Performance Based Design of Laterally Loaded Drilled Shafts

Prepared by:
Robert Y. Liang
Haijian Fan

Prepared for:
The Ohio Department of Transportation,
Office of Statewide Planning
& Research

State Job Number 134709

December 2013

Final Report

U.S. Department of Transportation
Federal Highway Administration

Technical Report Documentation Page

1. Report No.	2. Government Accession No.	3. Recipient's Catalog No.
FHWA/OH-2013/15		

4. Title and Subtitle	5. Report Date
Performance Based Design Of Laterally Loaded Drilled Shafts	**December 2013**
	6. Performing Organization Code

7. Author(s)	8. Performing Organization Report No.
Robert Y. Liang **Haijian Fan**	

9. Performing Organization Name and Address	10. Work Unit No. (TRAIS)
Department of Civil Engineering **The University of Akron** **244 Sumner Street, ASEC 210** **Akron, OH 44325**	
	11. Contract or Grant No.
	SJN 134709

12. Sponsoring Agency Name and Address	13. Type of Report and Period Covered
Ohio Department of Transportation **1980 West Broad Street** **Columbus, Ohio 43223**	**Final Report**
	14. Sponsoring Agency Code

15. Supplementary Notes

16. Abstract

Reliability-based design of deep foundations such as drilled shafts has been increasingly important due to the heightened awareness of the importance of risk management. The load and resistance factor design has been implemented by FHWA since 2007. Nevertheless, there are still many unsolved issues regarding the implementation of load and resistance factor design. In an attempt to address these issues, a performance-based design approach has been developed in which Monte Carlo simulation is employed to conduct reliability analysis. A series of computer codes were developed and validated. It was found that the spatial variability of soils is an important consideration in reliability analysis.

17. Keywords	18. Distribution Statement
Performance based design, drilled shaft, reliability, LRFD, soil variability, deep foundation	**No restrictions. This document is available to the public through the National Technical Information Service, Springfield, Virginia 22161**

19. Security Classification (of this report)	20. Security Classification (of this page)	21. No. of Pages	22. Price
Unclassified	**Unclassified**		

Form DOT F 1700.7 (8-72) **Reproduction of completed pages authorized**

Performance Based Design of Laterally Loaded Drilled Shafts

Prepared by:

Robert Liang

Haijian Fan

The University of Akron

December 2013

Prepared in cooperation with the Ohio Department of Transportation
and the U.S. Department of Transportation, Federal Highway Administration

ACKNOWLEDGMENTS

The authors would like to acknowledge the support and guidance provided by the ODOT Subject Expert Panel: Chris Merklin and Alexander Dettloff of the Office of Geotechnical Engineering.

ABSTRACT

With the implementation of load and resistance factor design (LRFD) by the U.S. Federal Highway Administration, the design of deep foundations is migrating from Level I (e.g., allowable stress design) codes to Level II codes (e.g., LRFD). Nevertheless, there are still unsolved issues regarding the implementation of load and resistance factor design. For example, there is no generally accepted guidance on the statistical characterization of soil properties. Moreover, the serviceability limit check in LRFD is still deterministic. No uncertainties arising in soil properties, loads and design criteria are taken into account in the implementation of LRFD. In current practice, the load factors and resistances are taken as unity, and deterministic models are applied to evaluate the displacements of geotechnical structures.

In order to address the aforementioned issues of LRFD, there is a need for a computational method for conducting reliability analysis and computational tools for statistically characterizing the variability of soil properties. The objectives of this research are: 1) to develop a mathematically sound computational tool for conducting reliability analysis for deep foundations; and 2) to develop the associated computational method that can be used to determine the variability model of a soil property.

To achieve consistency between the strength limit check and the serviceability limit check of the LRFD framework, performance-based design methodology is developed for deep foundation design. In the proposed methodology, the design criteria are defined in terms of the displacements of the structure that are induced by external loads. If the displacements are within the specified design criteria, the design is considered satisfactory. Otherwise, failure is said to

occur. In order to calculate the probability of failure, Monte Carlo simulation is employed. In Monte Carlo simulation, the variability of the random variables that are involved in the reliability analysis is captured by simulating a large number of samples according to their respective probability distributions. Next, the simulations of the random variables are used as the input to the commonly used *p-y* method and load transfer method to evaluate the load-displacement behavior. Once the displacements are calculated, it can be determined whether or not failure will occur. Accordingly, the failure probability is calculated as the number of failure events to the total number of simulations.

A series of computer programs have been developed and validated based on the proposed performance-based design methodology. These computer programs can be used to conduct reliability analysis for designing a drilled shaft. To determine the variability model of soil properties that will be used as input to the computer programs, a computational method has been developed in which the blow counts in a standard penetration test are required as inputs. It is found that the consideration of the dependence structure of soil properties is important for reliability analysis.

TABLE OF CONTENT

PAGE

LIST OF TABLES

LIST OF FIGURES

CHAPTER 1. INTRODUCTION

1.1 Problem Statement

1.1.1 Variability of Soil Properties

Soil properties are used as inputs to the deterministic models employed for calculating the capacity or predicting the load-displacement behavior of a designed structure. It is well known that soil properties will show spatial variability. As a result, the calculated capacity or displacement of a structure (such as a deep foundation) to external loads would also be expected to exhibit some variations. The variations of the capacity or the displacement should be properly considered in the design so that the structure can withstand an unforeseen extreme event that may be related to exceptionably weak soil strength or extremely large external loads. Structural failure or serviceability issues may occur if the designed structure is unable to handle the underlying risks.

Soil is a complicated material that is formed through a combination of physical and chemical processes, and thus its components vary significantly from one site to another. The variability in soil properties is a complex attribute that results from different sources of uncertainties. As recognized in Phoon and Kulhawy (1999), the primary sources of uncertainties for soil properties include the inherent variability of the soil, measurement errors, sampling process uncertainties, and transformation errors. Transformation error is introduced when the raw data from subsurface investigations, such as the standard penetration test (SPT) or cone penetration test (CPT), is converted to the desired soil properties such as undrained shear strength for cohesive soils or effective friction angle for granular soils. As a result of the

formulation process of soils and the sampling and measuring process, soil properties used in the calculation of the capacity and the displacement of the designed structure are always uncertain to some degree. The uncertainties of soil properties should be taken into account properly in the design process in order to guarantee the safety and the serviceability.

In the current practices, a site exploration program is run and *in situ* tests such as SPT and/or CPT are conducted in the subsurface investigation. The raw data from SPT or CPT is then converted to the desired soil properties that will be used in the calculation of capacity or displacement. In addition, the converted soil properties can also be used to conduct statistical analyses to determine the mean and the variance, using the following equations:

$$\mu_x = \frac{1}{n}\sum_{i=1}^{n} x_i \tag{1.1}$$

$$\sigma_x = \sqrt{\frac{1}{n-1}\sum_{i=1}^{n}\left(x_i - \mu_x\right)^2} \tag{1.2}$$

where x represents a soil property, n is the number of samples, μ_x denotes the mean of x, and σ_x denotes the standard deviation of x. The disadvantage in using this method of calculation, known as the method of moments, is that the spatial correlation of soil properties cannot be modeled. However, it has been demonstrated that the spatial correlation of soil properties is important in any reliability analysis (Fan and Liang 2013a, 2013b; Griffiths et al. 2009).

1.1.2 Simplified Reliability-Based Design

In order to tackle the influences of soil variability and other uncertainties on the reliability of geotechnical structures, reliability-based design (RBD) is proposed. As a simplified form of RBD, load and resistance factor design (LRFD) is being implemented by the American Association of State Highway and Transportation Officials (AASHTO). This is primarily due to the desire to achieve a reliable design for a foundation system. In the LRFD framework, it is

required that the summation of factored load effects should not exceed the summation of factored resistance, namely

$$\sum \eta_i \gamma_i Q_i \leq \sum \phi_i R_i \tag{1.3}$$

where η_i is a load modifier accounting for ductility of the structure, γ_i is a load factor applied to the load effect Q_i, and ϕ_i is a resistance factor applied to the resistance R_i (Brown et al. 2010). The format of LRFD expressed in the aforementioned inequality is compatible with allowable stress design (ASD), which enables design engineers to make a smooth transition from ASD to LRFD.

However, during the transition to LRFD, there are a number of implementation issues and problems confronting state departments of transportation. One of the outstanding problems is the calibration of the resistance factors (D'Andrea and Tsai 2009; Lai 2009). Currently, there are two approaches being used to calibrate the resistance factors: reliability theory and fitting to ASD.

In the reliability theories, assumptions or simplifications need to be made in order to calibrate the resistance factors. First of all, reliability analysis requires a design method. Then assumptions need to be made regarding the variability in soil properties. For example, Phoon et al. (1995) assumes that the soil properties, including the undrained shear strength of clay or the effective friction angle of sand, are described by an identical probability distribution such as the lognormal distribution. In addition, it is assumed in any reliability problem that the external loads may follow a probability distribution such as lognormal, normal or gamma distribution. The assumptions or simplifications (e.g. probability distributions of inputs in the design model as well as the overall design method) made during the calibration process may be invisible to designers, which can lead to potential misuse of these factors. When using calibrated load and

resistance factors, practicing engineers must accept all the associated assumptions and simplifications (Wang et al. 2011).

Furthermore, the load and resistance factors are only available for the predefined reliability indices β_T. The load and resistance factors for other β_T are not readily available, and recalibration is required. Because of this, it is not convenient to use the load and resistance factor design approach. As recognized by Phoon et al. (2003b), the load or resistance factors cannot be proposed independently of the definition of the nominal load effect or the nominal resistance. Note that the resistance factors or load factors can only be applied to the particular design method that is used in calibrating the load and resistance factors. A consistent level of reliability may not be achieved if the same factors are applied to a different design method. At best, the calibrated load and resistance factors are only applicable to a specific design model. Recalibration is required when using a different design model.

Instead of reliability theories, an approach that uses fitting to ASD may be used to calibrate the resistance factors if a database of load test results is not available (Lai 2009) or if the data is not adequate. However, the calibrated resistance factors only correspond to the particular factor of safety (FS) used in the calibration process, instead of the reliability index or probability of failure. Therefore, the application of these factors would be unable to achieve a safe foundation system design to a quantifiable and consistent level of reliability.

In the current LRFD approach, the spatial variability of soil properties is typically ignored. As noted in Griffiths et al. (2009), probabilistic approaches that do not model spatial variance may lead to an unconservative estimate of the probability of failure. Indeed, a parametric study such as the one described in Griffiths et al. (2009) indicates that the probability of failure for a deep foundation system is apparently sensitive to the variation in the covariance structure of the

soil properties. In geotechnical engineering, soil properties exhibit spatial dependence as noted by Fenton and Griffiths (2008). Soil properties are modeled as random fields in existing literature (Griffiths et al. 2009; Fenton and Griffiths 2008; and Paice et al. 1996). Unfortunately, the uncertainties of soil properties are only modeled at the point level and the spatial variability of soils is ignored, which in consequence may lead to a bias in load or resistance factors. Consequently, it may result in unsafe foundation design. Thus, there is a need to develop a novel methodology to account for the influence of the covariance structure of input on the probability of failure.

1.1.3 Serviceability Limit Check

In the LRFD framework, the serviceability requirements of any geotechnical structure should be satisfied. However, both resistance factors and load factors are taken as unity in the serviceability limit check. Unfactored loads are applied to calculate the displacements in response to external loads using deterministic models. If the displacement is within the specified tolerable displacement, the design is considered to be satisfactory. Otherwise, the design parameters such as the diameter and/or the length of a drilled shaft should be adjusted. In this calculation process, the uncertainties arising in the soil properties and external loads, as well as the model uncertainty, are ignored. In consequence, there could be a potential for a serviceability failure.

1.1.4 System Reliability

Under axial and lateral loading, a foundation system would usually have multiple failure modes. Unfortunately, the system reliability of foundation systems is usually ignored in the reliability analysis. In the current LRFD approach, the strength limit states and serviceability

limit states should be considered in the design. However, different limit states are considered separately without considering the effects of their interaction. Consequently, there is a potential that the overall failure probability may be underestimated.

1.1.5 Concluding Remarks

Based on the previous discussion, it can be concluded that the LRFD approach is deficient in the following aspects:

1. The load and resistance factors are only available for the predefined reliability indices. Recalibration of the factors has to be conducted for other reliability indices.
2. The process of fitting to ASD is used for calibrating the resistance factors when load test data is incomplete or limited. The resulting resistance factors only correspond to the particular factor of safety in the calibration process.
3. The calibration process of the load and resistance factors is almost unknown to practitioners, and practicing engineers cannot make any adjustments to the resistance factors.
4. The serviceability limit check is still deterministic, and the underlying uncertainties cannot be accounted for properly.
5. Different limit states of a foundation system are considered separately, and the system reliability is not considered in the design process.
6. The spatial correlation of soil properties is typically ignored in the design process.

Notice that the calibration of the resistance factors is conducted numerically, and there is usually no analytic solution for determining the resistance factors. Currently, a first order reliability method or a Monte Carlo simulation may be applied in the calibration process (Allen

et al. 2005). As a result of the calibration method and the assumptions that are made in the calibration process, practicing engineers cannot make any adjustments to the resistance factors tabulated in the design codes such as those provided by AASHTO (AASHTO 2010). The calibrated resistance factors can only apply to a particular design method. Moreover, the serviceability limit check is still deterministic in the LRFD framework. Hence, there is an obvious inconsistency between the design for strength limit states and the design for serviceability limit states. Although there are various limit states that need to be considered in the design process, they are indeed considered separately.

As a result of these deficiencies, the load and resistance factor design cannot achieve a consistent level of safety for the design. It has been noted that implementing LRFD factors independently of the stratum scenarios cannot produce a uniform level of safety (Ching et al. 2013) because the thickness of a particular soil stratum and the variability of the soil properties of the stratum may vary significantly from one site to another, resulting in different levels of variability for the resistance of the soil stratum.

1.2 Research Objectives and Scope

The purpose of the research is to improve the reliability analysis of deep foundation design so that the underlying risks in deep foundation design are properly taken into account. The objectives of this research are:

1. Develop a fundamentally sound methodology of conducting reliability analysis for deep foundation design;
2. Create computer programs to implement the developed methodology; and
3. Formulate the computational method for determining the soil variability model.

Because the calibration of the load and resistance factors in the LRFD framework invokes a number of assumptions or simplifications, the resulting LRFD factors would inevitably have their own limitations. Furthermore, the strategy of implementing the load and resistance factor independently of the stratum scenarios is problematic, since it is unable to achieve a uniform level of reliability for a diverse range of soil strata (Ching et al. 2013). Therefore, recalibration of the LRFD factors within the LRFD framework is not only tedious but also insignificant. Note that the recalibrated LRFD factors would likely be unable to achieve a consistent level of safety, just because the soil strata can vary significantly from one location to another. In addition, the limited number of stratum cases included in the calibration process cannot cover all possible cases!

It should be noted that the purpose of this research is not to recalibrate new load and resistance factors. Instead, the purpose is to develop a novel reliability-based design methodology. In order to accomplish the research objectives, the scope of the research project is defined as follows:

1. Conduct a literature review to identify numerical methods for analyzing drilled shafts under axial and lateral loads and identify state-of-the-art reliability methods;
2. Formulate a Monte Carlo simulation–based methodology for reliability analysis that is applicable to both axially loaded and laterally loaded piles;
3. Develop a statistical method for characterizing the variability of the uncertain parameters, particularly the parameters for soil properties; and
4. Conduct a comparative study on the developed methodology and the LRFD approach using data from a real-world project.

The purpose of the literature review is to identify the state-of-the-art methodologies pertaining to performance-based design of deep foundations. The numerical algorithms for analyzing piles under lateral loads and axial loads are reviewed, with particular attention to the uncertainties of the identified numerical algorithms. Since the main objective of this research is to develop a mathematically sound methodology for conducting reliability analysis, the advantages and the disadvantages of the first order reliability method and the Monte Carlo simulation are discussed.

In order to consider the spatial variability of soil properties, random field modeling is introduced in which a mean, a variance, and a correlation function are needed. To account for the influence of soil spatial variability, Monte Carlo simulation is applied. Following the Monte Carlo simulation–based methodology, a series of computer codes are developed. With a large number of realizations of the displacements, a statistical analysis can be conducted. Accordingly, feasible designs that achieve the target reliability index can be identified.

In an attempt to determine the soil variability model that will be used as input to the computer codes, a Bayesian approach is developed to model the spatial variability of the data of the standard penetration test. The objective of the approach is to obtain an estimate of the mean, the standard deviation, and the correlation length of a soil property, which are the parameters of interest in the Bayesian approach. The developed approach is applied to the data of a real-world project for validation purposes. Once the soil variability model is determined, the developed computer codes are used to conduct a reliability analysis, and a feasible design is obtained. A comparative study between the feasible design and the design obtained by using the LRFD approach is conducted.

1.3 Report Organization

A total of eight chapters are included in the report. The remaining chapters are organized as follows:

Chapter 2 presents a summary of the literature review. In the literature review, the widely used load transfer methods are briefly described. The assumptions and the uncertainties of the methods are discussed in detail, and the random field–based modeling of soil properties is explained. The reliability methods (such as the first order reliability method and Monte Carlo simulation) are discussed, and recent developments in reliability-based design methodology are reviewed.

Chapter 3 presents performance-based design for laterally loaded piles that considers the spatial variability of soil properties. This chapter discusses the selection of the numerical algorithm for analyzing laterally loaded drilled shafts, the choice in the distribution for statistically characterizing the load model, and the model uncertainties. Details are provided regarding the strength limit states and service limit states, the determination of the target reliability, and the proposed method to obtain a feasible design. Also included in this chapter is a design example for a very stiff clay site evaluated in a recent Federal Highway Administration (FHWA) report.

Chapter 4 presents a performance-based design for axially loaded piles, adopting the same approach as the method presented in Chapter 3 for laterally loaded piles. Details are provided regarding modeling of the spatial uncertainty of soil properties and the design criterion is defined in terms of the tolerable vertical movement. A design example is presented using boundary conditions of a drilled shaft and the statistical properties of shear strength of the soils taken from a published report identified during the literature search.

Chapter 5 presents the reliability analysis used to evaluate the serviceability performance of drilled shafts under combined lateral and axial loading, including details regarding the Monte Carlo simulation–based approach that was applied to analyze the system reliability. Random variables used in the analysis (namely, soil properties, material properties, model errors, allowable displacements, external loads) are discussed in detail. The chapter also includes an example of a reliability assessment for a drilled shaft and the importance analysis of the random variables that are considered in the example reliability analysis.

Chapter 6 presents a numerical algorithm for conducting efficient reliability analysis. The chapter discusses the benefits and drawbacks of using Monte Carlo simulation for reliability analysis, methods for analyzing the response to an axially loaded pile, and statistical parameters to characterize the variability of soil properties. The methodology for importance sampling is presented, including a discussion of the mathematical formulation for the probability of failure and considerations in applying importance sampling to the reliability evaluation of axially loaded piles, Details are also included regarding an implementation scheme, an approach for pinpointing the design point in order to characterize the region of interest, the use of the response surface method to construct a limit state function, and an algorithm for conducting fast reliability evaluation of axially loaded piles. Two examples for drilled shafts are presented: one for a shaft in a homogeneous soil deposit, and another for a shaft in a heterogeneous soil deposit.

Chapter 7 presents computational methods for determining the soil variability model, including details regarding the correlation with the standard penetration test, a discussion of the Bayesian approach, and applying Markov Chain Monte Carlo analysis to simulate various parameters. This chapter also presents geostatistical principals that can be applied to interpret the

soil profiles at potential shaft locations. An example is presented using data from a project in Ohio involving a grade-separation between a state route and existing railroad tracks.

Chapter 8 presents the summary of the research, the computational tools developed to facilitate the computation of the reliability analysis, the computational method for determining the soil variability, and the associated conclusions. This chapter also provides recommendations for future research.

CHAPTER 2. LITERATURE REVIEW

The focus of this chapter is to summarize the materials pertaining to the analysis of drilled shafts under axial and lateral loading, reliability methods, the variability of soil properties, and the recent developments in reliability-based design methods. In the analysis of the response of drilled shafts to external loads, the numerical methods (i.e., *p-y* method and *t-z* model) are presented; these methods are widely used in practice and have a reasonable level of accuracy. A brief discussion of the well-known first order reliability method is presented, followed by a short explanation of multiple resistance factor design.

2.1 Load Transfer Models

In the analysis of drilled shafts or driven piles subjected to axial and lateral loading, load transfer concepts have been widely applied. The *t-z* model (Coyle and Reese 1966) is used to calculate the vertical movement of the pile at a given axial load. For axial loading, the axial soil-structure interaction is modeled as *t-z* curves and *q-w* curves, where *t* and *q* represent side shear on the shaft and the tip resistance at the toe, respectively, and *z* and *w* represent the vertical displacements of the shaft segment and the toe of the drilled shaft, respectively. The *p-y* method (Reese 1977) is used to calculate the lateral deflection of a laterally loaded pile. For lateral loading, the lateral soil-structure interaction is modeled as *p-y* curves, where *p* represents the soil reaction and *y* represents the lateral deflection.

2.1.1 The *p-y* method

The *p-y* method (Reese 1977) has been widely accepted by practitioners because of the following advantages: 1) multiple layers of soils can be considered; 2) non-linear interaction

between the soil and the shaft can be modeled; 3) the flexural rigidity of the drilled shaft can be varied along the length of shafts; and 4) degradation of flexural rigidity of a drilled shaft under loading can be modeled. Figure 2.1(a) shows the model of a laterally loaded drilled shaft and Figure 2.1(b) shows a series of *p-y* curves along the length of the shaft for representing the lateral soil-drilled shaft interaction. The governing differential equation for the laterally loaded piles is given as:

$$EI\frac{d^4y}{dz^4}+Q\frac{d^2y}{dz^2}-p=0 \tag{2.1}$$

where *EI* is the flexural rigidity of the shaft, *y* is the lateral deflection of the shaft at point *z* along the shaft length, *Q* is the axial load acting on the shaft head, and *p* is the lateral soil reaction per unit length of the shaft. The soil–drilled shaft interaction is described by a set of discrete *p-y* curves, for which various criteria have been developed for different soil conditions. A finite difference numerical algorithm has been used to solve the governing differential equation, as in the commonly available computer programs such as *LPILE* (Reese et al. 2004).

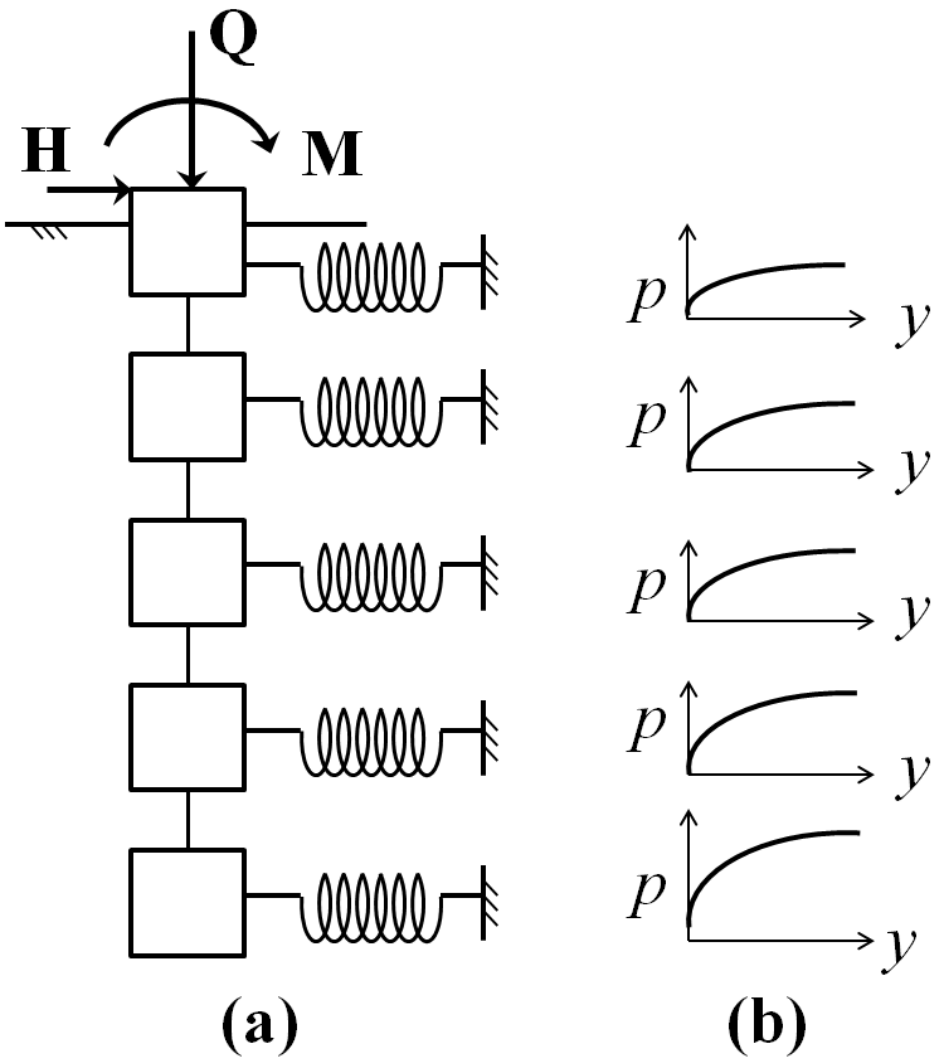

Figure 2.1 *p-y* method for lateral loading

2.1.2 The *t-z* Model

The *t-z* model (Coyle and Reese 1966) has been widely used for the analysis of axially loaded piles or drilled shafts. Figure 2.2 shows the schematic diagram of the *t-z* model. In this approach, the drilled shaft is divided into a finite number of segments, for which the interaction between the soil and the drilled shaft for each segment is modeled by discrete springs using the *t-z* curves for side friction and the *q-w* curves for end bearing, where *t* and *q* represent side shear on the shaft and the tip resistance at the toe, respectively, and *z* and *w* represent the vertical

displacements of the shaft segment and the toe of the drilled shaft, respectively. The advantages in using this method are that the load-transfer curves could be nonlinear and that multiple layers of soil could be considered. Numerous load-transfer curves have been developed for various types of soil conditions, which could be categorized as empirical or theoretical functions (e.g., Zhu and Chang 2002). The normalized load-transfer curves for cohesive soils contained in AASHTO (2010) are reproduced in Figure 2.3 and are adopted herein due to their wide acceptance. Likewise, the normalized load transfer curves for granular soils in AASHTO (2010) are incorporated into the program. Axial loading can be further categorized as compression and uplift. For compression, the total nominal resistance (i.e., R) of a drilled shaft can be evaluated using the following equation:

$$R = R_s + R_b - W \tag{2.2}$$

where W is the weight of the drilled shaft, R_s, R_b are the total nominal shaft resistance and toe resistance, respectively. For uplift, the nominal resistance of a drilled shaft can be evaluated as:

$$R = R_s + W \tag{2.3}$$

The toe resistance of the drilled shaft is usually ignored for the uplift loading.

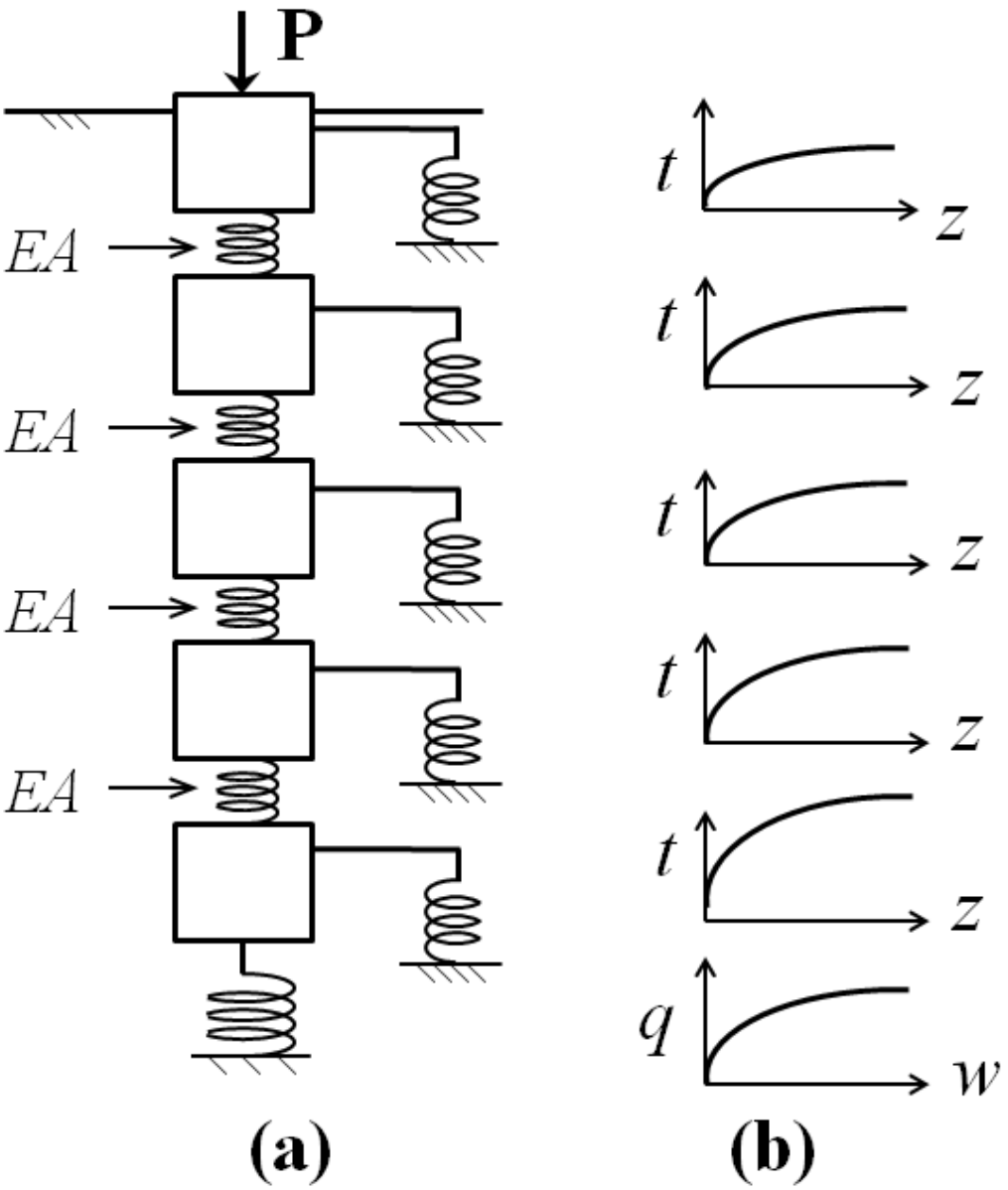

Figure 2.2 t-z model for axial loading

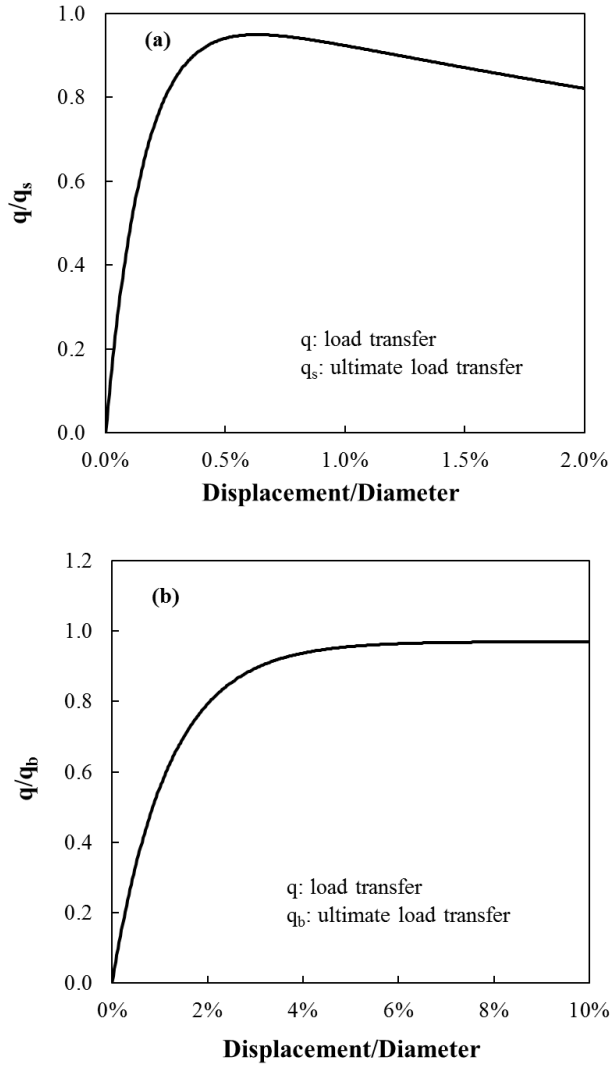

Figure 2.3 Normalized load transfer Curves for cohesive soil

2.1.3 Uncertainties Involved in Load Transfer Methods

The capacity or the displacement calculated based on the load transfer methods has some variations as a result of various uncertainties. The main sources of uncertainties include:

1. Soil properties;
2. Concrete properties;
3. Steel properties;

4. External loads including axial and lateral loads; and
5. Modeling of soil reactions to external loads.

In the load transfer methods, the soil properties are needed as input to construct the *p-y* curves, *t-z* curves and *q-w* curves. The strength and the stiffness of soil would directly influence the soil reactions that are represented by the load transfer curves (i.e., *p-y* curves, *t-z* curves and *q-w* curves). In addition, the properties of concrete and steel can influence the mechanical stiffness of the foundation system, thus affecting the capacity or the displacement of the system. The displacement of the foundation system is a response to the external loads. Hence, the variations in the external loads would cause some variations in the displacement. Finally, the soil reactions are represented by load transfer curves, which is a major assumption in the load transfer models. Thus, the accuracy of the load transfer curves would significantly affect the accuracy of the calculated capacity or displacement.

2.2 First Order Reliability Method

The first order reliability method (FORM) is widely used as a tool of reliability analysis that has been applied to calibrate the resistance factors in geotechnical engineering. FORM suffers from fundamental limitations that make it difficult to adapt for certain types of geotechnical problems, such as considering the spatial variability of soil properties. To describe the state of a system, a performance function is defined as:

$$G(\boldsymbol{x}) = C(\boldsymbol{x}) - D(\boldsymbol{x}) \tag{2.4}$$

where C and D denote the "capacity" and the "demand" in a broad sense, respectively, and $\boldsymbol{x}=(x_1,x_2,x_3,\ldots)$ denotes a vector of basic variates (i.e., random variables) in the design model. The system is considered to be in a safe region if $G>0$ and in the failure region if $G<0$.

In the context of FORM, the performance function is approximated using the first order Taylor series expansion, which is tantamount to replacing an *n*-dimensional failure surface with a hyper-plane tangent to the failure surface at the most probable failure point (Ang and Tang 1984). The resulting planar failure surface will be on the unconservative side if the performance function is concave towards the origin of the reduced variates, as illustrated in Figure 2.4. On the other hand, the failure surface will be on the conservative side if the performance function is convex towards the origin of the reduced variates. Ang and Tang (1984) point out that the accuracy of FORM may be improved through quadratic or polynomial approximation. Even so, the failure region is inevitably changed for non-linear performance functions, resulting in an inaccurate estimation of the probability of failure. It is concluded that the first order reliability method is mathematically exact only if the performance function is linear (Ang and Tang 1984), and the accuracy of this method deteriorates if second or higher derivatives of the function are significant (Fenton and Griffiths 2008). For a nonlinear performance function, the resulting probability of failure P_f evaluated by FORM will be biased since P_f is the generalized volume integral of the joint probability density function (PDF) over the failure region.

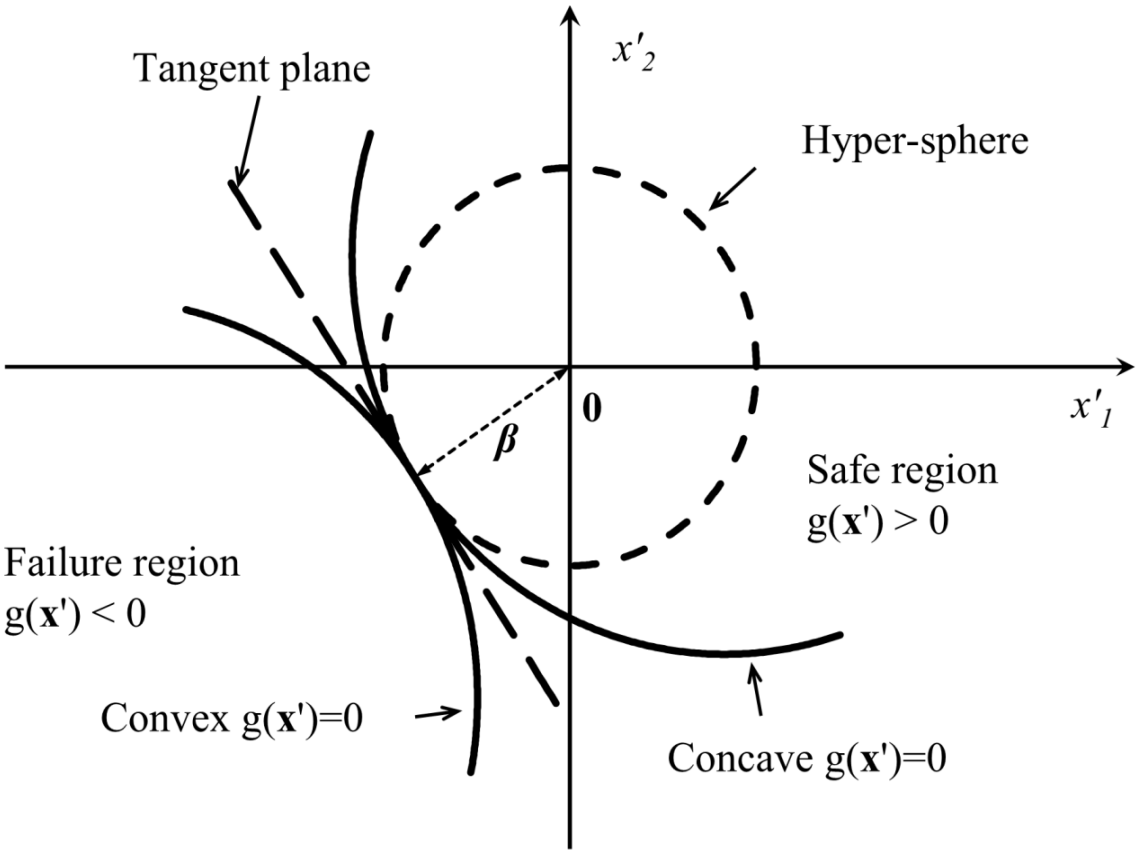

Figure 2.4 Implications of nonlinear limit state function

2.3 Soil Variability Model

2.3.1 Introduction

Soil properties such as effective friction angle for granular soils and undrained shear strength for cohesive soils are used as input to the *p-y* method and the load transfer method to model the soil reaction to external loads, which are characterized by *p-y* curves, *t-z* curves and *q-w* curves. These load transfer curves are then used in numerical algorithms to evaluate the load-displacement behavior iteratively. The prediction of the displacements of deep foundations due to external loads could vary if the soil properties needed to construct the load transfer curves have some variation. As a result, the stochastic nature of the soil properties plays an important

role on the reliability based design of deep foundations. An accurate variability model for soil properties is essential in the reliability analysis of deep foundations.

The objective of this section is to develop a mathematically sound model for statistically charactering the variability of soil properties. Because soil properties are spatially varying, the mean and the standard deviation may vary in space. Furthermore, a covariance matrix is needed to characterize the dependence structure of the soil properties. Therefore, the purposes of the statistical model are:

1. To model the variation of a soil property at the point; and
2. To model the spatial correlation of the soil property.

2.3.2 Random Variables

Soil properties used in the design of deep foundations have some variations because of the inherent variability of soils, the sampling process, and the measurement error that is related to equipment and operators. To statistically model the variations of the soil properties at the point level, a mean μ_x, a standard deviation σ_x and a probability distribution are needed. Suppose a soil property is denoted as x, and its distribution is shown in Figure 2.5. To statistically describe the data shown in Figure 2.5, a mean and a standard deviation are needed. The mean μ_x measures the center of x, which is defined as follows:

$$\mu_x = \frac{1}{n}\sum_{i=1}^{n} x_i \tag{2.5}$$

where n is the number of samples. The standard deviation σ_x measures the variation from the mean μ_x, which is defined as:

$$\sigma_x = \sqrt{\frac{1}{n-1}\sum_{i=1}^{n}\left(x_i - \mu_x\right)^2} \tag{2.6}$$

A dimensionless measure of variability is the coefficient of variation (COV) defined as:

$$\delta = \frac{\sigma}{\mu} \tag{2.7}$$

The COV for soil density and undrained shear strength of clay is in the range of 1% to 10% and 10% to 50% (e.g., Lee et al. 1983; Phoon et al. 1995), respectively. Depending on type of test and the equipment, the corresponding COV vary significantly from one soil property to another. The typical COVs for various soil properties could be found in Phoon and Kulhawy (1999).

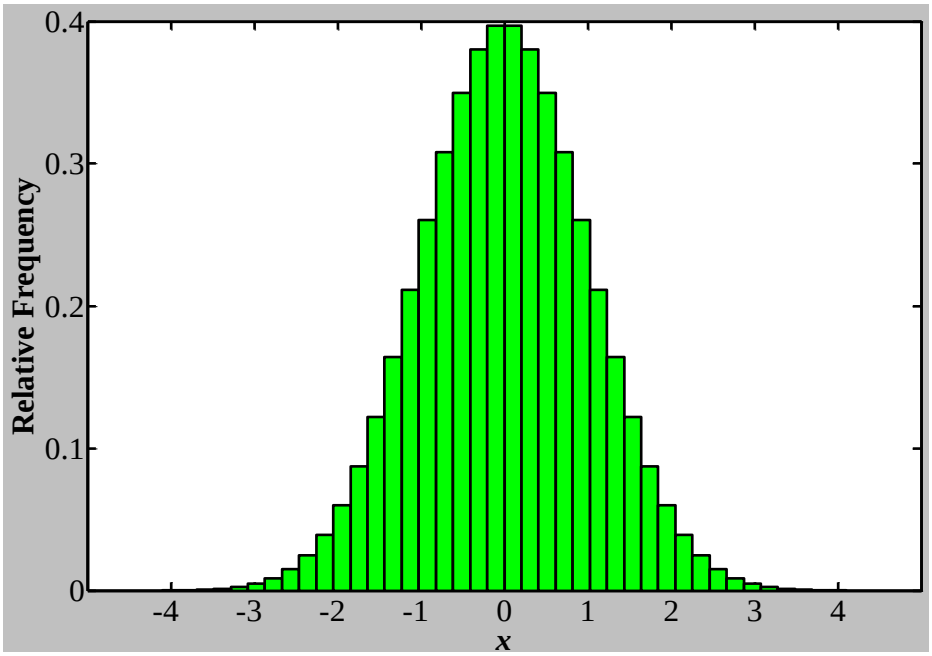

Figure 2.5 Histogram of random variable

In addition to the mean and the standard deviation, a probability distribution is required to describe how the random variable *x* is distributed. For soil properties such as unit weight of soils, effective friction angle and undrained shear strength, a commonly used probability distribution is lognormal distribution (see Fan and Liang 2012; Griffiths et al. 2009). There are two advantages in using lognormal distributions to model the variability of soil properties: 1) it guarantees that soil properties are always non-negative; and 2) logarithms of the strength parameters are

normally distributed. Two parameters, namely μ_{lnx} and σ_{lnx}, are needed to define a lognormal distribution. The two parameters are related to the mean μ_x and the standard deviation σ_x in the following equations:

$$\sigma_{\ln x} = \sqrt{\ln\left(1+\frac{\sigma_x^2}{\mu_x^2}\right)} \tag{2.8}$$

$$\mu_{\ln x} = \ln\left(\mu_x\right) - 0.5\sigma_{\ln x}^2 \tag{2.9}$$

With the distribution parameters, the probability density function of the lognormal distribution is written as

$$f\left(x|\mu_{\ln x},\sigma_{\ln x}\right) = \frac{1}{x\sigma_{\ln x}\sqrt{2\pi}}\exp\left[-\frac{1}{2}\frac{\left(\ln x-\mu_{\ln x}\right)^2}{\sigma_{\ln x}^2}\right] \tag{2.10}$$

From Equaiton (2.10), it can be seen that the logarithm of a lognormal variable follows normal distribution with mean = μ_{lnx} and standard deviation = σ_{lnx}. It should be noted that other probability distributions such as the normal distribution are potential choices for modeling soil properties.

2.3.3 Correlation Function

Soil properties are spatially varying. As a result, soil properties should be modeled as random fields. In addition to the mean and the variance, a third parameter called correlation length θ was suggested by Vanmarcke (1977) to characterize the spatial variability of a random variable. The correlation length is needed to define a correlation function, which describes how random variables are correlated at different separation distances. For example, the correlation function for Markov process is given below

$$\rho(\tau) = \exp\left(-\frac{2|\tau|}{\theta}\right) \tag{2.11}$$

where $\rho(\tau)$ is the correlation coefficient at the separation distance of τ, and θ is the correlation length. Equation (2.11) says the correlation coefficient decays exponentially with increasing separation distance. As a measure of the spatial correlation, the correlation length is essential in the definition of correlation function. A longer correlation length implies that the underlying random field is more uniform. If the correlation length is short, the underlying random field varies more rapidly. The following equation shows the covariance function for a stationary process:

$$C(\tau) = \sigma_x^2 \cdot \rho(\tau) \tag{2.12}$$

where σ_x is the standard deviation of the random variable at the point level. For simplicity, the correlation structure of soil properties is modeled as Markovian in this study so that Equation (2.11) and Equation (2.12) are employed to characterize the spatial variability of soil properties.

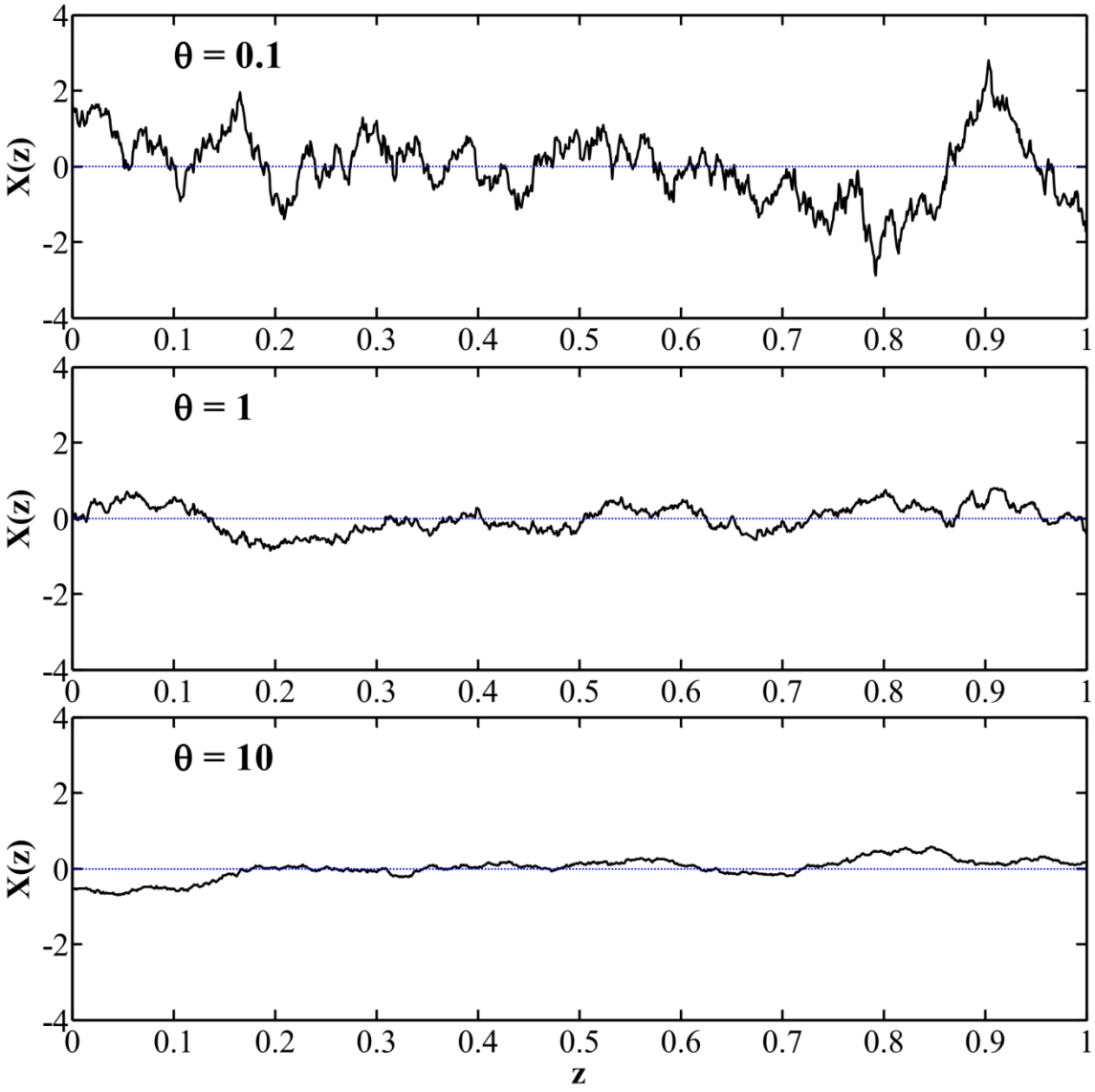

Figure 2.6 Random fields with different correlation lengths

2.3.4 Random Field Generation

The generation of random field samples is illustrated for the undrained shear strength of clay, which usually follows the lognormal distribution (Fenton and Griffiths 2008). In this research, Gaussian random fields (i.e., *X(z)*) are firstly generated with the prescribed correlation length using a selected random field generator and then transformed to the desired random fields by the following equation:

$$s(z) = \exp\left[X(z) \right] \tag{2.13}$$

where *s(z)* denotes the soil property at the depth *z*. Common methods for generating random fields include fast Fourier transform (FFT), local averaging subdivision (LAS), and covariance matrix decomposition (CMD). In this research, LAS is implemented to generate the random field samples, mainly because LAS is a fast and accurate method of producing random fields. The concept of local average subdivision was originated from the fact that quite a number of engineering measurements are the local averages of the properties under consideration. The algorithm used in this research to generate one-dimensional Gaussian random process is briefly described as follows:

1. Generate a random number to represent the global average, with the mean and variance obtained through the local averaging process theory.
2. Divide the process under consideration into two equal parts, and generate two random values that can preserve the local average of the parent cell to represent the local average of each cell. The two values are properly correlated with adjacent cells and exhibiting the variance according to the local averaging process theory.
3. Subdivide each cell into two equal parts and generate two random values to represent the local average of each part. Again, the two values have to preserve the local average of the parent cell. They are also required to be properly correlated with adjacent cells and exhibiting variance according to local averaging process theory.
4. Repeat Step 3 until the cell at the desired resolution is obtained.

Simply speaking, random fields in LAS are constructed recursively by subdividing the parent cell into equal parts. More technical details of generating random fields could be found in Fenton and Griffiths (2008). In this research, the size of local averaging process at the cell level

is chosen to be the same as the length of each drilled shaft segment, which is determined by the load transfer numerical methods. The corresponding load transfer curves (i.e., *p*-*y* curves, *t*-*z* curves and *q*-*w* curves) are constructed using the trend lines shown in Figure 2.3 and the randomly-generated soil properties are used as input.

2.4 Reliability Based Design

The reliability-based design methodologies for foundations have become increasingly popular. Just to name a few for example, multiple resistance factor design (MRFD) for shallow foundations for transmission line structures was developed based on the first order reliability method (Phoon et al. 2003a). The MRFD methodology was shown to achieve a more uniform level of safety compared with applying a single resistance factor. An expanded reliability-based design approach for drilled shafts based on Monte Carlo simulation (MCS) was proposed (Wang et al. 2011). The expanded reliability-based approach was not only robust and flexible, but it also is capable of addressing some of the deficiencies in load and resistance factor design. A quantile-based approach for calibrating reliability-based partial factors was proposed (Ching and Phoon 2011). In the proposed quantile-based method, the capacity is not required to lump into a single random variable in the LRFD format, nor is the mathematical optimization in the MRFD format required. The popularity of RBD methodologies was primarily driven by the desire to achieve a safe yet economical design in a rational way. It was noted that the geotechnical engineering community is known to be deep into empiricism (Phoon and Kulhawy 2005) and semi-empirical or empirical models are widely used. Nevertheless, the underlying assumptions for these models may not be always satisfied; therefore, the predictions based on the underlying assumptions are prone to errors. In addition, the soil properties used in geotechnical designs, such as shear strength and friction angle, are typically inherently difficult to quantify and thus uncertain to

some extent. As there are various uncertainties involved in the design models and soil parameters, it is still highly desirable to develop and implement the RBD methodologies that would enable the practicing engineers to design foundations rationally.

2.4.1 Multiple Resistance Factor Design

As mentioned earlier, LRFD has some deficiencies. Recent efforts in mitigating the fundamental flaws of LRFD approach include the work by Phoon et al. (1995, 2003a, 2003b) in which multiple resistance factor design (MRFD) for transmission line foundation structures was proposed. In MRFD, the uncertainties of the component resistance are separated and different resistance factors are applied to different component resistance. The rationale behind the MRFD is that different components of resistance have different magnitudes of uncertainty. As a result, the resistance factors for different components of resistance should be different. The main advantage of MRFD over LRFD is that a more consistent level of reliability can be achieved (Phoon et al. 2003a, 2003b).

In contrast, the resistance factors in the MRFD are implemented independently of the soil strata that are possibly present at the site. Consequently, MRFD is unable to achieve a consistent level of safety (Ching et al. 2013). In reality, it is common that multiple soil strata are present, and the thickness of each soil stratum may be different. Furthermore, the variability of various soils would also be different. If constant resistance factors are applied without considering the thickness and the variability of each soil stratum, it is likely that the resistance factors will be conservative for one site and unconservative for another site. This is understandable, because the variability of the resistance of a soil stratum is not only related to the soil properties of the stratum, but also related to the thickness of the soil stratum. Moreover, the geological

stratifications along the depth would matter, since the stratifications have different stiffnesses and can affect the load transfer.

Therefore, the strategy of implementing constant resistance factors is not able to achieve the desired consistent level of reliability. The study in Ching et al. (2013) indicates that the resistance factors should be calibrated considering the variability of each component resistance.

2.4.2 Monte Carlo Simulation–Based Approach

Wang et al. (2011) developed a more general reliability-based design approach for drilled shafts under axial loading. This approach formulates the design process as an expanded reliability problem in which Monte Carlo simulation is employed. The approach has a number of advantages over LRFD: 1) it enables designers to make adjustments on the target reliability index to accommodate specific needs for particular projects; 2) the process is transparent, enabling designers to gain insights on how the performance level changes as the pile diameter or penetration length changes; and 3) the estimate of probability of failure is accurate as long as the number of samples is large enough.

In this approach, the soil properties along the depth are modeled as independent random variables. The shortcoming of such a model is that the spatial correlation of soil properties cannot be accounted for. Note that the spatial correlation of soil properties is important in reliability analysis. As demonstrated in Griffiths (2009), it can lead to unconservative design if the dependence structure of soil properties is not considered in the reliability analysis.

2.4.3 Recognition of Soil Spatial Variability

Soil parameters are spatially variable, and the influence of soil spatial variability has attracted considerable attention. Griffiths et al. (2009) demonstrated a slope stability case in which ignoring soil spatial variability may lead to unconservative designs. Klammler et al. (2010)

demonstrated that the resistance factor in LRFD for a single drilled shaft is affected by soil spatial variability. More importantly, the resistance factors may be increased if the dependence structure of soil properties is taken into account. Luo et al. (2012) found that the reliability against basal heave for braced excavations is significantly influenced by soil spatial variability. As the spatial variability of soil parameters may affect the reliability of designs, it should be taken into account in reliability-based analysis.

2.5 Concluding Remarks

The objective of this research is to develop a novel reliability-based design methodology for deep foundations. The novel methodology consists of the following components:

1. Deterministic models for calculating the response of the pile under axial and lateral loads;
2. Monte Carlo simulation;
3. Evaluation of the probability of failure.

Although the *p-y* method and the *t-z* model have reasonably good accuracy, the results given by the two methods still have some variations because of the aforementioned uncertainties. Thus, it is highly desirable to develop a novel RBD methodology that can consider these uncertainties. In the proposed methodology, the *p-y* method and the *t-z* model are still used as numerical algorithms to evaluate the response of the pile to external loads. In addition to the *p-y* method and the *t-z* model, Monte Carlo simulation techniques are incorporated into the computational tools, so that various sources of uncertainties can be taken into account in the *p-y* method and the *t-z* model.

It is worth noting that soil properties are modeled as random fields. The advantage of using random field modeling is that the spatial variability of soil properties can be considered in the

reliability analysis. So far, the current LRFD approach has not considered the spatial variability of soil properties. Consequently, the design according to the LRFD approach might be potentially unconservative, as the variability of the related soil properties is not modeled correctly. On the other hand, this deficiency could be addressed in the proposed methodology.

More importantly, performance based design is implemented in the proposed methodology. The advantage of using performance-based design approach is that various sources of uncertainties can be considered consistently in both strength limit states and serviceability limit states. In contrast, the current LRFD approach is still deterministic for the serviceability limit state.

Furthermore, the system reliability of a design can be considered in the proposed performance-based design. In the developed methodology, not only are the individual limit states considered in the design but also the system failure is considered as well. The advantage of taking system failure events into account is that a more reliable design can be achieved.

CHAPTER 3. LATERALLY LOADED PILES

3.1 Introduction

In the current LRFD approach given in the AASHTO (2010) specifications, various resistance factors corresponding to different design methods have been provided for various strength limit states. However, there is an unresolved issue in the current AASHTO specifications in that the service limit check of a drilled shaft or driven pile is still carried out as in the Level I allowable stress approach. Unfactored loads are used to evaluate the deformation response of deep foundations using the deterministic computational models. The uncertainties arising from various sources, such as soil properties and their spatial variations, cannot be systematically taken into account. To provide a consistent framework for checking both strength limits and service limits, a Level III reliability-based design method for drilled shafts subjected to lateral loads is presented in this research.

The objective of this research is to present a performance-based reliability method and the associated computational algorithms for a laterally loaded drilled shaft or driven pile using a sampling-based approach. In the proposed approach, input to the computational model for the nonlinear soil structure interaction problem, such as *p*-*y* curves, is treated as random variables. In particular, soil properties, such as strength parameters, soil modulus (or subgrade reaction modulus), and unit weight, are modeled as random fields to account for the spatial variability and spatial correlations. The statistical parameters, including the mean, variance, and correlation length, are used to characterize a stationary random field. Random samples of the input are

generated according to the prescribed probability distributions. The deflection of the drilled shaft subjected to lateral loads is evaluated for each set of samples. In each realization, if the shaft head deflection exceeds the specified allowable value, then it is considered as an event of unsatisfactory performance. Consequently, the probability of failure (i.e., unsatisfactory performance) P_f, is simply calculated as the ratio of the number of events of unsatisfactory performance to the total number of realizations of random input. The design parameters of a deep foundation (i.e., shaft diameter D and shaft length L) are determined such that the desired target reliability level is met. A computer program, called *Probabilistic Laterally Loaded Piles* (*P-LPILE*), was developed by the authors to facilitate the computation according to the described sampling-based algorithms. The calculation of the deflection of a drilled shaft subjected to lateral loadings is based on the commonly-used *p-y* method (Reese 1977). A design example is given to demonstrate the application of the proposed methodology.

3.2 Numerical Algorithm for Analyzing Laterally Loaded Drilled Shafts

In the analysis of a laterally loaded drilled shaft, the widely used *p-y* method will be used as a numerical algorithm to calculate the response of a laterally loaded pile. The detailed discussion of the *p-y* method can be found in Chapter 2. It is noted that the non-linear *EI*-moment relationship is taken into account when calculating the displacement of the pile. The analytical method in Reese et al. (2004) is adopted for calculating the relationship between the bending moment and the flexural stiffness *EI*.

3.3 Probabilistic Load Description

The design loads applied to the foundations are uncertain to some degree. According to Nowak and Collins (2000), coefficients of variation for dead load could range from 0.08 to 0.10

for buildings and bridges, while those for live load including sustained live load and transient live load could range from 0.18 to 0.89. Previous investigations (e.g., Ellingwood and Tekie 1999; Ellingwood et al. 1980) have found that normal, lognormal, gamma, Type-I and Type-II Gumbel distributions are possible choices to statistically characterize load models. For example, the maximum live load for a structure can be statistically characterized by Type-I Gumbel distributions, while sustained live load can be modeled as a gamma distributed random variable.

3.4 Model Uncertainty

Model uncertainty is always present, as any computational model is an idealization or simplification of real-world conditions. The method for accounting for this uncertainty is described below. Suppose Y_p denotes the prediction based on a model, and N_M is a bias factor that describes the model uncertainty, then the actual behavior denoted as Y_m can be related to the prediction and bias as follows:

$$Y_m = N_M \cdot Y_p \tag{3.1}$$

It is noted that the error term N_M is a random variable whose statistical characters can be described as normal or lognormal distributions (e.g., Kung et al. 2007; Phoon and Kulhawy 2005).

In the *p-y* method, the soil reaction to lateral loading is modeled by *p-y* curves. To account for the uncertainty of the *p-y* curves, a random variable is generated in each simulation according to the prescribed probability distribution of the bias factor and is used to correct the soil reaction predicted by the *p-y* curve. As shown in Equation (3.1), the product of the generated bias factor and the prediction is viewed as the true soil reaction.

3.5 Performance-Based Reliability Analysis

3.5.1 Performance-Based Design

In current LRFD practices, strength limit states and service limit states are considered for various combinations of load effects. Appropriate load and resistance factors are applied to check that the design satisfies both limit states. The final design would be governed by either strength limit states or service limit states. However, as mentioned earlier, the service limit check for laterally loaded drilled shafts in the current AASHTO guidelines uses the traditional ASD approach, in which the load factor and the resistance factor are taken as unity and the deterministic *p-y* method (e.g., the *LPILE* program) is utilized for calculating the deflection of the foundation under lateral loads. As noted in Zhang and Ng (2005), currently serviceability limits are still considered using a conventional deterministic approach in most limit state design codes. The uncertainties arising from various sources (such as soil variability and load uncertainty) cannot be accounted for. Therefore, there is an obvious inconsistency in the design for considering the strength limits and service limits. To address this deficiency, a transition to the performance-based design (PBD) approach would be desirable, a viewpoint that is also noted by Nowak and Collins (2000). In the proposed framework, performance-based criteria can be established as the objectives for deep foundation design. The performance criteria are expressed in terms of allowable deflections of the foundation structures subjected to the design loads. In the PBD methodologies, a foundation design would be satisfactory provided the specified performance criteria are satisfied for the prescribed load effects.

3.5.2 Probability of Unsatisfactory Performance

The performance criteria of the proposed approach for laterally loaded shafts are stated in terms of the shaft head deflection. Failure is said to occur if the shaft head deflection exceeds the

allowable limits or if the numerical algorithm is unable to converge. Based on the described performance criteria, a general form for the probability of failure can be formulated as follows:

$$p_f = P(y_t \geq y_a) = \int_{G \leq 0} f(\boldsymbol{x})\, d\boldsymbol{x} = \int I[y_t \geq y_a] \cdot f(\boldsymbol{x})\, d\boldsymbol{x} \tag{3.2}$$

where y_t is the shaft-head deflection, y_a is the allowable displacement specified by the performance criteria, F is the failure region, $I[\cdot]$ is the indicator function, $\boldsymbol{x}$ is a vector of input and $f(\boldsymbol{x})$ is the joint probability density function. The indicator function in Equation (3.2) is equal to 1.0 if y_t is equal to or greater than y_a. It is zero for other conditions. The design objective can be written as:

$$P_f \leq P_T \tag{3.3}$$

where P_T is the target probability of failure. The design objective is therefore to optimize a deep foundation dimension so that the computed probability of failure P_f is equal to or less than the target probability of failure.

The determination of the target reliability is not an easy task. It involves the consideration of the consequence of failure, the construction costs, and the design life of the system under consideration, among others. A number of factors such as economic issues, social effects, and the existing levels of technology may have to be considered in order to determine an appropriate target probability of failure. It is noted that most civil engineering systems have a target probability of failure between 1/1000 and 1/100,000 (Fenton and Griffiths 2008). According to AASHTO (2010), a reliability index of 2.3 (approximately, P_f = 1/100) is used for shaft groups, while a reliability index of 3.0 (approximately, P_f = 1/1000) or higher is used for a single drilled shaft.

3.5.3 Sampling-Based Method

In the context of laterally loaded shafts, the reliability analysis simply becomes the evaluation of the failure probability defined in the previous section. In general, it is preferable to evaluate the integral expressed in Equation (3.2) analytically. Nevertheless, it is quite difficult to evaluate this integral directly for the following reasons: 1) $f(\boldsymbol{x})$ is a multivariate function for input vector $\boldsymbol{x}$, which may be of high dimensions; 2) it is hard to determine the failure region (i.e. F), particularly for a nonlinear soil structure interaction for which no analytic equation exists that can accurately predict the response of a drilled shaft under the lateral loads. The Monte Carlo integration (Robert and Casella 2004) is a realistic alternative for evaluating the integral.

Monte Carlo simulation (MCS) is a standard statistical method in which the response of a complex system is calculated repeatedly using a sequence of the generated random samples as input. The Monte Carlo approach of evaluating the probability of failure is expressed as follows:

$$P_f \approx \frac{1}{n}\sum_{i=1}^{n} I_i\left[y_t \geq y_a\right] \tag{3.4}$$

where n is the number of samples. By the law of large numbers, the unbiased estimator for P_f expressed in Equation (3.4) converges to the exact value as $n \rightarrow inf$ with a probability of 1.0. The Monte Carlo statistical method offers several advantages: 1) the Monte Carlo method gives the unbiased estimate of the probability of failure; 2) the accuracy of the estimate increases with increasing n; and 3) the method is mathematically simple. The accuracy of the estimate can be evaluated by its coefficient of variation, which can be estimated by the following equation:

$$\delta\left(P_f\right) \approx \sqrt{\frac{1}{n\left(n-1\right)\cdot P_f}\sum_{i=1}^{n}\left(I_i\left[y_t \geq y_a\right]-P_f\right)^2} \tag{3.5}$$

The flow chart for the proposed approach using the Monte Carlo technique is presented in Figure 3.1. The objective of the approach is to find feasible foundation dimensions (i.e., D and L)

that are able to achieve the target reliability for the prescribed performance criteria and design loads. In the proposed framework, a deterministic computational method is coupled with Monte Carlo simulation techniques in which the uncertainties of soil properties are quantified by field means, field variances, and the correlation structures. For loads and model errors, the probability distributions, mean values, and variances should be determined. For each trial foundation dimension, the probability of failure (unsatisfactory performance) is evaluated. The design process entails finding the optimum foundation dimension that is economical while meeting the reliability requirements. A computer program named *P-LPILE* was developed to incorporate the *p-y* method and the Monte Carlo simulation techniques described in this research.

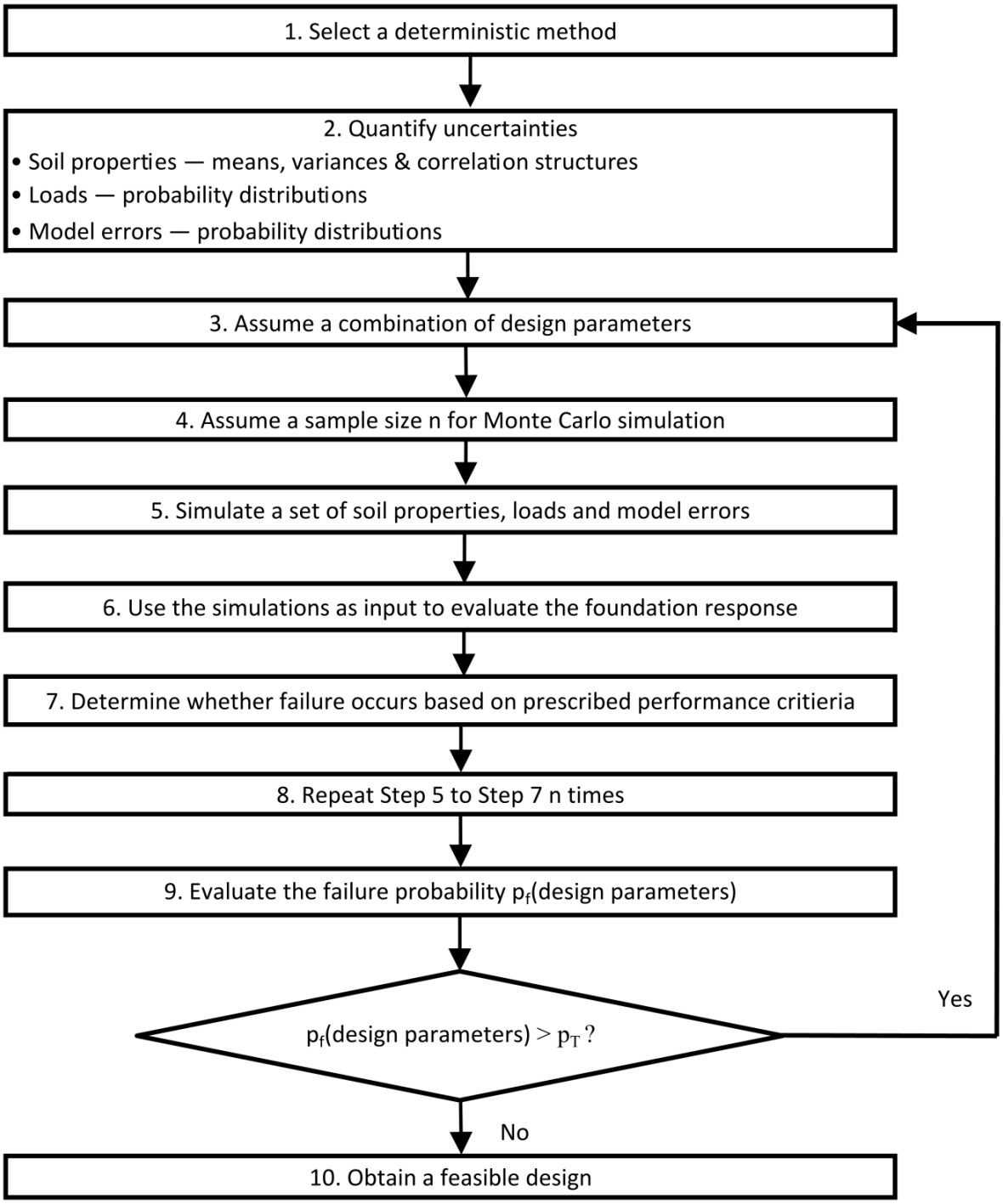

Figure 3.1 Flow chart of the proposed method

3.6 Design Example

Consider an example presented in a recent FHWA report (Brown et al. 2010). As shown in Figure 3.2, a drilled shaft is to be designed in a very stiff clay site with the design loads of 111.2

kN (i.e., 25 kips) in shear and 677.9 kN·m (i.e., 500 kip-ft) in moment applied at top of the drilled shaft on the ground level. The *p-y* curve for stiff clay (Reese et al., 2004) without free water was used in the report to represent the lateral soil–pile interaction. For generating the *p-y* curves, the mean values of the pertinent soil properties are as follows: the undrained shear strength is 103.4 kPa (i.e., 15 psi), the unit weight is 19 kN/m^3 (i.e., 0.07 pci), and the strain corresponding to 50% of the maximum principle stress difference (ε_{50}) is 0.005. The probability distributions of these soil properties are assumed to be lognormal. The example in the FHWA report does not provide values for COV for soil properties; therefore, the following COV values are assumed: a COV for undrained shear strength of 40%, a COV for ε_{50} of 20%, and a COV for effective unit weight of 4%. The maximum allowable lateral deflection at the shaft head was given in the FHWA report as 12.7 mm (i.e., 0.5 inch), which is deterministic. For calculating the Young's modulus of concrete, the compressive strength of concrete (31027.5 kPa, 4500 psi) is used. The properties of the reinforcing steels are as follows: the yield strength is 413700 kPa (i.e., 60,000 psi), and the elastic modulus of steel is 200 GPa (29,000 ksi). These values are used to calculate the values of *EI* of the drilled shaft as a function of the bending moment (see Reese et al. 2004). In the FHWA report, a resistance factor of 0.67 was used in the strength limit check for determining the foundation size, while the computer program *LPILE* was used to calculate the lateral deflection of the drilled shaft head under the unfactored loads at the pile head. The foundation dimension of 1.22 m (i.e., 4 ft) in diameter and 6.10 m (i.e., 20 ft) in length, with a total of 12 No. 11 rebars and a cover of 7.62 cm (3 in), was used for the final design according to the current LRFD methodologies documented in the FHWA report. This design is re-examined herein using the *P-LPILE* computer program and the proposed approach. Three soil parameters, namely ε_{50}, the undrained shear strength (denoted as S_u), and the effective unit weight (denoted

as γ'), are required to construct the *p-y* curve. For clarity, the correlation lengths for undrained shear strength, ε_{50}, and effective unit weight are denoted as $\theta_{\ln(Su)}$, $\theta_{\ln(\varepsilon 50)}$ and $\theta_{\ln(\gamma')}$, respectively. The correlation lengths of soil parameters are varied in a typical range to investigate their influences on the computed probability of failure.

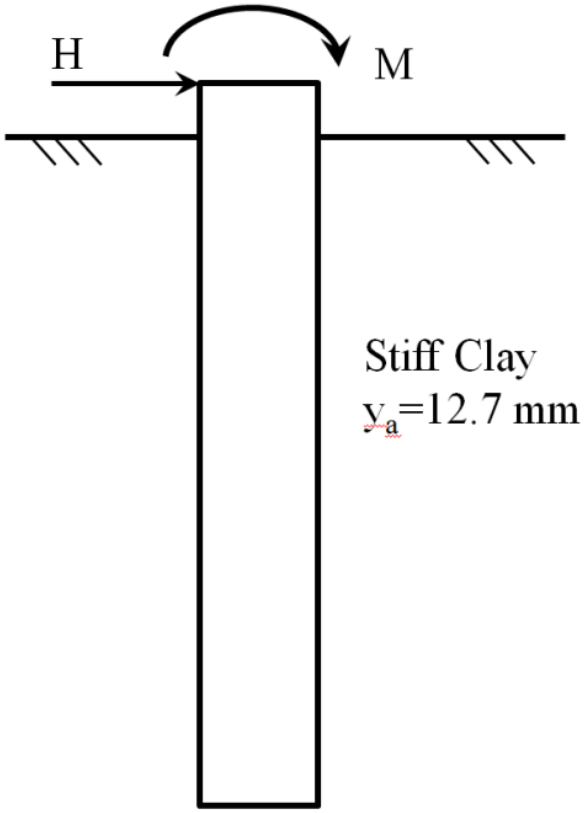

Figure 3.2 Example of a drilled shaft

3.6.1 Influence of Incremental Length

The random soil properties are generated using local averaging subdivision (LAS). The sensitivity of the computed probability of failure as affected by the unit cell length of the LAS is investigated in this section. The unit shaft length in the numerical *p-y* computational algorithm (denoted as *h*) is also set as the cell length for LAS; the number of segments is set to 400, 200,

100, and 50 in the sensitivity analysis. The corresponding ratio of h over D is 0.0125, 0.025, 0.05, and 0.1 for a diameter of 1.22 m (4.0 ft). Failure is said to occur when the lateral deflection at the top of the drilled shaft exceeds 12.7 mm (0.5 in). Figure 3.3 shows the relationship between p_f and the unit shaft length when the correlation length of undrained shear strength is varied from 2 m (6.56 ft) to 64 m (209.97 ft), while keeping $\theta_{\ln(\varepsilon 50)}$ equal to 1.0 m (3.28 ft) and $\theta_{\ln(\gamma')}$ equal to 1.0 m (3.28 ft). Figure 3.4 shows the relationship between P_f and the unit shaft length as the correlation length of ε_{50} is varied from 2 m (6.56 ft) to 64 m (209.97 ft), while fixing both $\theta_{\ln(Su)}$ and $\theta_{\ln(\gamma')}$ at 1.0 m (3.28 ft). Similarly, Figure 3.5 shows the relationship between P_f and the unit shaft length as the correlation length of unit weight is varied from 2 m (6.56 ft) to 64 m (209.97 ft), while fixing both $\theta_{\ln(Su)}$ and $\theta_{\ln(\varepsilon 50)}$ at 1.0 m (3.28 ft). It can be seen from these three figures that P_f does not vary, regardless of the number of segments used in the *p-y* method. Therefore, the selection of the unit shaft length can be determined based on the computational algorithm of the *p-y* method rather than the LAS method. A unit shaft length on the order of 10% of the drilled shaft diameter can be conveniently selected for numerical computation. It can also be observed from these three figures that the computed probability of failure for various correlation lengths of ε_{50} and γ' is about the same. On the other hand, the computed probability of failure for different correlation lengths of undrained shear strength is significantly different. This finding highlights the importance of considering the correlation length of undrained shear strength in the reliability analysis.

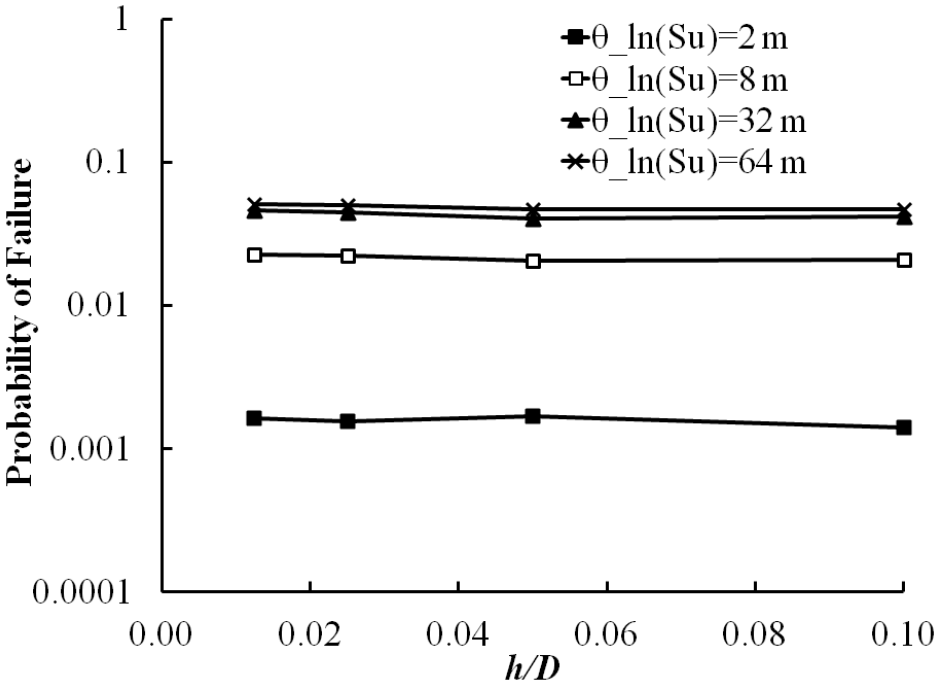

Figure 3.3 Influence of *h*/*D* for different values of $\theta_{ln(Su)}$

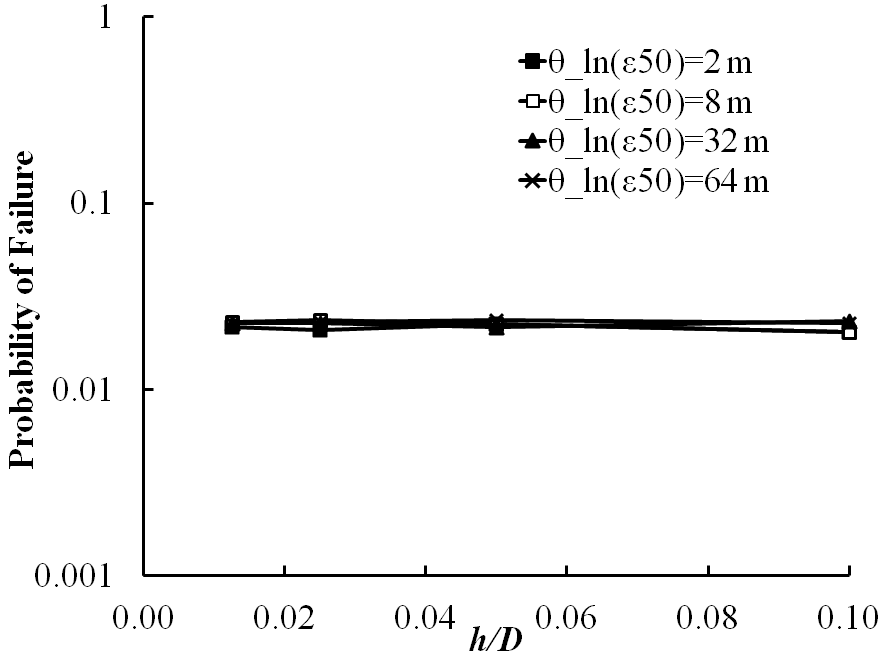

Figure 3.4 Influence of *h*/*D* for different values of $\theta_{ln(\varepsilon 50)}$

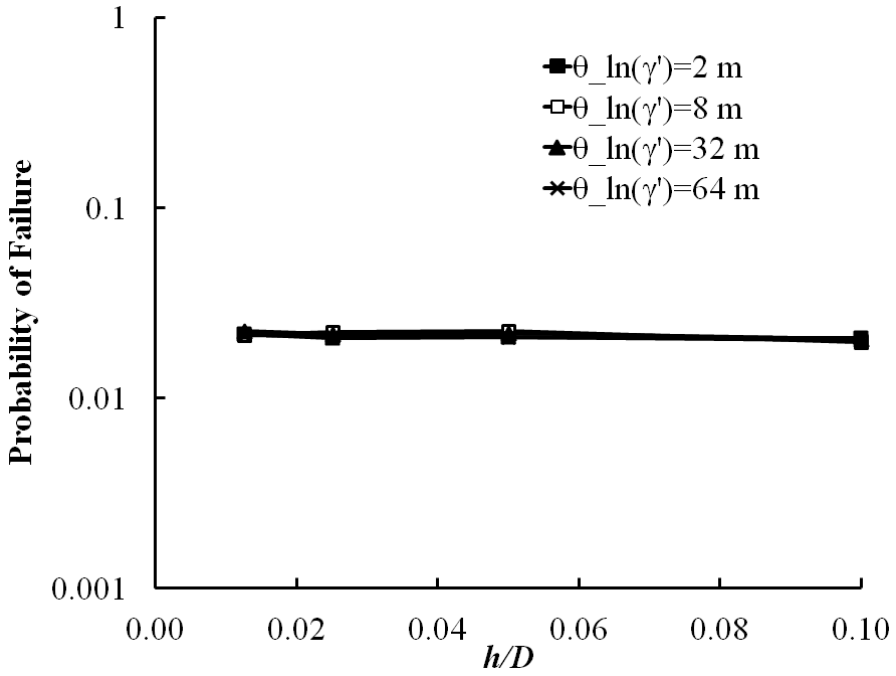

Figure 3.5 Influence of *h*/*D* for different values of $\theta_{\ln(\gamma')}$

(Note: 2 m =6.56 ft; 8 m = 26.25 m; 32 m = 104.99 ft; 64 m = 209.97 ft.)

3.6.2 Realizations of the Drilled Shaft Head Displacement

In this section, the influences of $\theta_{\ln(Su)}$ on the realization of the computed drilled shaft deflection are discussed. As mentioned earlier, the correlation length of undrained shear strength could exert significant influence on the computed probability of failure based on the specified performance criterion (i.e., 12.5 mm (0.5 in) lateral deflection at the top of the drilled shaft). Figure 3.6 shows the histograms of the drilled shaft-head deflection y_t for different correlation lengths of shear strength ranging from 0.1 m (0.33 ft) to 64 m (209.97 ft), while keeping the values of correlation length for both ε_{50} and γ' as 1.0 m (3.28 ft). The means and the standard deviations of y_t denoted as μ_{yt} and σ_{yt} are plotted in the histograms. It can be seen that the means and standard deviations of y_t are noticeably different for different correlation length of undrained shear strength. This finding indicates that the mean and the standard deviation of y_t are clearly sensitive to the spatial variability of shear strength. Figure 3.7 shows the convergence of the

computed P_f using Equation (3.4) for different values of $\theta_{ln(Su)}$. The estimated probabilities of failure for $\theta_{ln(Su)}$ of 2 m (6.56 ft), 8 m (26.25 ft), 32 m (104.99 ft), and 64 m (209.97 ft) are 0.0016, 0.022, 0.044, and 0.048, respectively. The COVs of these estimates range from 2% to 13%. It is evident that the computed probability of failure is highly dependent upon the correlation length of undrained shear strength. It can be concluded that the estimate of P_f could be biased, if the spatial variability (or correlation length) of undrained shear strength is ignored.

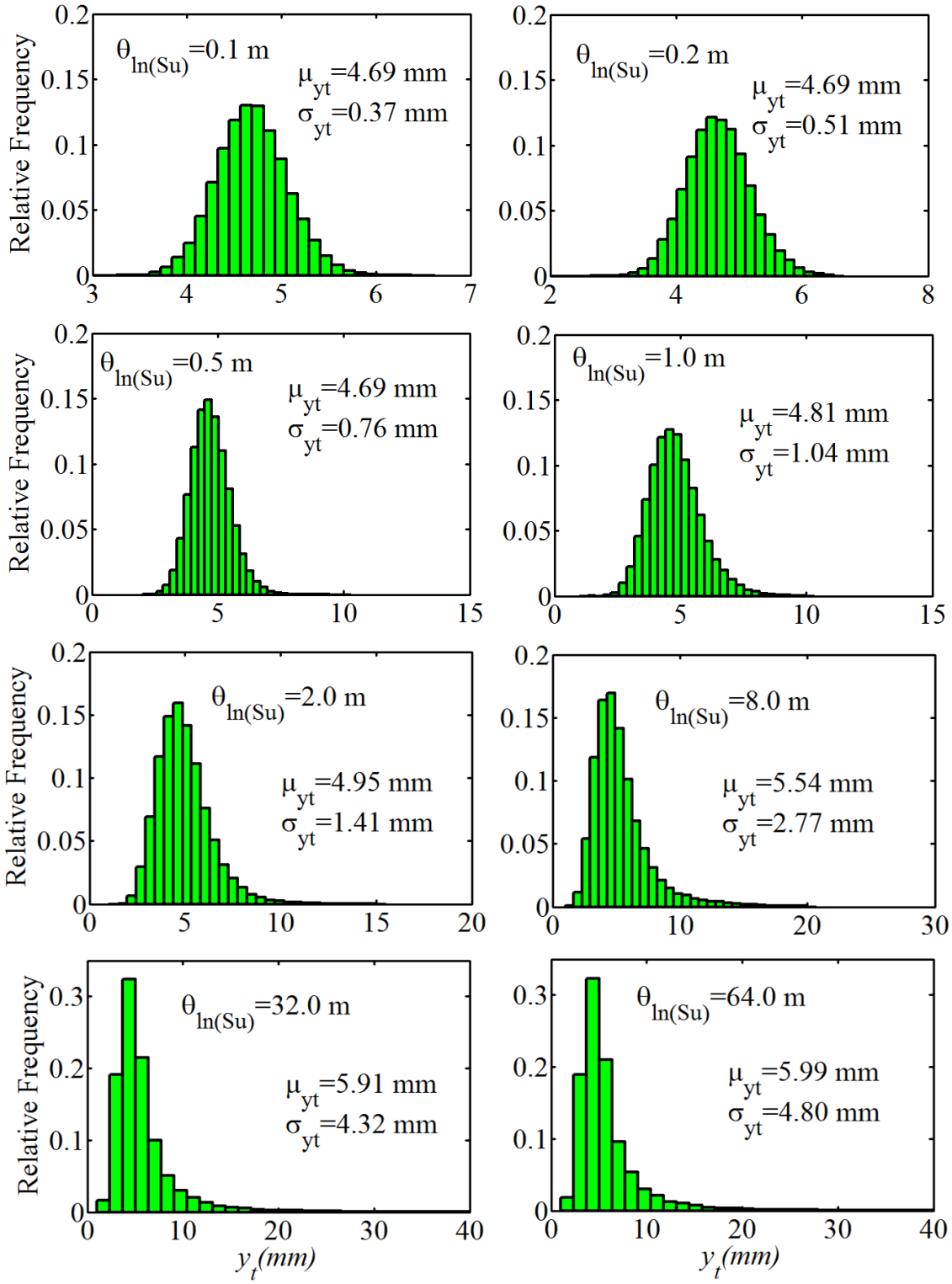

Figure 3.6 Realizations of the lateral deflection for different values of $\theta_{\ln(\gamma')}$

(Note: 1 mm = 0.0394 in and 1 m = 3.28 ft.)

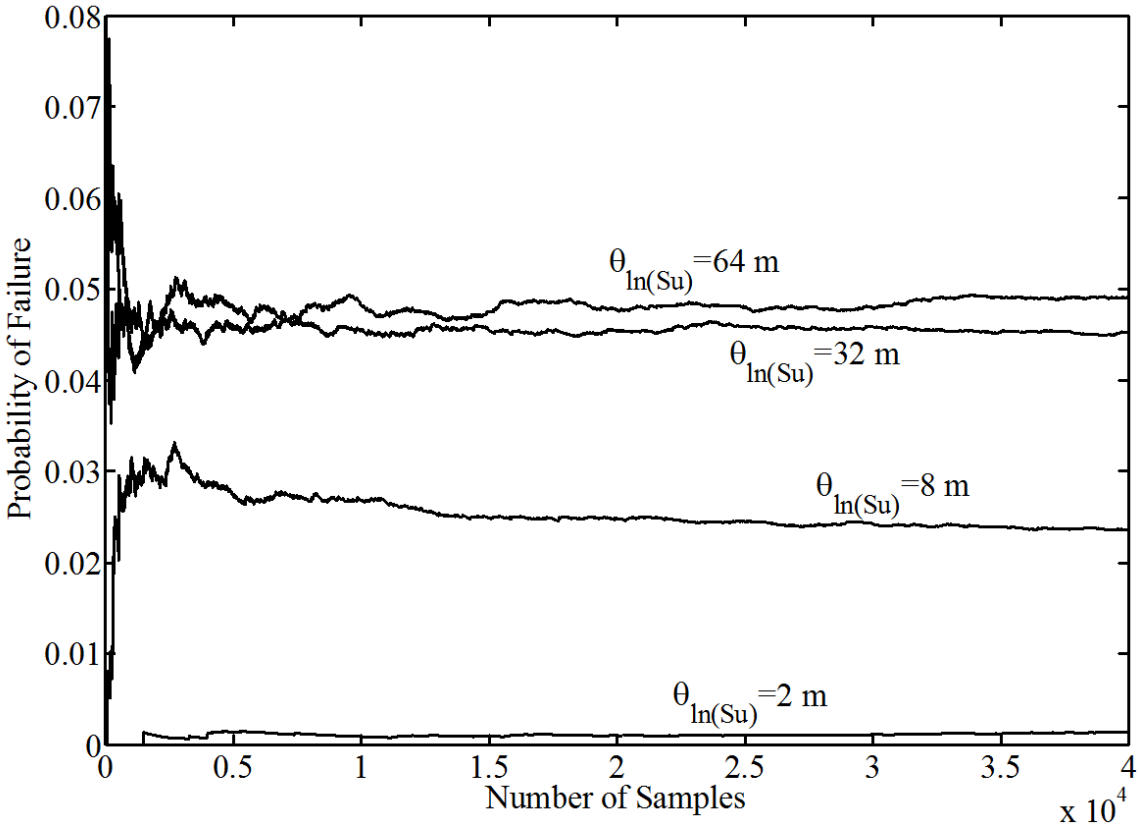

Figure 3.7 Convergence of the estimates

(Note: 2 m =6.56 ft; 8 m= 26.25 ft; 32 m = 104.99 ft; 64 m = 209.97 ft.)

3.6.3 Influence of Variability of Soil Properties

The variability of soil properties is characterized by COV and correlation length. The effects of varying COV and correlation length of the undrained shear strength for the design example are shown in Figure 3.8. In the sensitivity analysis, both $\theta_{\ln(\varepsilon 50)}$ and $\theta_{\ln(\gamma')}$ are set to 1.0 m (3.28 ft), while the COVs of ε_{50} and γ' are set to 20% and 4%, respectively. It can be seen that P_f increases with increasing COV of undrained shear strength. In addition, P_f varies significantly with different $\theta_{\ln(Su)}$.

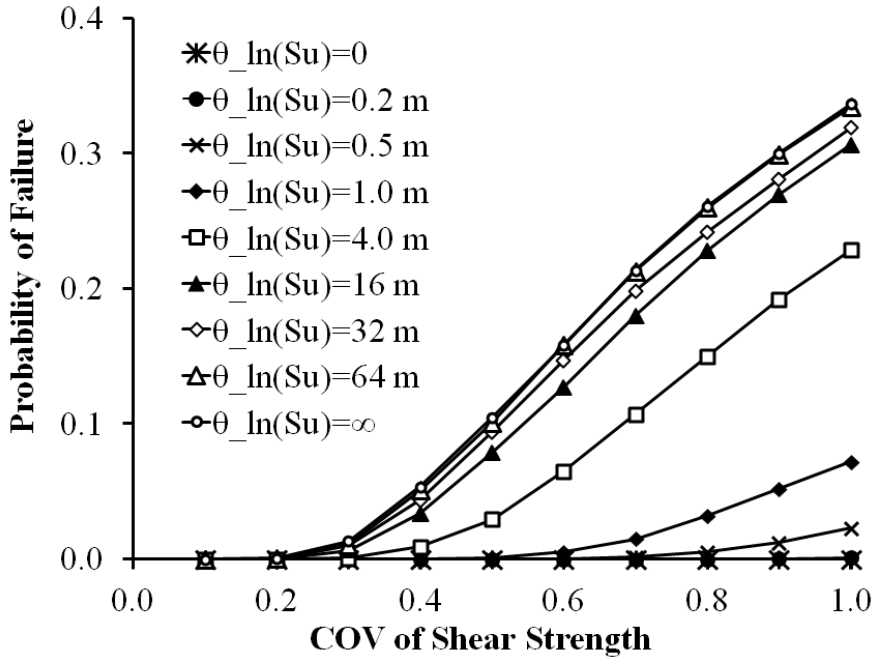

Figure 3.8 Influence of the spatial variability of S_u

(Note: 0.2 m =0.66 ft; 0.5 m = 1.64 ft; 1 m = 3.28 ft; 4 m = 13.12 ft; 8 m= 26.25 ft; 32 m = 104.99 ft; 64 m = 209.97 ft.)

The design outcome in the FHWA report is re-examined by means of the *P-LPILE* program, in which the effects of COV and correlation length of undrained shear strength are varied as shown in Table 3.1. The other relevant parameters are set as follows: both $\theta_{\ln(\varepsilon 50)}$ and $\theta_{\ln(\gamma')}$ are set to 1.0 m (3.28 ft), while the COV of ε_{50} and γ' are set to 20% and 4%, respectively. For the selected P_T =0.001, it can be seen that FHWA design may not be satisfactory for cases where the COV and correlation length of undrained shear strength are large. For example, if $\theta_{\ln(Su)}$ is equal to 1.0 m (3.28 ft) and the COV of undrained shear strength is equal to 60%, the foundation dimension is unsatisfactory.

Table 3.1 Design Performances under Various Assumptions

COV	$\theta_{ln(Su)}$ (m)								
	0	0.2	0.5	1	4	16	32	64	∞
0.1	S	S	S	S	S	S	S	S	S
0.2	S	S	S	S	S	S	S	S	S
0.3	S	S	S	S	S	U	U	U	U
0.4	S	S	S	S	U	U	U	U	U
0.5	S	S	S	S	U	U	U	U	U
0.6	S	S	S	U	U	U	U	U	U
0.7	S	S	U	U	U	U	U	U	U
0.8	S	S	U	U	U	U	U	U	U
0.9	S	S	U	U	U	U	U	U	U
1.0	S	U	U	U	U	U	U	U	U

Note: 1) COV is the coefficient of variation for the shear strength; and 2) "S" denotes a satisfactory design and "U" denotes an unsatisfactory design; 3) 0.2 m =0.66 ft; 0.5 m = 1.64 ft; 1 m = 3.28 ft; 4 m = 13.12 ft; 8 m= 26.25 ft; 32 m = 104.99 ft; 64 m = 209.97 ft.

3.6.4 Influence of Uncertainties of *p-y* Curves

For an illustration of the effects of COV of soil parameters, a baseline model of soil parameters pertinent to the design example is set as follows: the correlation lengths for all the soil parameters are set to 1.0 m (3.28 ft), and the COVs of S_u, ε_{50}, and γ' are set to be 40%, 20%, and 4%, respectively. The reinforcement ratio is assumed to be 1% of the sectional area with No. 11 rebars and a cover thickness of 7.62 cm (i.e., 3 inches) for evaluating *EI* in the *P-LPILE* computation. In this section, the effects of uncertainties of *p-y* curves are examined by assuming that the bias factor N_M follows a lognormal distribution with a mean value of 1.0 and standard deviation of 0.15. A mean of 1.0 implies that the *p-y* curve gives unbiased predictions of soil reaction. The assumed mean and standard deviation of N_M are for illustration purposes. Figure 3.9 shows the probabilities of failure computed by MCS considering the uncertainty of *p-y* curves as a solid line. The probabilities of failure for the baseline soil properties are also shown in the same graph as a dashed line. As can be seen that in order to achieve a P_T of 0.001, a drilled

shaft of L = 6 m (19.68 ft) and $D \geq$ 1.2 m (3.94 ft), or $L \geq$ 7 m (22.97 ft) and $D \geq$ 1.1 m (3.61 ft) would be sufficient for the baseline soil properties. However, if the uncertainty of the *p-y* curves is considered, the foundation dimensions for the feasible design would be L = 6 m (19.68 ft) and $D \geq$ 1.3 m (4.27 ft), or $L \geq$ 7 m (22.97 ft) and $D \geq$ 1.2 m (3.94 ft). Therefore, the uncertainties of *p-y* curves have resulted in a larger foundation dimensions for the same soil properties and design loads.

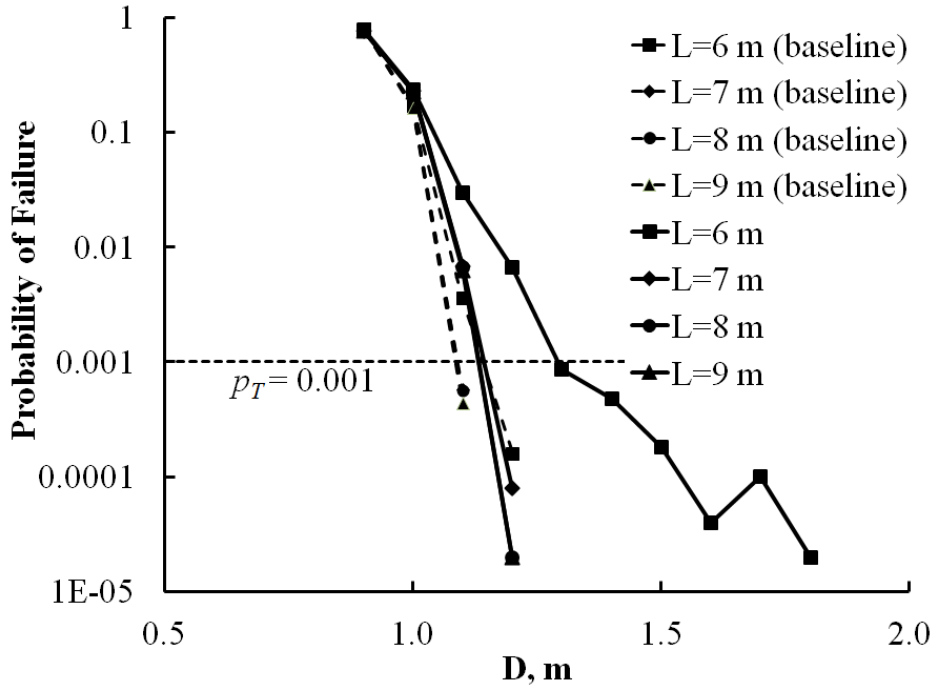

Figure 3.9 Influence of uncertain *p-y* curves

(Note: 1 m = 3.28 ft; 2 m = 6.56 ft; 6 m = 19.68 ft; 7 m 22.97 ft; 8 m = 26.25 m; 9 m = 29.53 ft.)

3.6.5 Influence of Uncertainties of Loads

As discussed previously, sustained live loads can be modeled as a gamma-distributed random variable. In this section, it is assumed that the shear force applied at top of the drilled shaft is a gamma-distributed variable with a mean of 111.2 kN (25 kips) and a COV of 30%. In addition, it was assumed that the bending moment at the top of the drilled shaft is proportional to

the shear force. The probabilities of failure computed by MCS for the assumed uncertain loads under the same soil conditions are shown in Figure 3.10, with the P_f values for the baseline soil properties depicted as a dashed line. It can be seen that the feasible foundation dimensions would be L = 6 m (19.69 ft) and $D \geq 2.1$ m (6.89 ft), L = 7 m (22.97 ft) and $D \geq 1.6$ m (5.25 ft), or $L \geq 8$ m (26.25 ft) and $D \geq 1.4$ m (4.59 ft). The feasible foundation sizes with the consideration of load uncertainty are larger than for those that do not consider the load uncertainties.

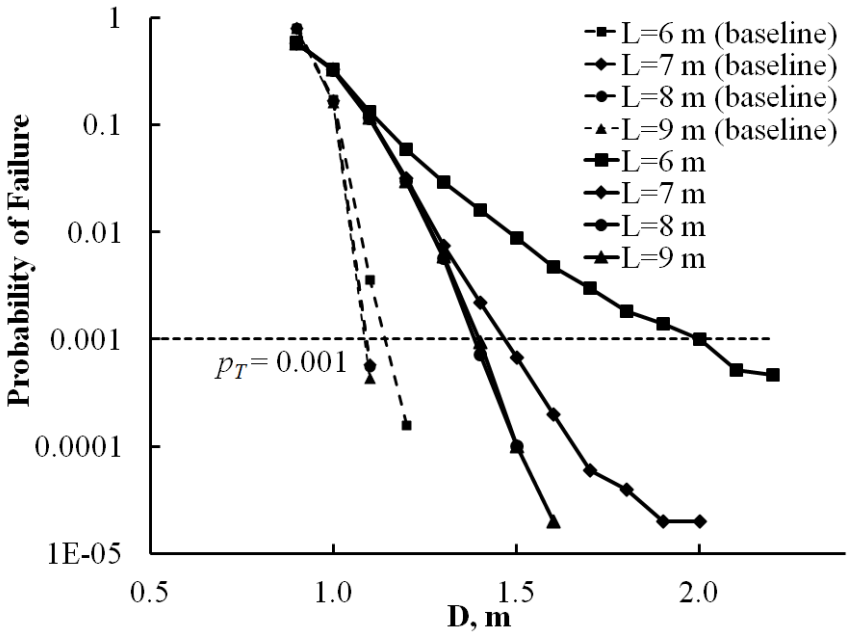

Figure 3.10 Influence of uncertain loads

(Note: 1 m = 3.28 ft; 2 m = 6.56 ft; 6 m = 19.68 ft; 7 m 22.97 ft; 8 m = 26.25 m; 9 m = 29.53 ft.)

3.6.6 Influence of Cross-correlation

A parametric study is conducted to investigate the influence of cross-correlation. In the parametric study, the COVs of S_u, ε_{50}, and γ' are set as 45%, 20%, and 4%, respectively. The correlation lengths of both ε_{50} and γ' are set at 1.0 m (3.28 ft), while $\theta_{\ln(Su)}$ is varied. It is believed that the cross-correlation between the unit weight and the undrained shear strength (ε_{50}) is largely minimal. Only the cross-correlation between undrained shear strength and ε_{50} is considered. The

Pearson linear correlation coefficient is used to measure the cross-correlation that is defined with respect to logarithms of both variables. Figure 3.11 shows the influence of the cross-correlation between S_u and ε_{50} for a drilled shaft with a 1.10-m (3.61 ft) diameter and 8.0-m (26.25 ft) length. It is clear that the probability of failure exhibits significant variation for different cross-correlations. This finding indicates that the cross-correlation should be considered in order to have an accurate evaluation for the failure probability.

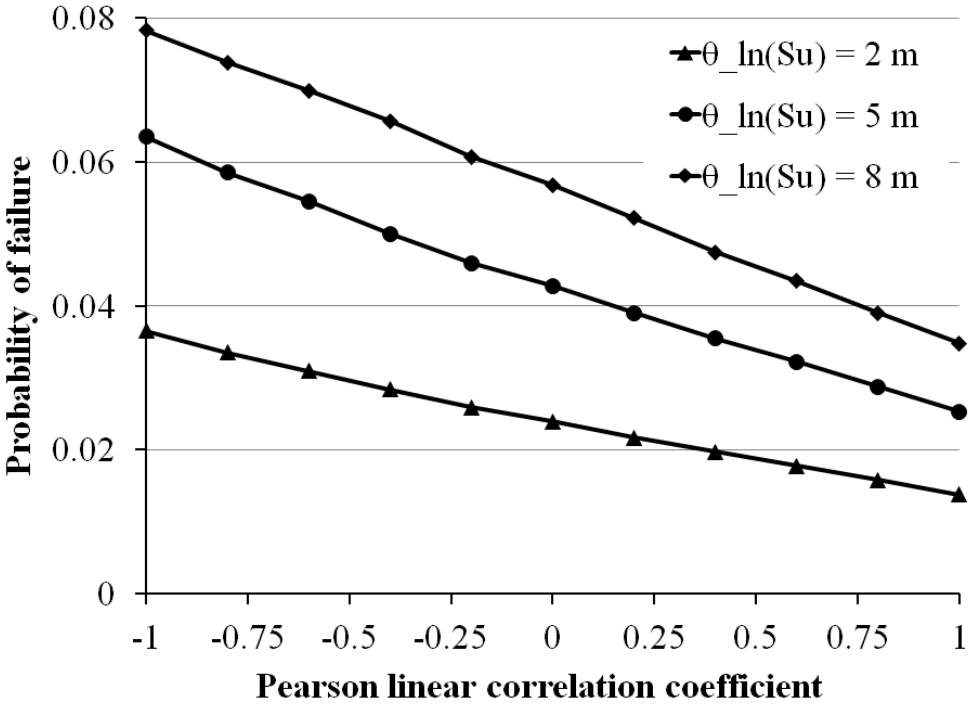

Figure 3.11 Influence of the cross-correlation

(Note: 2 m = 6.56 ft; 5 m = 16.40 m; 8 m = 26.25 m.)

3.7 Summary and Conclusions

In this chapter, a performance-based reliability method that considers the spatial variability of soil properties for a laterally loaded drilled shaft was presented. The spatial variability of soil properties is considered by using random field theories. The random field of a soil parameter is statistically characterized by the field mean, field variance, and the correlation structure. In

addition, uncertainties of the applied loads and the computational models can also be accounted for using Monte Carlo simulation according to the prescribed probability distributions. The performance criteria for the laterally loaded drilled shaft are stated in terms of the lateral deflection at the top of the pile. Failure, or unsatisfactory performance, is defined as the event that the pile-head deflection exceeds the allowable displacement. A computation program called *P-LPILE* was developed that incorporates the Monte Carlo simulation techniques and the *p-y* method for computing the reliability of the laterally loaded drilled shafts. Based on the numerical results presented in this research, the following conclusions can be made:

1. The spatial variability of soil properties, particularly the COV and correlation length of the undrained shear strength for cohesive soils, could exert significant influence on the computed probability of failure for the specified performance criteria. The difference in the computed probability of failure caused by different correlation lengths of S_u could be several orders of magnitude. Additionally, the cross-correlation between S_u and ε_{50} is critical in the evaluation of the failure probability. The failure probability would be biased if the cross-correlation is not considered.

2. Apart from soil spatial variability, the proposed approach provides a systematic procedure to consider uncertainties due to the computational model and applied loads. A random bias factor is introduced to account for the uncertainty of *p-y* curves. The estimated probability of failure increases if the uncertainty of the adopted *p-y* curves is considered. The uncertainty of loads is considered by sampling from their probability distributions and using the samples as input. The calculated probability of failure increases when the uncertainty of loads is considered.

3. The proposed approach is useful for conducting reliability analysis to check the serviceability limit in the current LRFD framework. Based on the conducted parametric studies, the reliability for the serviceability limit design of a laterally loaded pile is sensitive to the spatial correlation of soil properties, soil variability, and the uncertainty of *p-y* curves and loads.

4. The proposed approach is very versatile, as it allows practicing engineers to input the means, variances, and probability distributions of the load model; site-specific soil properties; and the bias factor for the *p-y* curves. Furthermore, engineers can specify the target reliability index according to the intended functions of the structures under consideration.

CHAPTER 4. AXIALLY LOADED PILES

4.1 Introduction

The objective of this chapter is to present a fundamentally sound and robust performance-based design method for drilled shafts subjected to axial loads. In the performance based design framework, the input of soil properties in the computational model and the model error are treated as random variables. Monte Carlo simulation techniques are used to generate a large number of random samples according to the prescribed probability distributions. Next, the response of a drilled shaft to random input is evaluated repeatedly using the deterministic computational models per sample trial. The performance-based acceptance criteria are specified in terms of the allowable drilled shaft settlement. The computation of the load-settlement curve of an axially loaded drilled shaft is carried out using the load transfer curves specified in the current AASHTO guidelines (AASHTO 2010) and a computer code *P-TZPILE* developed recently by the authors. Failure is said to occur if the settlement of the shaft head exceeds the allowable limit. The probability of failure P_f is computed as the ratio of the number of unsatisfactory results to the total number of samples. In the context of performance-based design, the basic design parameters such as drilled shaft diameter D and length L can be adjusted to achieve the desired reliability level to meet the needs of a particular project. Two design examples are given to illustrate the application of the Monte Carlo simulation algorithms for the design of an axially loaded drilled shaft. The proposed method not only addresses the current shortcoming of the LRFD for the service limit check, but it also offers the following advantages: 1) it is conceptually simple and gives an unbiased estimate of the probability of failure; 2) it is a

true reliability-based design that explicitly accounts for the uncertainties arising from the input of computational models and model errors; 3) it can explicitly account for the spatial variance of soil properties; 4) it is a sampling-based and robust process; and 5) it is project-based, since site-specific information is used in the reliability analysis.

4.2 Performance-Based Design

It is anticipated that in the future, many code-writing organizations will make a transition towards performance-based design codes (Nowak and Collins 2000). In the context of performance-based design (PBD), the design objectives are defined in terms of the allowable or tolerable displacement of the foundation structures under the design loads. There are several advantages of using performance-based design. In the traditional design methodologies, the strength limit state or the ultimate limit state is checked to assure the summation of the load effects does not exceed the summation of the resistance. However, the interpretation of nominal resistance can be problematic due to various criteria being suggested for interpreting nominal resistance from the load settlement curve obtained from the load test (Roberts and Misra 2010). The use of a performance-based design approach can remove the ambiguity in interpreting nominal resistance from the load-settlement curve obtained from actual load tests. In traditional design methodologies, in addition to checking the ultimate limit state or the strength limit state, the service limit state is also checked to assure the functionality of the structure. Indeed, only one of the limit states governs the design. If excessive displacement is induced on the structure, the structure either fails due to the overstress on the materials or is not able to serve the desired function in a satisfactory manner. Therefore, the adoption of a performance-based design methodology could eliminate the need to check for both strength limits and service limits.

In the probability-based design approaches, the safety of a system is defined in terms of the probability of failure (Nowak and Collins 2000). For axially loaded drilled shafts, the performance-based design approach uses the performance criteria stated in terms of the drilled shaft head settlement. Failure is said to occur when the drilled shaft head settlement exceeds the specified allowable limit. Then, the probability of failure P_f can be defined as follows:

$$P_f = P(y_t \geq y_a) = \int_F f(\boldsymbol{x})\, d\boldsymbol{x} = \int I[y_t \geq y_a] \cdot f(\boldsymbol{x})\, d\boldsymbol{x} \tag{4.1}$$

where y_t is the drilled shaft head settlement, y_a is the allowable settlement, F is the failure region, $I[\cdot]$ is the indicator function, $\boldsymbol{x}$ is a vector of variables, and $f(\boldsymbol{x})$ is a joint probability density function. The indicator function in Equation (4.1) is equal to 1.0 if y_t is equal to or greater than y_a; otherwise, it is zero.

4.3 Framework of Reliability-Based Design

In the context of the axially loaded drilled shafts, the reliability analysis simply becomes an evaluation of the integral expressed in Equation (4.1). In general, it is preferable to evaluate it analytically. However, it is quite difficult to evaluate this integral directly for the following reasons: 1) $f(\boldsymbol{x})$ is a multivariate function for input $\boldsymbol{x}$ which may be correlated or of high dimensions; 2) it is difficult to determine the failure region (i.e., F), in particular in the context of the implicit solution involving nonlinear soil-foundation interaction analysis, where an iteration is involved for force equilibrium and strain compatibility and no analytic equation exists that can predict the load-displacement curve of a drilled shaft under axial loading. Therefore, the Monte Carlo integration technique (Robert and Casella 2004) is a realistic alternative to evaluate the integral.

4.3.1 Monte Carlo Simulation

Monte Carlo simulation (MCS) is a standard statistical method in which the response of a complex system is calculated repeatedly using a sequence of the generated random samples as inputs (e.g., Ang and Tang 1984; Fenton and Griffiths 2008). More details on Monte Carlo statistical method can be found elsewhere (e.g., Robert and Casella 2004; Fishman 1996). In MCS, a large number of random field samples are generated, and each set of samples is used as input to the developed *P-TZPILE* computer program. Next, the settlement of a drilled shaft subjected to axial loads is computed repeatedly until a desired or prescribed sample size is achieved. With the performance criteria defined (i.e., the allowable drilled shaft head settlement), it is possible to determine whether or not failure will occur. The Monte Carlo approach for evaluating the probability of failure, based on the performance criterion, is expressed as follows:

$$P_f = \frac{1}{n}\sum_{i=1}^{n} I_i\left[y_t \geq y_a\right] \tag{4.2}$$

where n is the number of samples. By the law of large numbers, the estimation for P_f expressed in Equation (4.2) converges to the exact value as $n \rightarrow inf$ with the probability of 1.0. There are several advantages of using the Monte Carlo statistical method: 1) the Monte Carlo method gives an unbiased estimate of the probability of failure; 2) the accuracy of the estimate increases with increasing n; and 3) the method is conceptually and mathematically simple. The accuracy of the estimate can be evaluated by its coefficient of variation (COV), which can be estimated by the following equation:

$$\delta\left(P_f\right) \approx \sqrt{\frac{1}{n\left(n-1\right)\cdot P_f}\sum_{i=1}^{n}\left(I_i\left[y_t \geq y_a\right] - P_f\right)^2} \tag{4.3}$$

Figure 4.1 shows the flow chart for the performance-based design framework. The purpose of the design procedure is to find out feasible combinations of basic design parameters (i.e.,

diameter D and length L) of a drilled shaft that can provide the target reliability for the specified performance criteria. It starts with characterizations of the probability distributions of the input for the computational model. In the next step, the basic design parameters and a sample size are assumed. To guarantee convergence of the P_f estimate in Equation (4.2), the sample size has to be sufficiently large. With the assumed foundation dimensions, the response of the foundation to random input is calculated repeatedly using a different set of randomly-generated samples as input. If uncertainties of load effects can be characterized probabilistically, the load effects could also be simulated in the same fashion as the resistance in the proposed framework. The probability of failure can be evaluated with Equation (4.2) using the resulting output from the repetitive calculations. The process is executed iteratively by adjusting the foundation dimensions until the calculated probability of failure is equal to or smaller than the target probability of failure.

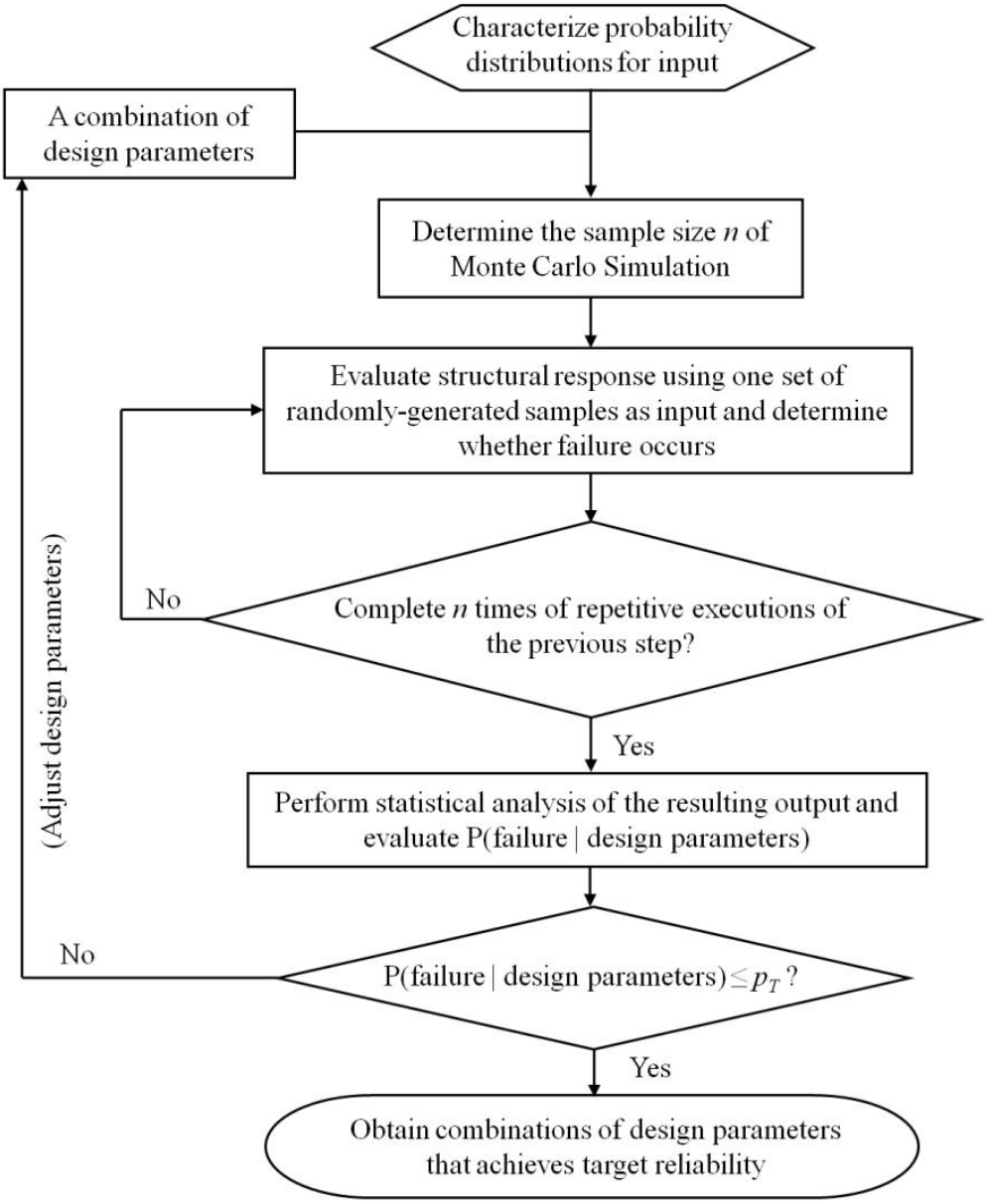

Figure 4.1 Flow chart of Performance-Based Reliability Design

The determination of the target reliability is not an easy task. It involves determination of the consequence of failure, the construction costs, the design life, and so on. A number of factors such as economic issues, societal effects, and existing technical levels of computational models

may have to be considered simultaneously to determine the appropriate target probability of failure. Previous research (e.g., Phoon et al. 1995) indicates that a reliability index of 3.2 (i.e., P_f = 6.8714 $\times 10^{-4}$) is appropriate for ultimate limit state and 2.6 (i.e., P_f = 0.0047) for the service limit state. It is noted that most civil engineering systems have a target probability of failure between 1/1000 and 1/100,000 (Fenton and Griffiths 2008). In this research, for the purpose of illustration, a target probability of failure of 1/1000 is adopted.

4.3.2 Uncertainties of Soil Properties

Soil properties are needed as inputs to evaluate the load-displacement behavior. As a result, the variations in the soil properties can directly influence the calculated displacement. Therefore, it is important to recognize the presence of the underlying uncertainties or risk during the design process, and it is necessary to quantify the variability of inputs in the reliability-based design. In this research, soil properties are modeled as random fields to account for the spatial variability. The detailed discussion of random field modeling and the random field generation can be found in Chapter 2.

4.3.3 Uncertainties of Model Error

Model error or bias is defined as the ratio of the measured to the estimated, namely:

$$b = \frac{Y_m}{Y_e} \tag{4.4}$$

where Y_m denotes the measured value and Y_e denotes the estimated value. In most cases, the computational models used to represent the reality do not produce a bias of 1.0 due to the simplifications and the imperfect knowledge regarding the soil-foundation interaction. For the axially loaded drilled shaft, the underlying assumption is that the soil–drilled shaft interaction behavior is known and could be modeled using the load-transfer curves. In the past, a number of

t-z and *q-w* criteria have been developed. However, these criteria are simply idealizations of the soil behavior. Therefore, it is not surprising that these criteria contain uncertainties to some degree, and there is an ongoing need to quantify the uncertainties involved in these existing load transfer criteria. The available literature (e.g., Phoon and Kulhawy 2005; Kung et al. 2007) indicates that the model error could be modeled as a normally or lognormally distributed variable. In this study, the probability distribution of the model error is assumed to be lognormal, although other distributions could also be used.

4.4 Design Example: A Drilled Shaft Subjected to Uplift Loads

The drilled shaft in the example was designed using LRFD in a report by Phoon et al. (1995). The boundary conditions of the drilled shaft and the statistical properties of shear strength of the soils are taken from the report and are shown in Figure 4.2. The uplift force of 400 kN (89.92 kips) applied at the top of the shaft is the same as the one in the published report, so the load effects are treated the same. The performance criterion is specified using the allowable vertical displacement of 25 mm (1 in)at the top of the drilled shaft. The structural section of the reinforced concrete shaft has a steel ratio of 1%. The elastic modulus of concrete is taken as 26.60 GPa (3857 ksi) and that of steel is 200.00 GPa (29,000 ksi); both of these values are typical. A typical value of 24 kN/m^3 (149.76 pcf) is used for the unit weight of reinforced concrete. With these material properties, *EA*, the stiffness of the structural section of the drilled shaft is 3.204×10^7 kPa·m^2 (7.198×10^9 psf·ft^2). Furthermore, the material properties of the drilled shaft are treated as deterministic since the focus of this example is on the uncertainties of soil properties. The undrained shear strength of the cohesive soils is modeled as a lognormal variable whose mean is constant along the depth. Since the standard deviation and the correlation length are not provided in the cited original report, these two parameters are therefore varied

within a typical range in the parametric study. Also, it should be noted that the ultimate unit shaft resistance of the load-transfer curves is calculated based on the alpha method outlined in the AASHTO guidelines (AASHTO 2010).

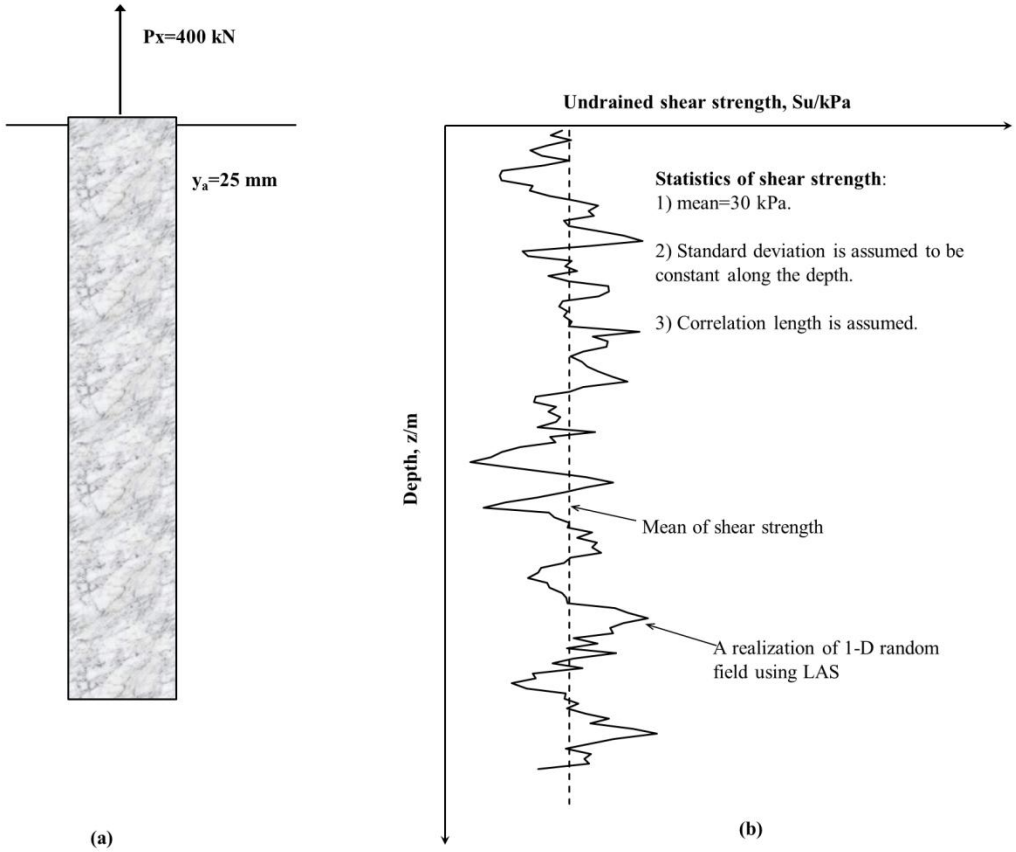

Figure 4.2 Drilled shaft in uplift

(Note: 400 KN = 89.92 kips; 30 KPa = 4.35 psi; 1 KPa = 0.145 psi.)

It should be noted that the resistance factors given in the report were calibrated using a first order reliability method for a computational model that is different from the one in either the AASHTO guidelines or the load transfer method developed in this research. The computational model for predicting the load-displacement relationship of the drilled shaft head in the report was assumed to follow the hyperbolic equation, in which the curve fitting parameters are determined by fitting to the test results of a number of load tests. Furthermore, the contribution from the toe

of drilled shaft is taken into account in the report, but it is ignored in the present model due to the uplift mode of loading. Therefore, it should be noted that even for the same soil profile and soil properties, the predicted load-displacement curves of a drilled shaft would be different for the two deterministic computational methods adopted in the report and this research. The comparisons presented in this research should be viewed from the perspective of the effects caused by the consideration of soil uncertainties and spatial correlations.

According to Phoon et al. (1995), if the COV of the undrained shear strength ranges from 10% to 30%, a drilled shaft with a 1.20-m (3.94 ft) diameter and 6.60-m (21.65 ft) length can achieve a reliability index of 3.2 (i.e., P_f = 0.0006814) for the strength limit state and 2.6 (i.e., P_f = 0.0047) for the service limit state. This foundation dimension is used for examination using the developed PBRD methodology and the accompanied computational algorithms. Since LAS is employed in the current study to construct random fields for soil parameters, it is important to investigate the influence of the local averaging process at the cell level on the computed probability of failure. Suppose the length of each shaft segment chosen for the *t-z* curve analysis (denoted as *h*) is also the chosen dimension of the local averaging process. In the local averaging process, the variance reduction of a local average would increase with the increasing dimension of the local averaging process. In other words, the variance of a local average would diminish as the size of the local averaging process increases. For the foundation dimension mentioned, the drilled shaft is discretized into 100, 50, 30, 15, 10, and 6 segments in different cases, and the corresponding *h/D* ratios are 0.06, 0.11, 0.18, 0.37, 0.55, and 0.92, respectively. The computed probability of failure is shown in Figure 4.3 for various correlation lengths. It can be seen that for each correlation length, the probability of failure is invariant with respect to *h/D*. It is concluded that the probability of failure is sensitive to the correlation length but insensitive to the

normalized cell size in LAS. Based on this parametric study, the number of increments used in the design example is taken as 30. The adopted use of the shaft segment size in the discretization process of the drilled shaft in the numerical algorithm would be acceptable, as it does not affect the outcome of the computed probability of failure. Figure 4.4 shows examples of the computed load-settlement curves using the developed computer program for a case with an assumed COV of the shear strength of 30% and an assumed correlation length of 4.0 m (13.12 ft).

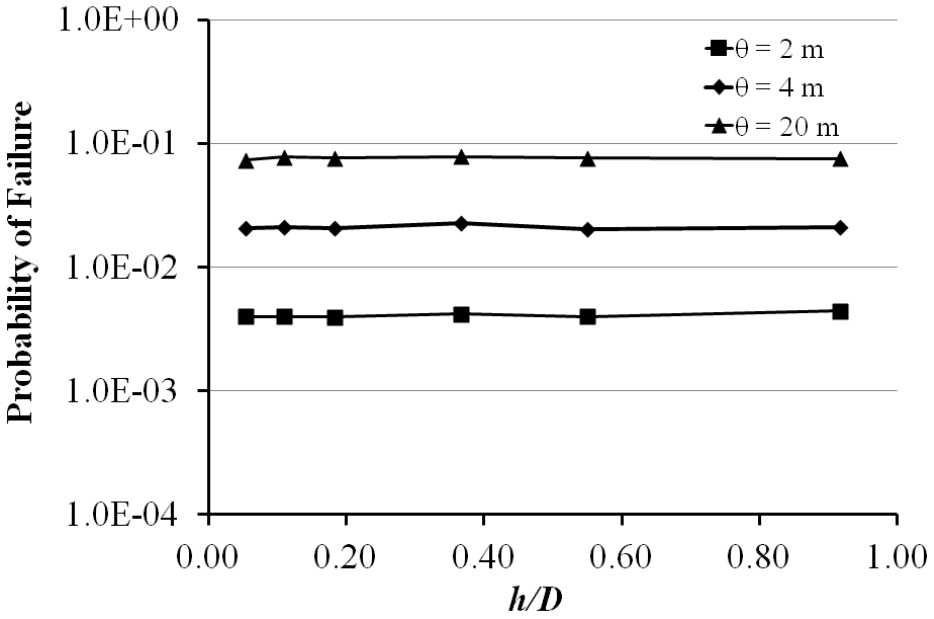

Figure 4.3 Relationship between P_f and the normalized size of local averaging process

(Note: 2 m = 6.56 ft; 4 m = 13.12 ft; 20 m = 65.62 ft.)

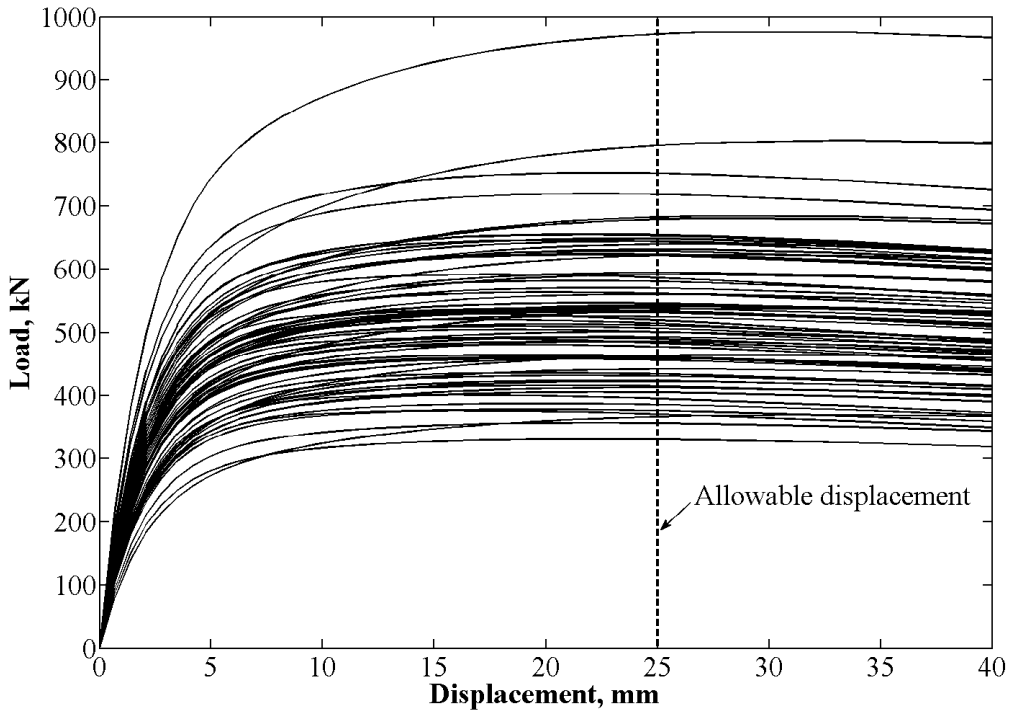

Figure 4.4 Uncertainty of the load-displacement curves

(Note: 25 mm = 1 in; 40 mm = 1.57 inch; 100 KN = 22.48 kips; 400 KN = 89.92 kips; 1000 KN = 224.8 kips.)

The effects of uncertainties of the load transfer curves are investigated by a series of parametric studies in which the model errors for different *t-z* curves along the shaft are assumed to be independent of each other but have a mean of 1.0. In addition, it is further assumed that model errors will follow a lognormal distribution. The parametric results shown in Figure 4.5 indicate that the computed probability of failure increases as the COV of the model error increases, indicating that the use of more accurate *t-z* criteria would give more confidence in the design. The effects of the variance and the correlation length of shear strength on the computed probability of failure are also investigated in a parametric study. If the variance of shear strength is large, then it implies that the shear strength is highly uncertain. Furthermore, as the correlation length increases, the generated random field tends to be more uniform. Figure 4.6 shows the

relationship between the probability of failure and the correlation length. It can be seen that there is a significant variation of P_f due to the variation of the correlation length. Additionally, P_f increases significantly as the variance of shear strength increases. Hence, from this example, applying a single value of the calibrated resistance factors in the foundation design could be problematic, as it cannot achieve a uniform level of safety.

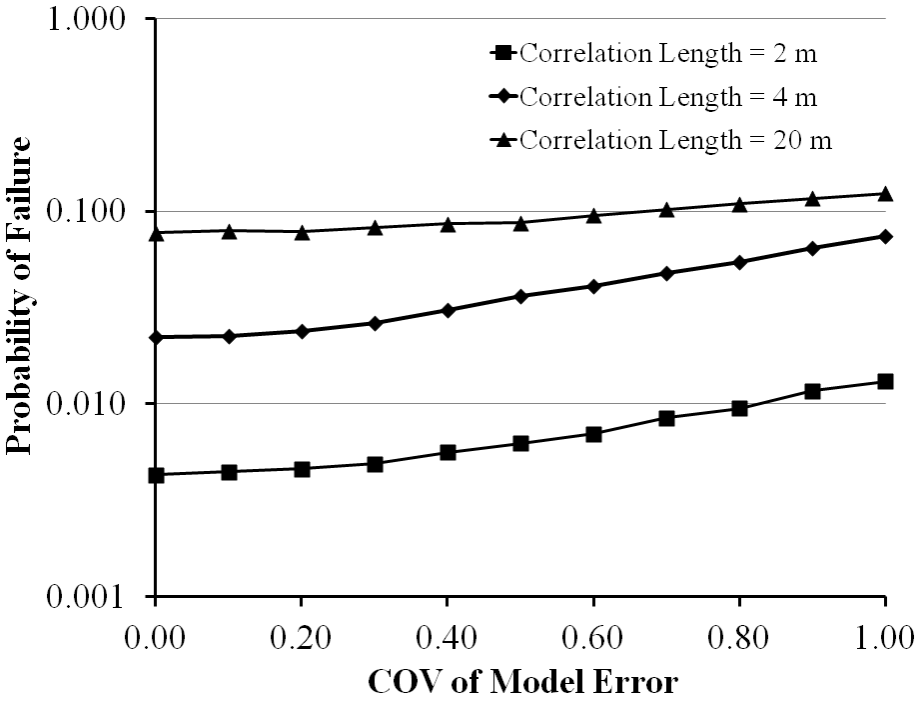

Figure 4.5 Relationship between P_f and the uncertainty of *t-z* criteria

(Note: 2 m =6.56 ft; 4 m = 13.12 ft; 20 m = 65.62 ft.)

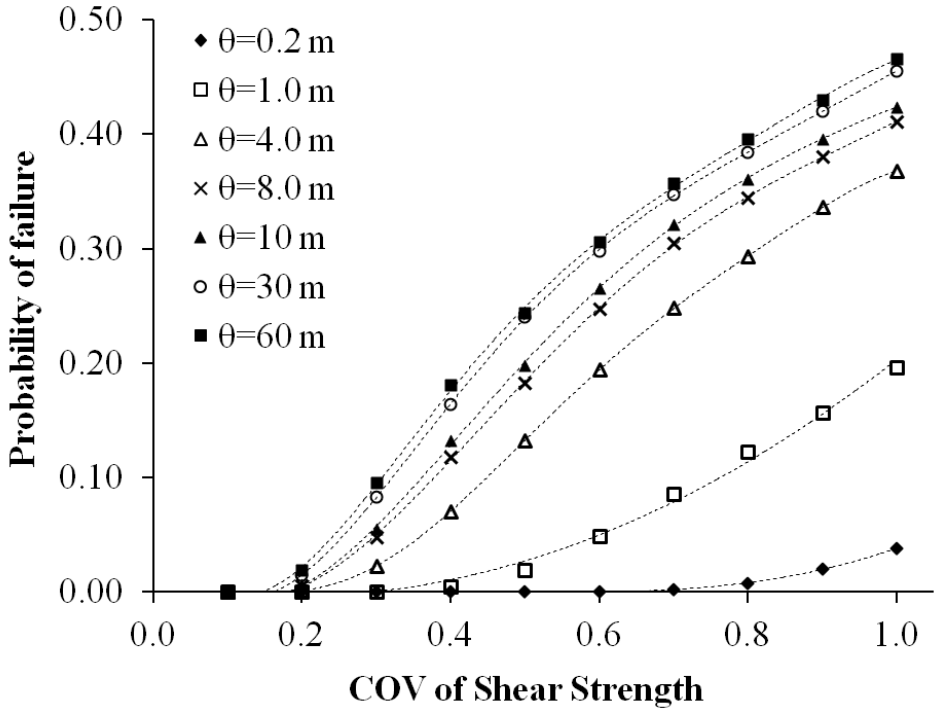

Figure 4.6 Relationship between P_f and correlation length

(Note: 0.2 m = 0.66 ft; 1 m = 3.28 ft; 4 m = 13.12 ft; 8 m =26.25 ft; 10 m = 32.81 ft; 30 m = 98.43 ft; 60 m = 196.85 ft.)

The proposed sampling-based reliability methodology is compared with the previous LRFD based design outcome (i.e., D = 1.20 m (3.94 ft) and L = 6.60 m (21.65 ft)) for different design assumptions in which the COV and the correlation length of the strength are varied. Because the proposed methodology adopts a performance-based approach, only the service limit state design is compared. Nevertheless, if the strength limit state is defined by the ultimate or limiting settlement, then the strength limit could also be checked. Table 4.1 tabulates the performance of the design for different assumed COV values and correlation lengths of undrained shear strength. As can be seen from this table, if the correlation length is assumed to be 0.20 m (0.66 ft), the foundation dimension is satisfactory but is overly conservative for the COV range of 10% to 30%. In fact, the foundation dimension is still satisfactory even when the

COV of the shear strength is equal to 70%. However, if the correlation length is assumed to be 8.0 m (26.25 ft), the foundation dimension is satisfactory for a COV of 10% but unsatisfactory for a COV of 20% or greater.

The performance of the aforementioned design outcome for two special cases (i.e., $\theta = 0$ and $\theta = \infty$) were also tabulated. If the correlation length is equal to zero, then the random field becomes an infinite sequence of independent and identically distributed random variables. In this case, the variance of a local average for any finite averaging dimension is equal to zero, which means a random field based analysis become a deterministic analysis. For θ equal to 0, it can be observed from Table 4.1 that the design outcome is satisfactory even when the COV of shear strength is equal to 100%. At the other end of the scale, the correlation length is equal to infinity. In this case, the random field is perfectly correlated, meaning that the random variables for a stationary and perfectly correlated random field are identical. For θ equal to ∞, it can be observed from Table 4.1 that the design outcome is satisfactory when the COV of shear strength is equal to 10%, but it becomes unsatisfactory if the COV of shear strength is equal to or greater than 20%. There may be a number of reasons for the observed differences between the design outcomes given by these two approaches when various assumptions are made regarding the COV and correlation length. First of all, the deterministic computational models for predicting the load-displacement relationships are obviously different between these two approaches. In addition, the correlation structures of soil parameters were not included in the calibration of resistance factors in the report by Phoon et al. (1995).

Table 4.1 Performances of the design for different assumptions

COV	Correlation Length (m)								
	0	0.2	1	4	8	10	30	60	∞
0.1	S	S	S	S	S	S	S	S	S
0.2	S	S	S	S	U	U	U	U	U
0.3	S	S	S	U	U	U	U	U	U
0.4	S	S	S	U	U	U	U	U	U
0.5	S	S	U	U	U	U	U	U	U
0.6	S	S	U	U	U	U	U	U	U
0.7	S	S	U	U	U	U	U	U	U
0.8	S	U	U	U	U	U	U	U	U
0.9	S	U	U	U	U	U	U	U	U
1.0	S	U	U	U	U	U	U	U	U

Note: 1) COV is the coefficient of variance for the shear strength, "S" denotes a satisfactory design and "U" denotes an unsatisfactory design; 2) 0.2 m = 0.66 ft; 1 m =3.28 ft; 4 m= 13.12 ft; 8 m = 26.25 ft; 10 m = 32.8 ft; 30 m = 98.43 ft; 60 m = 196.85 ft.)

If the correlation structure is ignored and only the mean and variance are used to characterize the uncertainty of a spatially variable soil parameter, it implies that the soil parameter is either perfectly correlated or uncorrelated in space. If a soil parameter is perfectly correlated in space, then its correlation length must be infinite. In the case of infinite correlation length, the shear strength is constant along the depth. That is to say, in each simulation a single value of shear strength is generated and assigned to each segment in order to construct the load transfer curves, which clearly simplifies the calculation. If we suppose the COV of shear strength is 30%, the P_f estimate for the case of infinite correlation length will be obtained as shown in Figure 4.7. The final estimate for P_f is 0.1013 with a COV of 2.11%. For comparison purposes, the P_f estimate for θ = 30,000 m (98425.2 ft) by using the developed computer program is also presented in Figure 4.7. A correlation length of 30,000 m (98425.2 ft) is assumed here, mainly because it is so long that it may be deemed infinite when compared with the shaft dimension (6.60 m (21.65 ft) in length and 1.20 m (3.94 ft) in diameter). The corresponding P_f estimate is

0.1015 with a COV of 2.10%. It is clear that the results obtained by the two simulation approaches agree very well.

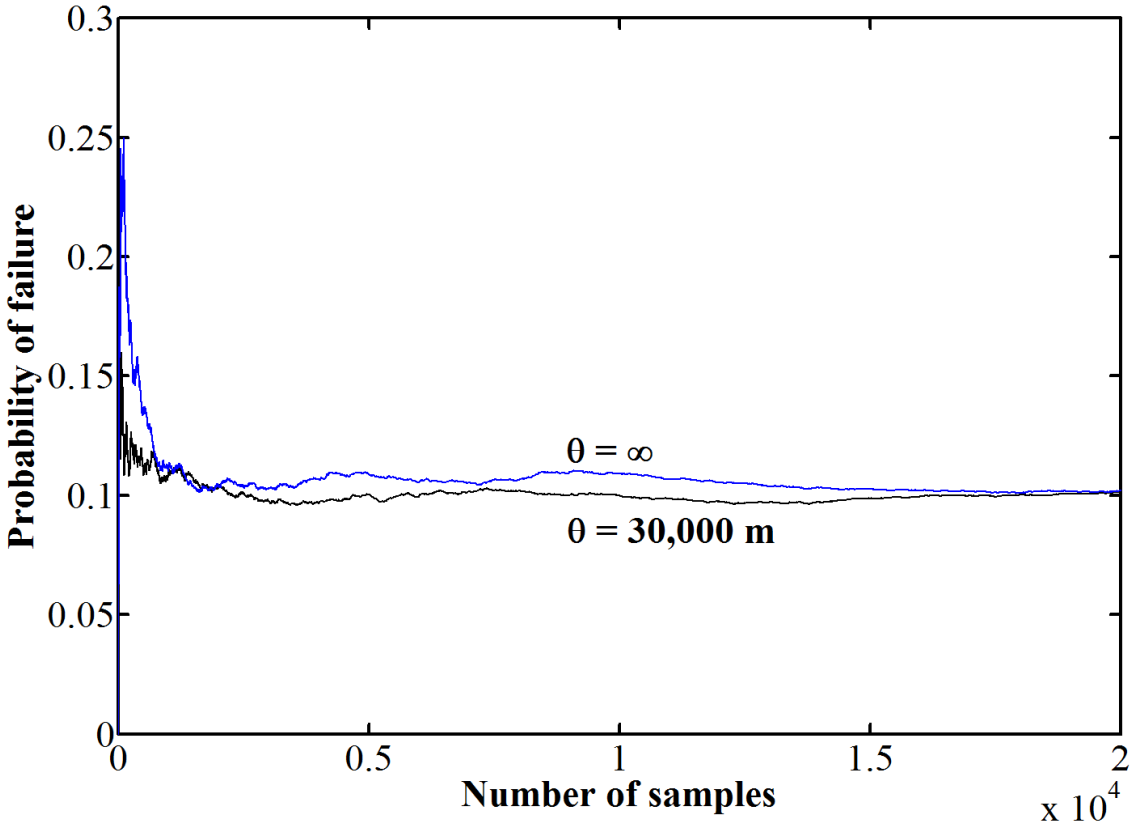

Figure 4.7 Convergence of P_f estimates based on simplified MCS and *P-TZPILE*

(Note: 30,000 m = 98425.2 ft.)

In contrast, if the soil parameter is uncorrelated in space, then the correlation length has to be equal to zero. Again suppose that the COV of shear strength is 30% for a lognormal variable with zero correlation length; its median of 28.73 kPa (4.16 psi) is assigned to each segment as the shear strength. A deterministic analysis was conducted and the uplift capacity was determined to be 499.0093 kN (112.18 kips) based on the allowable displacement. For comparison purposes, a random field–based analysis was conducted for this case with a θ equal to 1.0×10^{-7} m (3.28×10^{-7} ft). Correlation length of 1.0×10^{-7} m (3.28×10^{-7} ft) is assumed here,

mainly because it is so short that it may be deemed to be zero, when compared with the shaft dimension. Using the developed computer program, samples of the uplift capacity can be obtained based on the allowable displacement. The mean of the samples is 499.0092 kN (112.18 kips) and the COV of the samples is 0.0023%. Note that the sample size is 20,000 and the resolution of the numerical results should be reasonably good. It is very clear that the results based on deterministic analysis and those based on random field theory agree quite well. Indeed, soil parameters are usually correlated to some degree and the correlation between two points will typically decrease as the separation distance increases. Therefore, as demonstrated in this example, the estimated probability of failure based on this simplification of correlation structure would easily become biased or inaccurate. It is illustrated in this example that the use of the calibrated resistance factors may not achieve the target reliability level, especially when the spatial variability of the strength parameter is not taken into account in the calibration.

As can be seen from Table 4.1, the LRFD based design outcome could be unsatisfactory for some design assumptions. If the correlation length of shear strength is 1.0 m (3.28 ft) and the COV of shear strength is 50%, the design outcome is unable to achieve the prescribed reliability level (i.e., P_T = 0.0047) based on the proposed methodology. To increase the reliability level, either the diameter or the length should be increased. Figure 4.8 shows that the probability of failure decreases as the shaft length increases. It also indicates that the probability of failure decreases with an increase in the shaft diameter. The target probability of failure is also shown in the dashed line. It can be found from Figure 4.8 that a feasible design can be a drilled shaft with D = 1.40 m (4.59 ft) and $L \geq$ 5.60 m (18.37 ft), D = 1.30 m (4.27 ft) and $L \geq$ 6.20 m (20.34 ft), or D = 1.20 m (3.94 ft) and $L \geq$ 7.00 m (22.97 ft). If the target probability of failure is specified as 0.001, a feasible design could be a drilled shaft with D = 1.40 m (4.59 ft) and $L \geq$ 5.80 m (19.03

ft), D = 1.30 m (4.27 ft) and $L \geq$ 6.60 m (21.65 ft), or D = 1.20 m (3.94 ft) and $L \geq$ 7.20 m (23.62 ft). Likewise, the feasible designs for other prescribed reliability levels can be found conveniently from this figure. Among the feasible designs, one can find the optimal design with consideration of the economic constraints (e.g., Wang et al. 2011).

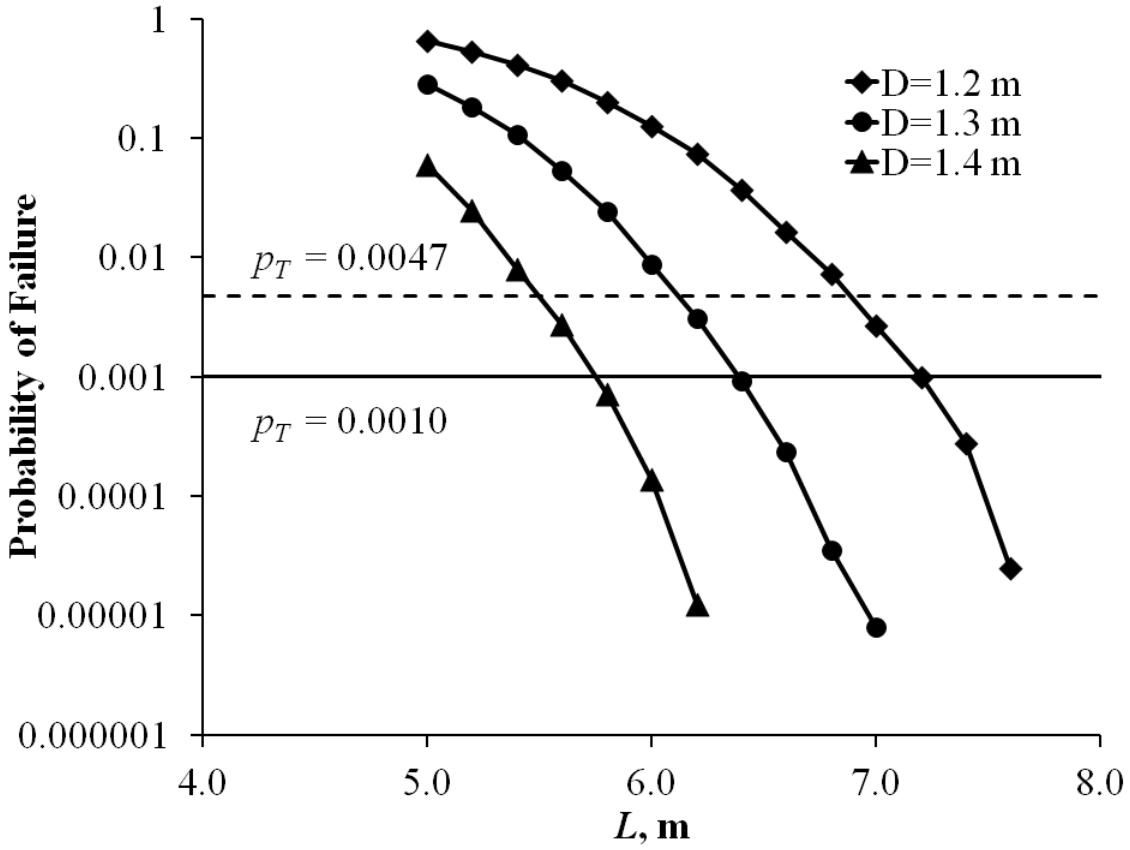

Figure 4.8 Probabilities of failure for different designs

(Note: 1.2 m = 3.94 ft; 1.3 m 4.27 ft; 1.4 m = 4.59 ft; 5 m =16.4 ft; 6 m= 19.68 ft; 7 m = 22.97 ft; 8 m = 26.25 ft.)

4.5 Design Example: A Drilled Shaft Subjected to Compression

Consider the example drilled shaft shown in Figure 4.9. The compressive force applied at the top of the shaft is 600 kN (134.88 kips) and is assumed to be deterministic. The limiting vertical displacement is assumed to be 25 mm (1 in). Failure is said to occur if the shaft head

displacement exceeds 25 mm (1 in). The section of the reinforced concrete shaft has a steel ratio of 1%. The compressive strength of concrete is given as 31027.5 kPa (4.5 ksi), and a typical value of 200 GPa (29,000 ksi) is used for the elastic modulus of steel. A typical value of 24 kN/m^3 (149.76 pcf) is used for the unit weight of reinforced concrete and is assumed to be deterministic. The undrained shear strength of cohesive soils is modeled as a lognormal variable with a standard deviation of 30 kPa (4.35 psi). The mean of the shear strength is constant at the top three meters and then increases linearly with depth (see Figure 4.9). Indeed, it is not unusual for the soil properties to vary with depth. The shear strength of clay along the depth is modeled as one-dimensional (1-D) random fields, which are generated using LAS. The aforementioned values are used as inputs in the developed computer program. The alpha method outlined in AASHTO (2010) is used to calculate the ultimate load transfer of the load-transfer curves. For illustration purposes, the normalized load-transfer curves shown in Figure 2.3 are assumed to be certain, and they are employed to predict the load-settlement curves.

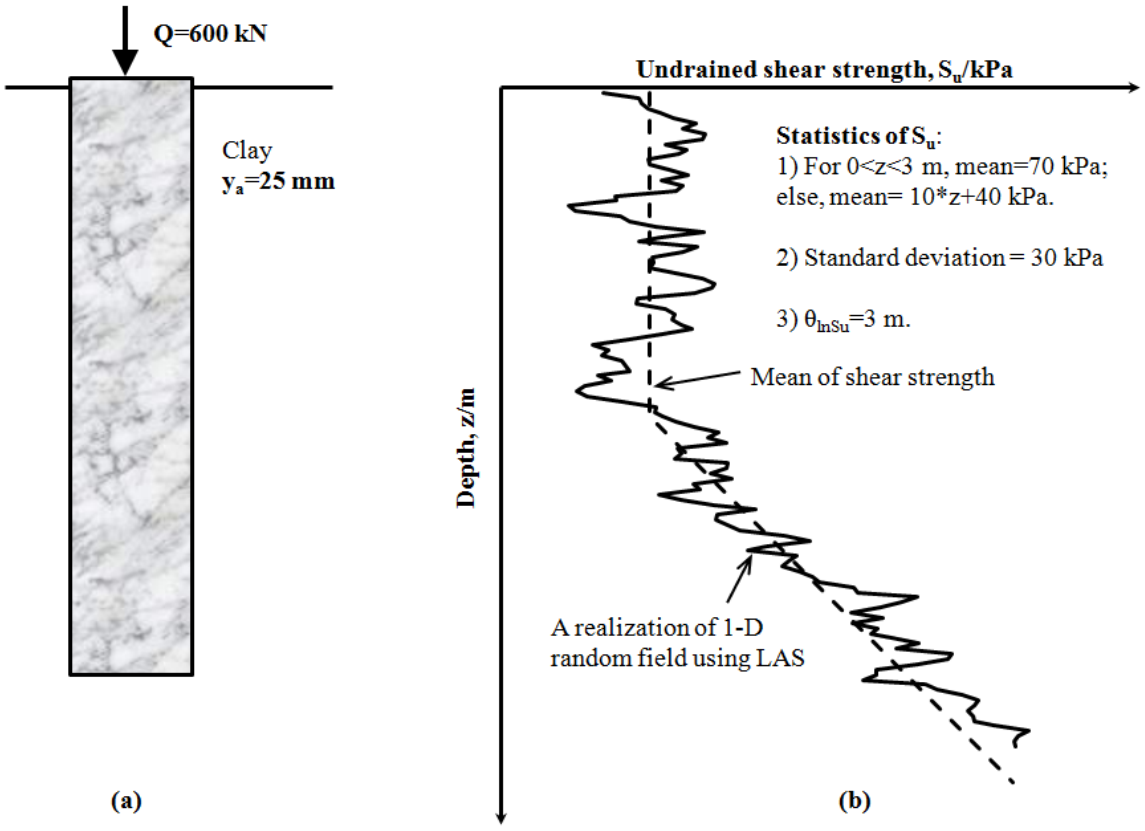

Figure 4.9 Drilled shaft in compression

(Note: 600 KN = 134.88 kips; 25 mm = 1 in; 3 m = 9.84 ft; 70 KPa = 10.15 psi; 30 KPa = 4.35 psi.)

Figure 4.10 shows partial examples of randomly-generated load-settlement curves for a drilled shaft that is 1.2 m (3.94 ft) in diameter and 6.6 m (21.65 ft) in length using the *P-TZPILE* program, which incorporates the load-transfer method. Using the performance-based design approach, the nominal resistance provided by the side friction and end bearing is determined to be the load that corresponds to the allowable settlement (i.e., y_a = 25 mm (1 in)) and it can be used to determine if failure will occur by comparing the resistance corresponding to the allowable displacement with the applied load. For the first trial, the shaft diameter and

penetration length are assumed to be 1.4 m (4.59 ft) and 4.0 m (13.12 ft), respectively. A sample size of 10,000 is used to ensure convergence of the P_f estimate.

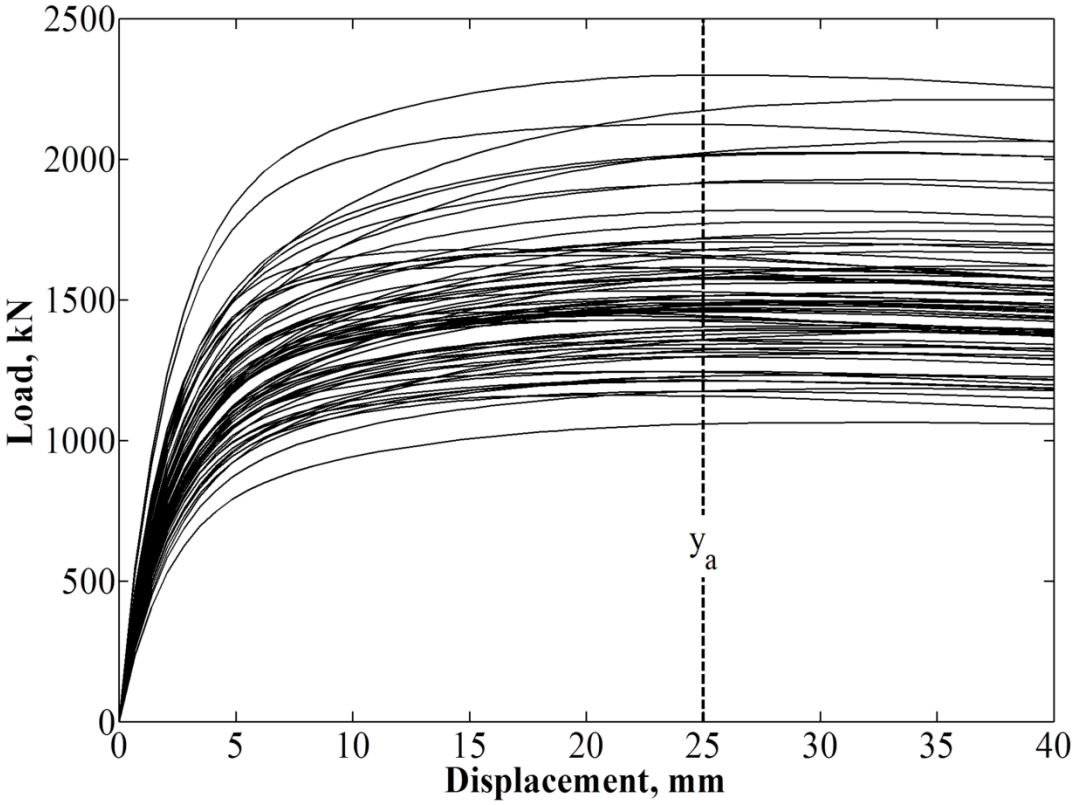

Figure 4.10 Uncertainty of the load-settlement curves

Figure 4.11 shows the convergence of the P_f estimate for different correlation lengths. It can be observed that the P_f estimate converges as the number of samples increases. The computation for a sample size of 10,000 takes an average of 2.76 seconds, using an i7-2600 processor (3.40 GHz). Thus, Monte Carlo method is quite attractive in the reliability analysis for axially loaded piles. In addition, it can be seen that the probability of failure exhibits significant variation as the correlation length of undrained shear strength increases. Here for illustration purpose, the correlation length is assumed to be 3.0 m (9.84 ft). For this correlation length, P_f is 5.89% with a COV of 4.00%. To achieve a P_T of 1/1000, other shaft dimensions are tried and the

results are summarized in Table 4.2. From the tabulated results, it can be seen that drilled shafts with D = 1.20 m (3.94 ft) and $L \geq$ 6.00 m (19.68 ft), or D = 1.40 m (4.59 ft) and $L \geq$ 5.40 m (17.72 ft) would meet the specified performance criteria. It is noted that other feasible designs (i.e., combinations of D and L) should be checked as well for choosing final optimal design.

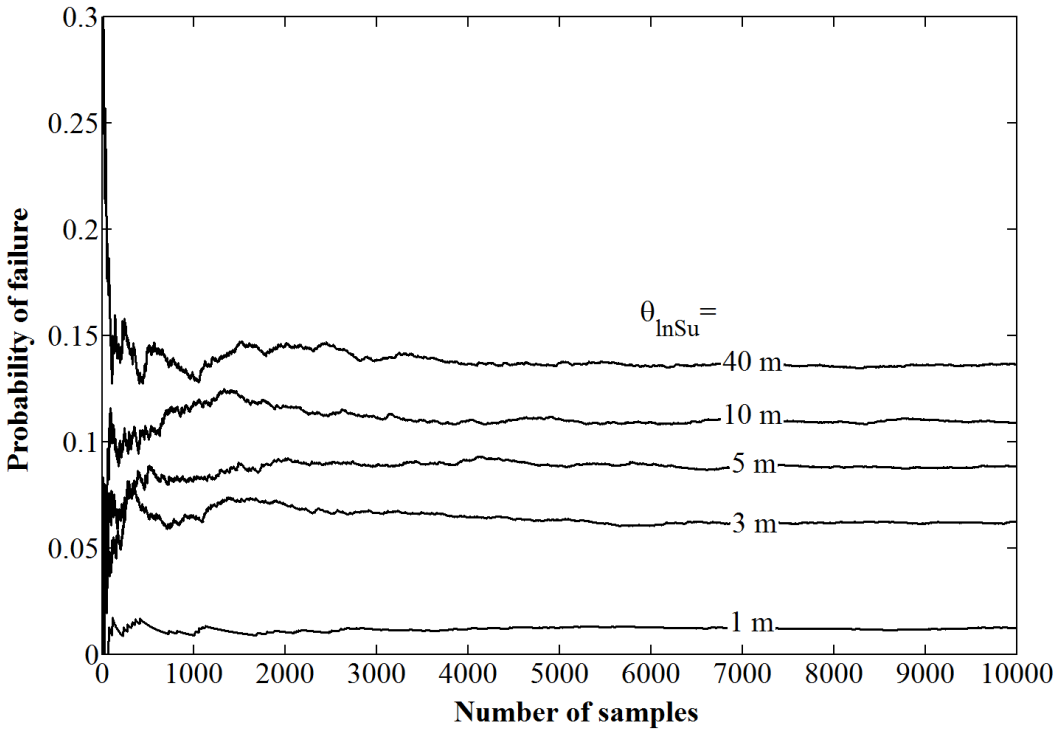

Figure 4.11 Convergence of P_f estimates by MCS

(Note: 1 m = 3.28 ft; 3 m = 9.84 ft; 5 m = 16.40 ft; 10 m = 32.81 ft; 40 m = 131.23 ft.)

Table 4.2 Probabilities of Failure obtained by MCS

L (m)	D = 1.2 m			D = 1.4 m		
	P_f	n	COV(P_f)	P_f	n	COV(P_f)
4.0	1.64E-01	10000	2.26%	5.89E-02	10000	4.00%
4.2	1.24E-01	10000	2.65%	4.12E-02	10000	4.82%
4.4	9.05E-02	10000	3.17%	2.45E-02	10000	6.31%
4.6	6.45E-02	10000	3.81%	1.49E-02	10000	8.13%
4.8	4.20E-02	10000	4.78%	7.60E-03	10000	11.43%
5.0	2.42E-02	10000	6.35%	3.00E-03	10000	18.23%
5.2	1.64E-02	10000	7.74%	1.50E-03	10000	25.80%
5.4	7.20E-03	10000	11.74%	5.67E-04	30000	24.25%
5.6	3.60E-03	10000	16.64%	3.67E-04	30000	30.15%
5.8	1.90E-03	20000	16.21%	3.33E-05	30000	100.00%
6.0	5.50E-04	20000	30.14%	3.33E-05	30000	100.00%

Note: 1) n is the sample size for MCS; 2) COV(P_f) is the coefficient of variation for P_f; 3) 1.2 m = 3.94 ft; 1.4 m = 4.59 ft; 4 m = 13.12 ft; 5 m = 16.40 ft; 6 m = 19.69 ft.

4.6 Summary and Conclusions

A performance-based design computational method based on Monte Carlo statistical methods was presented in this chapter for the analysis and design of a drilled shaft subjected to axial loads. In the proposed framework, the uncertainties arising from the input (e.g., the undrained shear strength for cohesive soils) for the computational model and the model error (i.e., the error of *t-z* and *q-w* criteria) were treated as random variables. In particular, the spatial variance of soil properties is explicitly accounted for by using random field modeling. The local averaging subdivision technique was used to generate a large number of random samples according to the statistical descriptors including mean, variance, probability distribution function, and correlation length. The generated samples are used as input to evaluate the axial displacement of the drilled shaft under the applied axial loads. The probability of failure determined on the basis of the specified performance criteria (i.e., the allowable drilled shaft head movement) can be computed accordingly. The performance-based design involves

adjusting the design parameters (i.e., the diameter and length of the drilled shaft) until the calculated probability of failure is equal to or smaller than the target probability of failure. A computer program called *P-TZPILE*, which uses the traditional load transfer concepts involving nonlinear *t-z* and *q-w* curves, was developed to implement the proposed methodology for the reliability analysis of an axially loaded drilled shaft.

Two design examples were presented in this chapter to illustrate the application of the developed method. The examples demonstrated that the probabilistic approaches that do not take into consideration the spatial variance of soil properties may potentially result in a foundation design that would not meet the performance criteria with the target reliability. There is a strong incentive to use a reliability-based method that considers the correlation structure of soil properties for deep foundations.

CHAPTER 5. ANALYSIS OF SYSTEM RELIABILITY

5.1 Introduction

In the LRFD approach LRFD, different limit states are considered separately and no system reliability is taken into account. Therefore, it is desirable to develop a probabilistic approach to tackle the uncertainties in the reliability-based design to address those issues described earlier. In this chapter, the serviceability performance of drilled shafts under combined lateral and axial loading is investigated using reliability analysis. Note that the terms "pile" and "drilled shaft" will be used interchangeably in this report.

Drilled shafts are widely used to resist axial and lateral loads. Under the loading, a drilled shaft typically has three distinctive displacements: lateral deflection (δ), angular distortion (ψ), and axial movement (w) at the top of the shaft. The performance of the pile is defined in terms of these displacements. To conduct reliability analysis for each limit state and assess the system reliability, Monte Carlo simulation (MCS) is applied. Since there are various sources of uncertainties involved in the reliability analysis, importance analysis is conducted in order to identify the sources of uncertainties that will significantly affect the serviceability performance.

5.2 Reliability Assessment

The failure (or unsatisfactory performance) event in this study is said to occur if the induced displacements at the top of the pile are greater than the corresponding allowable displacements. System failure in this study is defined as the event in which any of the individual

failure modes occurs. Following the conventional notation in structural reliability theory (Ditlevsen and Madsen 1996), probability of system failure, P_f, can be expressed by

$$P_f = P\left(\bigcup_k g_k\left[C_k, D_k\left(\mathbf{x}\right)\right] \le 0\right) \tag{5.1}$$

where the subscript k represents a serviceability failure mode (i.e., $k = \delta$, ψ and w), $g_k(\cdot)$ refers to the k-th limit state function, C_k represents the allowable displacement, D_k is the induced displacement due to the external loads, and $\mathbf{x} = (\mathbf{x}_r, \mathbf{x}_d)$ refer to the input variables (e.g., geometry and material properties) in which $\mathbf{x}_r$ are random variables and $\mathbf{x}_d$ are deterministic variables. In this study, the limit state function for the k-th failure mode is defined as

$$g_k = C_k - D_k\left(\mathbf{x}\right) \tag{5.2}$$

Using the probability of failure for the k-th limit state ($P_{f,k}$), the corresponding reliability index, β_k, can be determined by

$$\beta_k = -\Phi^{-1}\left(P_{f,k}\right) = \Phi^{-1}\left(1 - P_{f,k}\right) \tag{5.3}$$

where $\Phi^{-1}(\cdot)$ is the inverse of the cumulative distribution function of the standard normal variable.

In this study, the induced displacement D_k is obtained through the analysis of drilled shafts subjected to axial and lateral loading where the load transfer methods—for example, the *t-z* model proposed by Coyle and Reese (1966) and the *p-y* method proposed by Reese (1977)—are applied to model the nonlinear soil-pile interactions. The *t*-z model can be used to calculate the vertical movement where the axial soil-pile interaction is modeled as *t-z* curves and *q-w* curves, in which *t* and *q* represent side shear on the shaft and the tip resistance at the toe, respectively, and *z* and *w* represent the vertical displacements of the shaft segment and the toe of the drilled

shaft, respectively. The *p-y* method can be used to calculate the lateral deflection and the angular distortion where the lateral soil-pile interaction is modeled as *p-y* curves, in which *p* represents the soil reaction and *y* represents the lateral deflection. The schematic diagrams of the *p-y* method for lateral loads and the *t-z* model for axial loads and are shown in Figure 2.1 and Figure 2.2, respectively.

The reliability can be assessed using MCS method so as to simulate various sources of prevailing uncertainties. In MCS, the probability of failure for the *k*-th failure mode, $P_{f,k}$, is written as

$$P_{f,k} = \int I\left[g_k \le 0\right] f\left(\mathbf{x}_r\right) d\mathbf{x}_r \approx \frac{1}{n}\sum_{i=1}^{n} I_i\left[g_k \le 0\right] \tag{5.4}$$

where $I[\cdot]$ is an indicator function, $f(\cdot)$ is the joint probability density function of $\mathbf{x}_r$, and n is the number of samples. As $n \rightarrow inf$, the estimator in Equation (5.4) approaches its exact value. The advantage of using MCS is that it is mathematically simple and provides unbiased estimation. Furthermore, the accuracy of the probability estimate by MCS is not affected by the shape of the failure surface.

5.3 Importance Measure

There are a number of random variables entering the limit state functions. The variations of some random variables would cause significant variations in the reliability index β of the designed drilled shaft, while the variations of other random variables only produce minimal variations in β. The former are classified as important while the latter are classified as less important or unimportant. It is instructive to identify the random variables that have maximum influences on the performance reliability so that practicing engineers can pay more attention to the random variables that are the most critical.

The importance measure can be used to identify the importance of random variables. According to Der Kiureghian and Ke (1995), an importance measure $\boldsymbol{\kappa}$ is defined as follows

$$\boldsymbol{\kappa}^T = \frac{\boldsymbol{\alpha}^T \mathbf{J}_{u^*,x^*} \mathbf{B}}{\left\| \boldsymbol{\alpha}^T \mathbf{J}_{u^*,x^*} \mathbf{B} \right\|} \tag{5.5a}$$

$$\boldsymbol{\alpha} = -\frac{\nabla G(\mathbf{u})}{\left\| \nabla G(\mathbf{u}) \right\|} \tag{5.5b}$$

$$\boldsymbol{\Sigma} = \mathbf{J}_{x^*,u^*} \mathbf{J}^T_{x^*,u^*} \tag{5.5c}$$

where $G(\mathbf{u}) = g(\mathbf{x}(\mathbf{u}))$, $\nabla G(\mathbf{u})$is the gradient vector evaluated at the design point $\mathbf{x_r}^*$ in the standard normal space $\mathbf{u}$, $\mathbf{J}_{\mathbf{u}^*,\mathbf{x}^*}$ is the Jacobian matrix of the probability transformation from the original space $\mathbf{x}_r$ to the standard normal space $\mathbf{u}$ with respect to the design point and is equal to the inverse of $\mathbf{J}_{x^*,u^*}$, the superscript "*T*" denotes transpose, $\mathbf{B}$ is a diagonal matrix consisting of the standard deviations of equivalent normal variables $\mathbf{x'_r}$ that can be calculated with respect to the design point, $\sum$ is the covariance matrix of $\mathbf{x_r}$. If a random variable is not normally distributed, it has to be transformed to an equivalent normal variable according to its distribution type, mean, and variance.

5.4 Random Variables

In this study, there are a number of sources of uncertainty. These sources include soil variability; the variability of concrete and reinforcement material properties; the model errors in *p-y* curves, *t-z* curves, and *q-w* curves; the uncertainty in the performance criteria; and the load variability. These uncertainties are considered through the random variables $\mathbf{x_r}$. This section describes the probabilistic modeling of these random variables.

It should be noted that the performance of the designed drilled shafts is clearly affected by construction. Even if the design is appropriate, the actual performance may be unsatisfactory when the construction quality is poor. Therefore, the construction-related uncertainty should be treated as a factor that is as important as the aforementioned uncertainties. However, it is difficult to quantify construction-related uncertainty because the construction process is complex and has many implications. For example, the construction process may directly affect the surrounding soils and the strength of the concrete. As the complexity of these implications is beyond the research scope of this research, it is assumed that the drilled shafts in this study are properly constructed such that the influence of the construction-related uncertainty can be ignored.

5.4.1 Soil Properties

The analysis of a pile subjected to axial load and lateral load is a complex problem in which the soil-structure interaction is involved. In the analysis, the uncertainty of soil properties propagates through the *p*-*y* curves, *t*-*z* curves, and *q*-*w* curves used in the soil-structure interaction analysis. Cohesive soils can be used as an example. Soil properties are needed for constructing *t*-*z* curves, *q*-*w* curves, and *p*-*y* curves; these soil properties include undrained shear strength S_u, effective unit weight γ', and ε_{50} (where ε_{50} is defined as 50% of the strain corresponding to the maximum principal stress difference). . Soil itself is a complicated material in which physical process and chemical process are involved, resulting in relatively large variability in the soil properties. In addition, statistical uncertainty and transformation error are introduced in the sampling process and the testing process (e.g., Phoon and Kulhawy 1999). Thus, an appropriate soil variability model is needed in the reliability analysis. To capture the spatial correlation, each soil property (S_u, γ', and ε_{50}) is modeled as a random field that is

statistically characterized by three parameters: the mean μ, variance σ^2 and correlation length θ. The mean measures the center of a dataset and the variance measures the dispersion from the center, while the correlation length measures how rapidly a random field varies in space. The way in which a random field varies depends on its correlation structure, which is considered through a correlation function.

5.4.2 Material Properties

The materials for constructing drilled shafts include concrete and steel reinforcing bars (or rebar). The strength of concrete inevitably has some degree of variation. According to the American Concrete Institute (2002), the coefficient of variation (COV) for concrete compressive strength, f'_c, is generally in the range of 3% to 10%, depending on the concrete production and transportation process, the sampling process, and the testing process. The mechanical properties of reinforcement also have some degree of variation. It is known that a number of factors, including the rate of loading and the cross-sectional area of the rebars, can directly affect the yield strength of rebars. According to Mirza and MacGregor (1979), the COV for the yield strength of rebars, f_y, is typically in the range of 1% to 12%.

5.4.3 Model Errors

Model uncertainty is always present, as any computational model is an idealization or simplification of real-world conditions. Suppose Y_m denotes the prediction based on a model it assumes to be unbiased, and e_m is a model factor for capturing the model error that leads to potential under- or over- estimates. Thus, the true behavior (denoted as Y_t) can be expressed as follows:

$$Y_t = e_m \cdot Y_m \tag{5.6}$$

It should be noted that the error term e_m should be considered as a random variable whose statistical characters can be described using lognormal distributions (e.g., Phoon and Kulhawy 2005).

The accuracy of the *p-y* method (for calculating lateral deflection and angular distortion) and the *t-z* model (for calculating vertical movement) is primarily affected by the modeling of soil-pile interactions, which are represented by the *p-y* curves, *t-z* curves, and *q-w* curves. However, the development of these curves is usually based on limited load tests, and the curves may not truly represent the reality in which soils can vary significantly from one site to another. Furthermore, various errors are involved in the load test data. For example, there are measurement errors in the strain gauges used for estimating the axial deformations and curvatures induced by bending moment. Therefore, the model error in the *p-y* curves, *t-z* curves, and *q-w* curves needs to be considered for the soil-pile interaction analysis.

5.4.4 Allowable Displacements

The design of drilled shafts must satisfy strength and serviceability performance requirements. The serviceability check requires that the displacement induced by external loads should not be greater than the maximum allowable displacement. Maximum allowable displacements are traditionally treated as deterministic.

However, the specified allowable displacement is uncertain to some extent. The allowable displacement is primarily determined by the superstructure under consideration through structural analysis. The outcome of the structural analysis is dependent on the models employed and the corresponding input (i.e., material and geometry properties). Therefore, the outcome of interest (i.e., the allowable displacements in this study) has some variations due to the uncertainties in the models and the inputs used in the structural analysis.

5.4.5 External Loads

The variability in the design loads applied to the pile foundations should be considered, as the external loads can directly affect the displacement of a designed structure. According to Nowak and Collins (2000), the COV for dead load could range from 0.08 to 0.10 for buildings and bridges, while those for live load (including sustained live load and transient live load) could range from 0.18 to 0.89. Previous investigations (e.g., Ellingwood and Tekie 1999; Ellingwood et al. 1980) have found that normal, lognormal, gamma, Type-I and Type-II Gumbel distributions are possible choices to statistically characterize load models. For example, the maximum live load for a structure can be statistically characterized by Type-I Gumbel distributions, while sustained live load can be modeled as a gamma-distributed random variable.

5.5 Example

This section presents an example of reliability-based assessment for a drilled shaft and the importance analysis of the random variables that are considered in the reliability analysis. The configuration of the example of a drilled shaft is shown in Figure 5.1. It is assumed that the pile is constructed in a stiff clay site. The drilled shaft is 1.0 m (3.28 ft) in diameter and 8.0 m (26.25 ft) in length. The cross-section of the shaft is reinforced by a total of 12 No. 11 rebars (with a nominal diameter equal to 3.581 cm (1.41 in)), a reinforcement ratio of 1%, and a cover thickness of 7.62 cm (3 in).

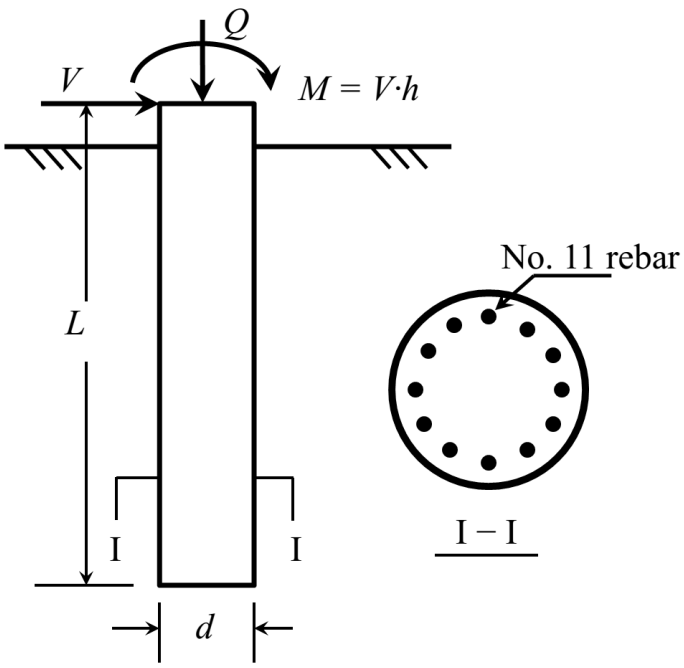

Figure 5.1 Example of a drilled shaft

5.5.1 Modeling of Random Variables

In the previous discussion, we have identified different sources of uncertainties that affect the performance of the designed drilled shafts. This subsection shows the models of the random variables used in this example. The random variables include soil properties (S_u, ε_{50}, and γ') for constructing the load transfer curves; concrete compressive strength f'_c; yield strength of reinforcement f_y; elastic modulus of reinforcement E_s; model factors e_{py}, e_{tz}, and e_{qw} for *p-y* curves, *t-z* curves and *q-w* curves, respectively; three allowable displacements (C_δ for lateral deflection, C_ψ for angular distortion, and C_w for vertical movement); lateral load *V;* and axial load *Q*. The load eccentricity (*h*) of the lateral load is assumed to be deterministic, and an *h* value of 3.0 m is used in this study. As such, the bending moment at the top of the drilled shaft, denoted by *M*, is calculated by multiplying the lateral load *V* by *h*. Overall, there are a total of 14 random variables, and the distributions and statistical properties of those random variables are summarized in Table 5.1.

Table 5.1 Statistical properties of random variables.

Variable	Distribution	Mean	COV
S_u	Lognormal	120 KPa	50%
ε_{50}	Lognormal	0.002	15%
γ'	Lognormal	19 KN/m^3	3%
f'_c	Gumbel	32 MPa	7%
f_y	Gumbel	415 MPa	5%
E_s	Lognormal	200 GPa	5%
e_{py}	Lognormal	1.0	5%
e_{tz}	Lognormal	1.0	5%
e_{qw}	Lognormal	1.0	5%
C_δ	Gumbel	2.0 cm	10%
C_ψ	Gumbel	0.01	10%
C_w	Gumbel	2.5 cm	10%
V	Gamma	200 KN	15%
Q	Gamma	1000 KN	10%

(Note: 120 KPa = 17.4 psi; 19 KN/m^3 = 118.56 pcf; 32 MPa = 4640 psi; 415 MPa = 60.18 ksi; 200 GPa = 29000 ksi; 2 cm = 0.79 in; 2.5 cm = 1 in; 200 KN = 44.96 kips; 1000 KN = 224.8 kips.)

It is noted that the mean values and the COVs listed in Table 5.1 are typical for the random variables of interest except for those of ε_{50} and the model factors (e_{py}, e_{tz}, and e_{qw}). To the best knowledge of the authors, the statistical properties of the model factors for the load transfer curves and ε_{50} are not widely available in the literature. In this example, the mean values of the model factors are assumed to be 1.0, implying that they are not under- or over-estimated in predicting soil reactions, and the COVs of the model factors are assumed to be 5%. The mean of ε_{50} for stiff clay is assumed to be 0.005 (the default value when test data is unavailable), and the COV of ε_{50} is taken as 15%. The typical variability levels for the remaining random variables can be readily found in the literature (e.g., Zhang and Ng 2005; Phoon and Kulhawy 2005; Nowak and Collins 2000; Ellingwood et al. 1980).

To simulate the lateral soil-pile interaction, the *p-y* curve for stiff clay without free water is used (Reese et al. 2004). The *t*-z curves and the *q-w* curves in this example are adopted from AASHTO (2010) to represent the axial soil reaction for cohesive soils. Three soil properties (namely S_u, γ' and ε_{50}) are used to construct the load transfer curves. As mentioned earlier, soil properties are modeled as random fields in which the correlation lengths are needed to characterize the dependence structure. In this example, the correlation lengths for S_u, γ' and ε_{50} are taken as 1.0 m.

5.5.2 Reliability Analysis

Once the statistical properties of the random variables are defined, MCS is employed to conduct reliability analysis. In MCS, the soil properties are simulated using the local averaging subdivision (LAS) technique (Fenton and Griffiths 2008), which has proven to be a fast and accurate method of producing random fields. In each realization, the displacements (δ, ψ and w) at the top of the pile are evaluated repeatedly using a different set of soil properties as inputs to the *t-z* model and the *p-y* method. With the resulting realizations of the displacements and the realizations of the allowable displacements, the failure probabilities for each limit state and the system can be evaluated accordingly.

Figure 5.2 shows the estimates of the failure probabilities for lateral deflection ($P_{f,\delta}$), angular distortion ($P_{f,\psi}$), vertical movement ($P_{f,w}$), and system failure (P_f). As expected, the failure probabilities converge as the number of samples increases. As shown in Figure 5.2, the failure probability of the system P_f is greater than that for any of the three individual failure modes and is less than the summation of the failure probabilities of the individual failure modes. The system failure probability will be underestimated if multiple failure modes are not considered simultaneously, while the system failure probability will be overestimated as different

failure modes are not disjoint. This observation indicates a critical deficiency in the current LRFD approach in which different limit states are considered separately.

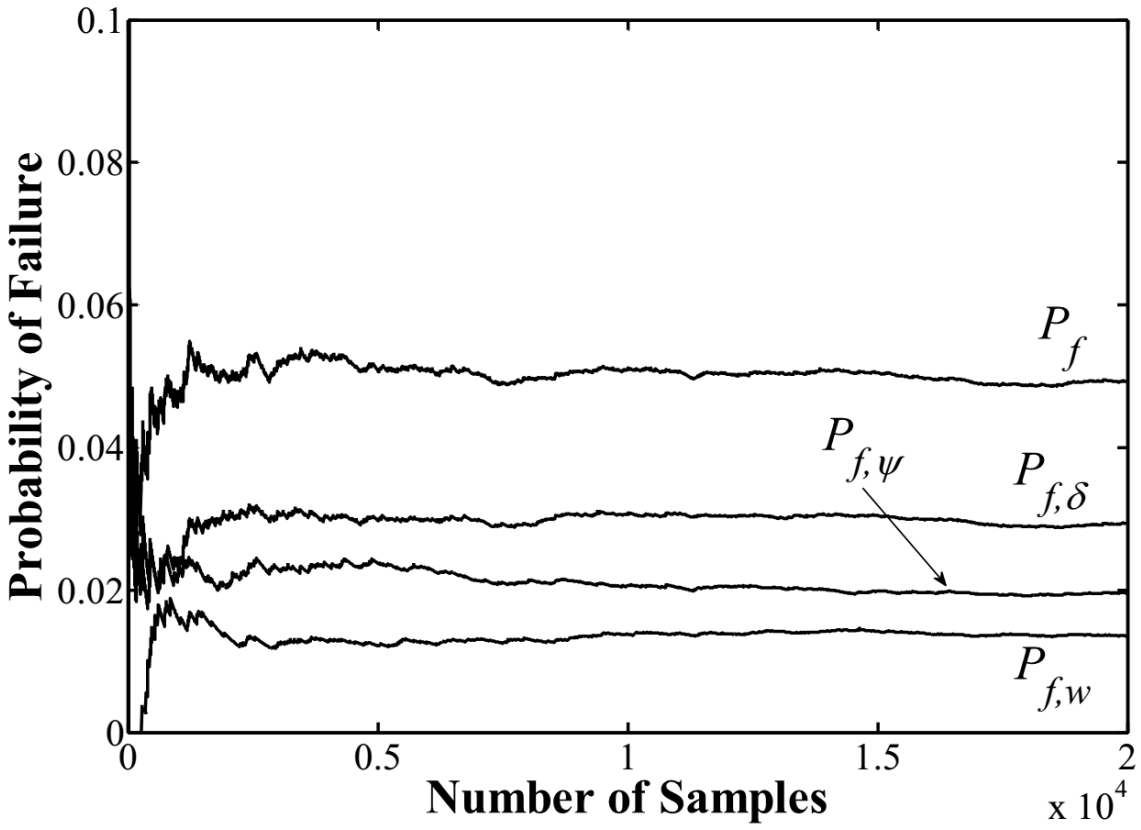

Figure 5.2 Probabilities of failure by MCS

5.5.3 Importance Measures

The importance measure of the random variables depends on the limit state function and the statistical properties of the variables, and it provides important insights on which are the major sources of uncertainties affecting the reliability of the designed structures.

The displacements of interest (δ, ψ and w) are evaluated based on the commonly used *p-y* method and *t-z* model, which do not have an explicit solution. The governing differential functions in the *p-y* method and the *t-z* model are solved by finite difference–based numerical algorithms. However, an explicit form of the limit state function can be defined using the

response surface method. A quadratic form of the limit state function is adopted in this study and is defined as follows:

$$G(\mathbf{x}_r) = c + \sum_{i=1}^{m} a_i x_{r,i} + \sum_{i=1}^{m} b_i x_{r,i}^2 \tag{5.7}$$

where a_i, b_i and c are regression coefficients, and $\mathbf{x}_r = (x_{r,1}, x_{r,2}, \ldots, x_{r,m})$ are the random variables. The regression coefficients are determined using the method of least squares. It should be pointed out that other forms of the limit state function may be applicable. For example, the interaction terms between different random variables (such as $x_{r,i} \cdot x_{r,j}$) may be included. The advantage of using a quadratic limit state function is that it becomes straightforward and efficient to evaluate the gradient of the function that is needed in the importance analysis.

Figure 5.3 shows the importance measures for the three failure modes. For lateral deflection ($k = \delta$) and angular distortion ($k = \psi$) failure modes, the most important variables are lateral load (V) and their corresponding allowable displacements. In contrast to the other two modes, the vertical movement failure mode ($k = w$) has S_u as the most important variable and Q as the second most important variable.

Although the COVs of V and Q are just 15% and 10%, respectively, the external loads overall still outweigh other random variables. This is understandable, since the lateral deflection and the angular distortion are the direct response of V, and the vertical movement is the direction response of Q. Furthermore, the allowable displacements are important, because they directly reflect the "capacity" in the limit state functions.

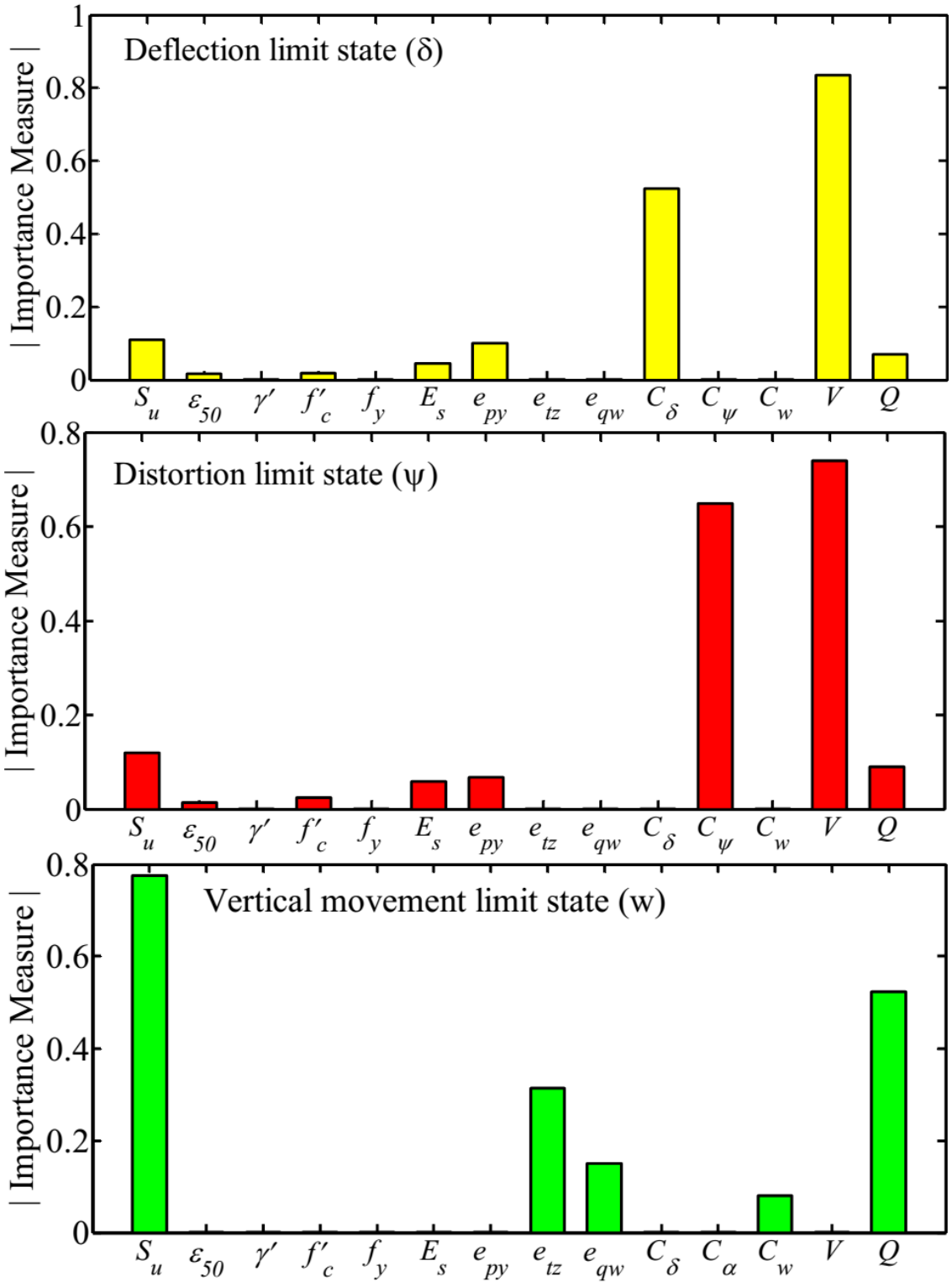

Figure 5.3 Importance measures of random variables

It should be noted that S_u is a measure of soil strength, and it is assumed to have a large variability (i.e., its COV is assumed to be as much as 50% in this example). Surprisingly, the variability of S_u is relatively less important for $k = \delta$ and $k = \psi$, but it is the most important variable for $k = w$. On the other hand, even though the COVs for the model factors (e_{py}, e_{tz}, e_{qw}) are just 5%, the importance measure of e_{py} is large for both $k = \delta$ and $k = \psi$, and the importance measures of e_{tz} and e_{qw} are large for $k = w$. This observation indicates that the accuracy of the load transfer curves is important in the reliability analyses. Moreover, f'_c, f_y, ε_{50} and γ', can be considered unimportant random variables for all three failure modes.

Based on the evaluation of importance measures, it is concluded that the major sources of uncertainties affecting the reliability of a designed drilled shaft come from the external loads, the allowable displacements, the variability of S_u, and the accuracy of the load transfer curves.

5.5.4 Influence of External Loads

In order to further investigate how the random variables affect the responses of the pile system, an importance analysis is conducted given certain values of the external loading. Figures 5.4 and 5.5 show the importance measures in which Q is kept equal to 1000 KN (224.8 kips) and V is varied, while Figure 5.6 shows the importance measures in which V is kept equal to 200 KN (44.96 kips) and Q is varied. Only the first four most important random variables are shown in these figures. Furthermore, it can be noticed that the change in V (168 KN (37.77 kips) to 270 KN (60.70 kips)) in Figures 5.4 and 5.5 leads to the changes in the reliability indices (β_δ ranges from 0.53 to 5.35, while β_ψ ranges from 0.70 to 5.50). Likewise, the change in Q (700 KN (157.36 kips) to 1600 KN (359.68 kips)) leads to the change in β_w, which ranges from -0.10 to 3.55. Although the variations in reliability indices are large, the order of importance of the random variables remains the same, consistent with what is found in Figure 5.3. For $k = \delta$ and k

= ψ, the allowable displacements (C_δ and C_ψ) dominate the contribution to the variability in the failure probability, while for $k = w$, S_u dominates. Note that in Figures 5.4 and 5.5, there is a sudden change in the importance measures when the lateral load V is at approximately 200 KN. This is because there is a sudden change in flexural stiffness due to the concrete cracking, which causes the lateral deflection and the angular distortion at the top of the pile to increase dramatically. The concrete cracking that leads to the reduction in the flexural stiffness is developed due to the bending moment developed along the pile that increases with an increase in V. According to the analytical method described in Reese et al. (2004), which is adopted in this study to evaluate the moment-stiffness relationships, the flexural stiffness of a reinforced concrete pile could be reduced by 70% to 80% after concrete cracking occurs.

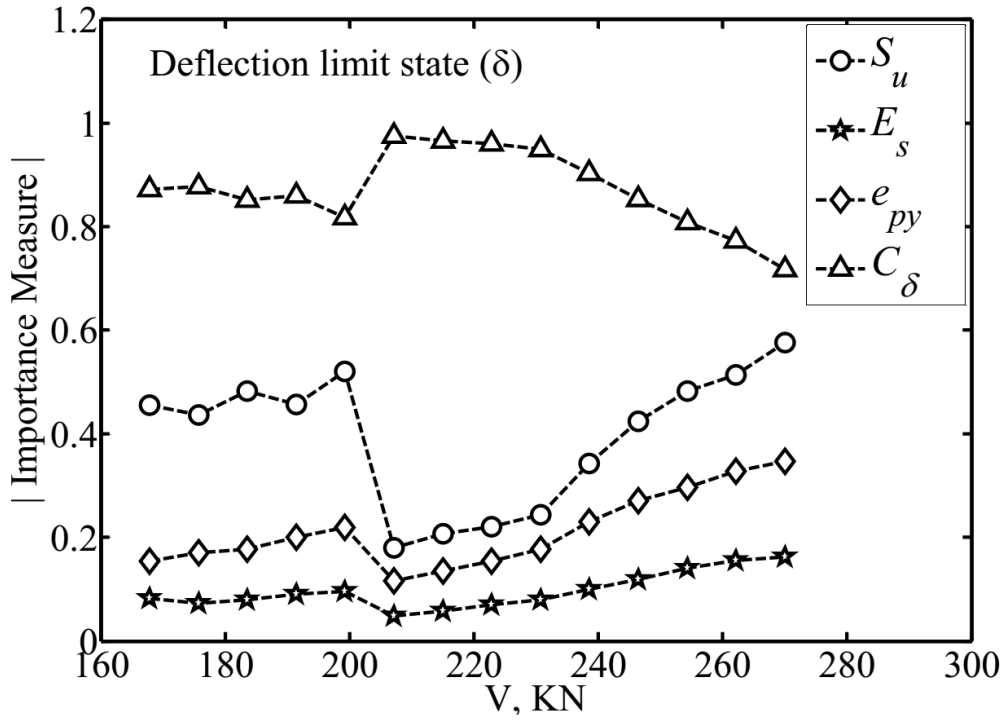

Figure 5.4 Influence of lateral load on the importance measure for deflection limit state

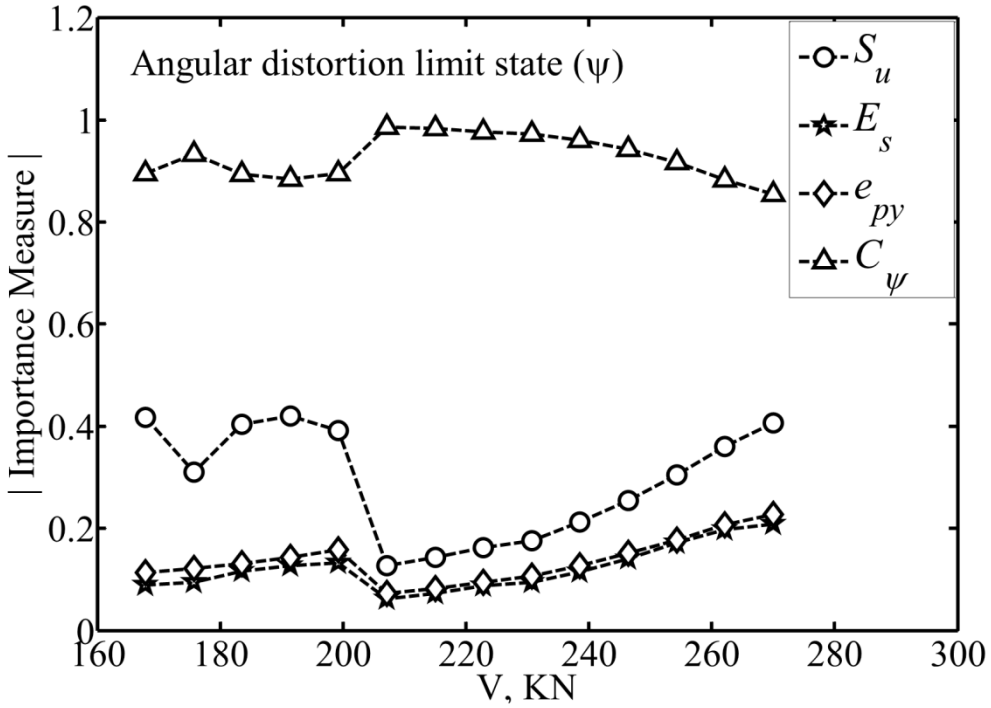

Figure 5.5 Influence of lateral load on importance measures for ψ limit state

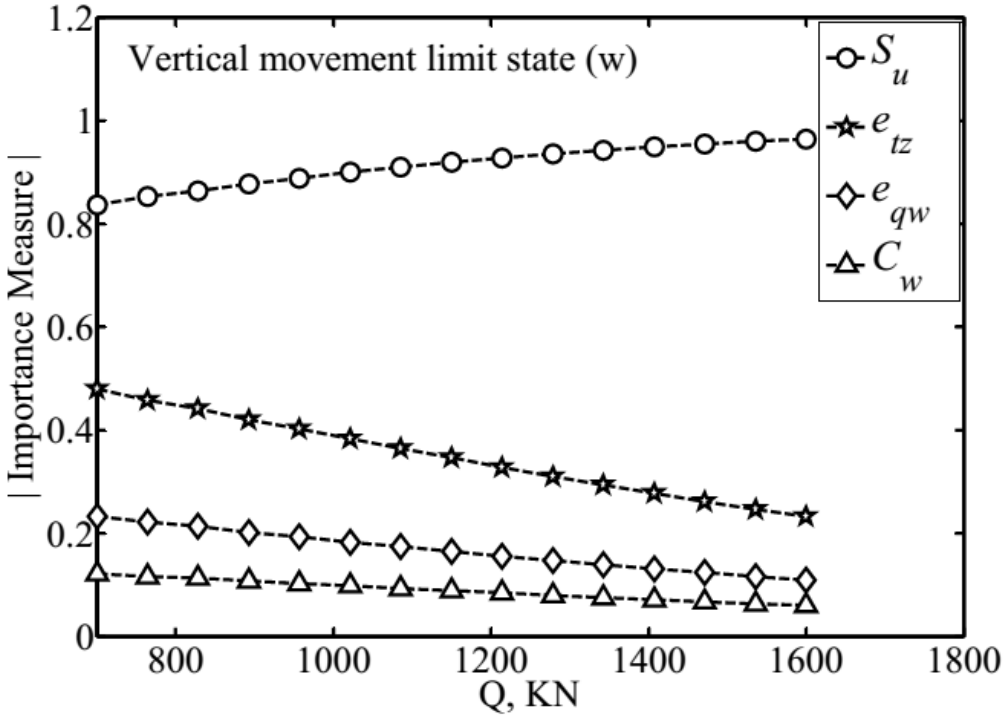

Figure 5.6 Influence of axial load on importance measures for vertical movement limit state

Additionally, as shown in Figures 5.4 and 5.5, the importance measures of S_u, E_s and e_{py} remain nearly constant, but they start to increase once cracking in the concrete occurs (when V is about 200 KN (44.96 kips)). Meanwhile, the importance measures of C_δ and C_ψ remain about the same prior to the concrete cracking but begin to decrease after the concrete cracks. For the vertical movement limit state shown in Figure 5.6, the importance measure of S_u slightly increases, while those of e_{tz}, e_{qw} and C_w slightly decrease with an increase in Q.

5.5.5 Influence of Correlation Length

As discussed previously, the correlation length is used to describe the correlation structure of a random field. It is important to study the influence of correlation length on the calculated probability of failure. The influence of ε_{50} and γ' on the failure probability is minimal, as shown in the prior discussion of importance measures. Consequently, this section only investigates the influences of the correlation length of S_u, θ_{Su}, on the calculated the probability of failure. A parametric study is conducted by varying θ_{Su} and the COV of S_u, COV(S_u), while the correlation lengths of γ' and ε_{50} are fixed at 1.0 m (3.28 ft).

Figures 5.7, 5.8, and 5.9 show the failure probabilities of the individual limit states and the system failure rates for COV(S_u) are 30%, 50%, and 70%, respectively. First, it can be seen that the P_f is greater than any of the failure probabilities of the component limit states, regardless of the value for θ_{Su}. Secondly, the system reliability would be governed by different limit states when θ_{Su} and COV(S_u) are varied. In Figure 5.7, when $\theta_{Su} < 0.7$ m (2.3 ft), $P_{f,\psi}$ is greater than the failure probabilities of the other two modes. But for $\theta_{Su} \geq 0.7$ m, $P_{f,\delta}$ is greater than those of the other two modes. This indicates that when the dependence of S_u is weak, the system more likely fails in distortion ($k = \psi$); otherwise, it will fail in lateral deflection ($k = \delta$). However, for a COV(S_u) equal to 50% (as shown in Figure 5.8), the system tends to fail in lateral deflection (k =

δ) if $\theta_{Su} \leq 4$ m (13.12 ft); it will tend to fail in vertical movement (w) if $\theta_{Su} > 4$ m (13.12 ft). Likewise, a similar observation can be found in Figure 5.9. Overall, Figures 5.7 through 5.9 indicate that θ_{Su} and COV(S_u) play important roles on reliability analysis. If θ_{Su} and COV(S_u) are not appropriately chosen, the estimate of the failure probabilities would become biased. Therefore, special attention is needed to determine the values of θ_{Su} and COV(S_u) to reflect the correct statistics of the undrained shear strength S_u of the soil.

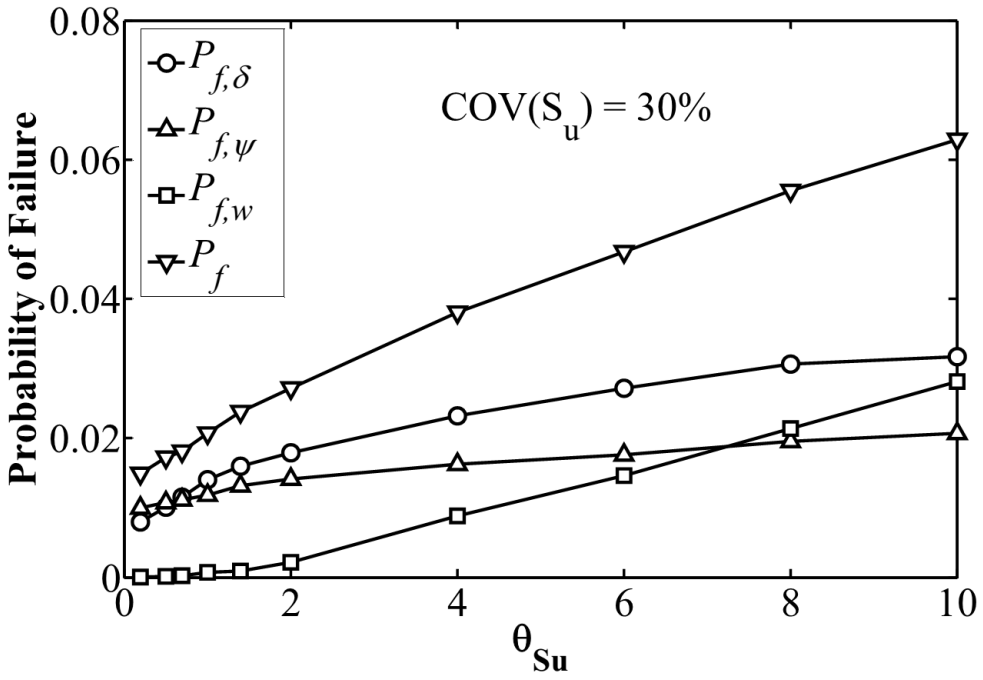

Figure 5.7 Influence of θ_{su} on failure probabilities for COV(S_u) = 30%

(Note: 2 m = 6.56 ft; 4 m = 13.12 ft; 6 m = 19.68 ft; 8 m = 26.25 ft; 10 m = 32.81 ft.)

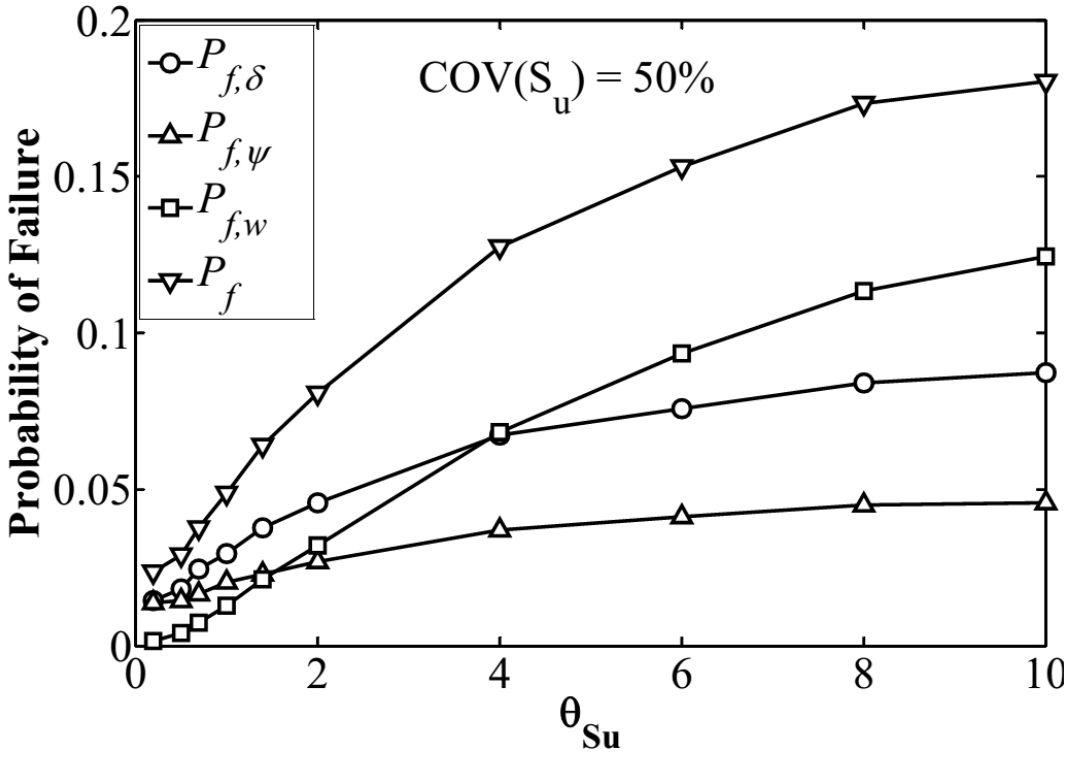

Figure 5.8 Influence of θ_{su} on failure probabilities for COV(S_u) = 50%

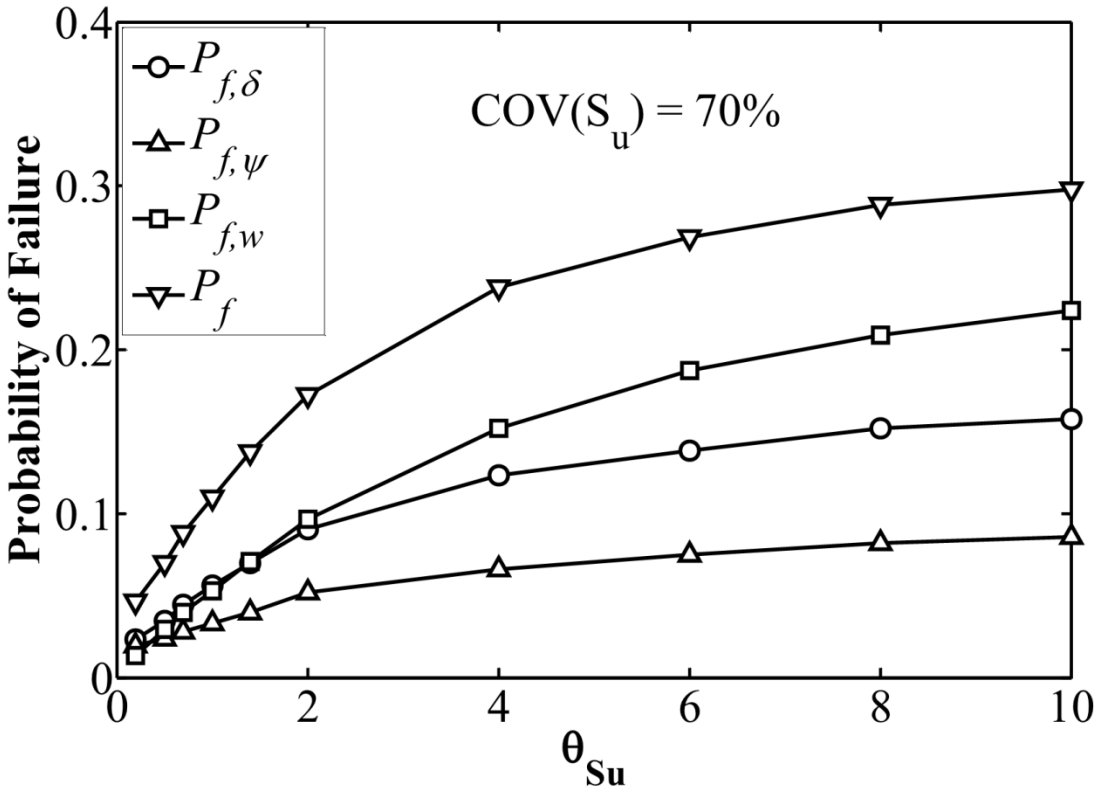

Figure 5.9 Influence of θ_{su} on failure probabilities for COV(S_u) = 70%

5.6 Summary and Conclusions

This chapter presents a probabilistic framework to evaluate the serviceability performance of a drilled shaft. This study addresses the limitations of the current LRFD approach that handles the serviceability limit state in a deterministic way. In the proposed framework, the uncertainties that affect the reliability of a designed drilled shaft are identified as the following: soil properties, material properties, model errors in the soil interaction analysis, performance criteria, and external loads. Particularly, the spatial variability of soil properties is considered using random field theory, in which each soil property is statistically characterized by the mean, variance, and correlation length. The model errors of the load transfer curves are accounted for by introducing model factors. This chapter concluded with an example, where reliability analysis and importance analysis are conducted for three failure modes (lateral deflection, angular distortion, and vertical movement at the top of the pile). Based on the results, the following conclusions are made:

1. The failure probability of the system, P_f, is greater than those of the individual failure modes. Besides, P_f is less than the summation of the failure probabilities of the three individual failure modes. The failure probability of the system may be underestimated if multiple failure modes are not considered simultaneously. It is recommended to conduct reliability analysis system-wise if multiple failure modes exist. In the current LRFD approach, different limit states are considered separately, which leads to an overestimation of the reliability.
2. The importance analysis of the random variables indicate that the major sources of uncertainties affecting the reliability of a designed drilled shaft come from external loads, the allowable displacement, soil property S_u, and the model factors of the load

transfer curves. The variability in concrete and reinforcement is relatively less important.

3. Considering the dependence structures of soil properties in reliability analysis is essential. If the dependence structures of soil properties are ignored or not considered appropriately, the calculated probability of failure will be biased. Therefore, guidance regarding how to determine the dependence structures of soil properties is needed.

CHAPTER 6. USE OF IMPORTANCE SAMPLING IN RELIABILITY ANALYSIS

6.1 Introduction

Monte Carlo simulation (MCS) is widely used for reliability analysis because of its mathematical simplicity and robustness. An important application of MCS is to evaluate the probability of failure P_f, as in the following equation:

$$P_f = P(G \le 0) = \int_{G \le 0} f(\boldsymbol{x})\, d\boldsymbol{x} = \int I[G \le 0]\, f(\boldsymbol{x})\, d\boldsymbol{x} \tag{6.1}$$

where $P(\cdot)$ denotes a probability measure, $f(\boldsymbol{x})$ denotes the joint probability density function (PDF) of random vector $\boldsymbol{x}$, $I[\cdot]$ denotes an indicator function, G denotes a limit state function, and failure is denoted as $G \le 0$. A general definition of the limit state function is written as follows:

$$G(\boldsymbol{x}) = C - D(\boldsymbol{x}) \tag{6.2}$$

where C and D denote the "capacity" and the "demand" in a broad sense. With the probability of failure, the reliability index β can be evaluated accordingly:

$$\beta = \Phi^{-1}(1 - P_f) = -\Phi^{-1}(P_f) \tag{6.3}$$

where $\Phi^{-1}(\cdot)$ denotes the inverse of the cumulative distribution function for the standard normal variable.

A common problem with the evaluation of the failure probability is that the number of dimensions in reliability problems may be large, making it difficult to evaluate the numerical integration (i.e., Equation 6.1) directly. In that case, the integration can be evaluated as the expectation of the indicator function using Monte Carlo integration (Robert and Casella 2004). Simply speaking, the probability of failure P_f is approximated as the ratio of the number of failure events to the total number of samples, as shown in the following equation:

$$P_{f,\mathrm{MCS}} = \frac{1}{n}\sum_{i=1}^{n} I_i\left[G \le 0\right] \tag{6.4}$$

where n is the sample size, the subscript "MCS" indicates that the estimate is evaluated using the crude MCS method. The indicator function is equal to 1.0 if G is less than or equal to 0; otherwise, it is zero. It should be noted that in the crude MCS method, the random variables $\boldsymbol{x}$ are drawn from the joint PDF f.

To guarantee the convergence of Equation (6.4), the sample size n has to be sufficiently large. According to Ang and Tang (2007), the degree of precision for the estimate of Equation (6.4) can be measured by its coefficient of variation (COV) δ_p, which is determined by:

$$\delta_p \approx \sqrt{\frac{1-P_{f,\mathrm{MCS}}}{n \cdot P_{f,\mathrm{MCS}}}} \tag{6.5}$$

Equation (6.5) indicates that the coefficient of variation is affected by the sample size n and P_f. Based on Equation (6.5), a back-calculation can be used to estimate the sample size n as follows:

$$n \approx \frac{1-P_{f,\mathrm{MCS}}}{\delta_p^2 \cdot P_{f,\mathrm{MCS}}} \tag{6.6}$$

Based on Equation (6.6), it is concluded that the sample size n is related to P_f and its COV δ_p. The smaller δ_p and P_f are, the larger n is. The probability of failure P_f is typically a small number. Thus, the sample size n is usually large enough that the convergence of Equation (6.4) is guaranteed. According to Robert and Casella (2004), a rule of thumb for selecting a sample size is that n is approximately ten times the reciprocal of the probability level, if the COV for P_f is taken as 30%. For example, the sample size is at least 10,000 if P_f is equal to 1/1000. A larger sample size is warranted if a smaller δ_p is desired. Based on the above discussion, it is well

understood that the crude Monte Carlo statistical methods are often computationally expensive as a result of repetitive evaluation of the indicator function. It becomes even more demanding if the evaluation of the indicator functions is complex.

In the reliability analysis for axially loaded piles, the authors previously developed a performance based design approach using the crude MCS method (Fan and Liang 2012). To improve the computational efficiency of the Monte Carlo method, this research presents an importance sampling (IS) based algorithm that can be applied to conduct fast reliability evaluation for an axially loaded pile. The spatial variability of soil properties is considered by random field modeling, in which each soil property is statistically characterized by the field mean, the field variance, and the correlation structure. The random fields for soil properties are simulated by using the local averaging subdivision (LAS) method (Fenton and Griffiths 2008). This well-accepted load transfer method is employed to evaluate the load-displacement behavior for the pile. In the proposed importance sampling algorithm, the instrumental function is constructed by shifting the original PDF such that the mean is at the point having the maximum probability density of the failure surface. By sampling more heavily from the region of interest and then scaling the indicator function back by a ratio of probability densities, a faster rate of convergence can be achieved while maintaining the accuracy of the estimate. Two examples – one for homogeneous clay sites and the other for non-uniform clay sites – are presented to illustrate the accuracy and efficiency of the developed importance sampling method.

6.2 Load Transfer Model

The analysis of axially loaded piles is a nonlinear soil-pile interaction problem that is solved by iterative numerical algorithms. Numerous methods are available to analyze the response of an axially loaded pile, such as the finite element method and the load transfer

method. The load transfer method (e.g., Coyle and Reese 1966) is widely used because of its accuracy and simplicity. The schematic diagram of the load transfer model is shown in Figure 2.2., and a detailed discussion of the load transfer model can be found in Section 2.1.2.

6.3 Random Field Modeling

Soil properties such as undrained shear strength and friction angle are needed as inputs to construct the load transfer curves (*t-z* curves and *q-w* curves). The soil properties are uncertain due to intrinsic variability, measurement errors, and interpretation errors. The variations of soil properties can directly affect the *t-z* curves and *q-w* curves in the load transfer model. Consequently, these variations can exert significant influence on the calculated load-displacement curve. Therefore, the modeling of soil variability is of great importance in reliability assessment.

Two statistical parameters, namely the mean μ and variance σ^2, are required to characterize the variability of a soil property at the point level. The mean measures the center of a dataset while the variance measures the dispersion from the mean. One commonly used probability distribution for soil properties is the lognormal distribution (e.g., Griffiths et al. 2009). The use of lognormal distribution ensures that soil properties are always non-negative. The PDF for lognormal distribution is given as follows:

$$f\left(x|\mu_{\ln x},\sigma_{\ln x}\right)=\frac{1}{x\sigma_{\ln x}\sqrt{2\pi}}\exp\left[-\frac{1}{2}\frac{\left(\ln x-\mu_{\ln x}\right)^2}{\sigma_{\ln x}^2}\right] \tag{6.7}$$

where $\mu_{\ln x}$ and $\sigma_{\ln x}$ are the distribution parameters. The distribution parameters can be determined based on the mean μ_x and the standard deviation σ_x, as shown in the following equation:

$$\sigma_{\ln x}=\sqrt{\ln\left(1+\frac{\sigma_x^2}{\mu_x^2}\right)} \tag{6.8}$$

$$\mu_{\ln x} = \ln \mu_x - 0.5\sigma^2_{\ln x} \tag{6.9}$$

For mathematical simplicity, it is preferable to have normal variables. By taking the logarithm, a lognormally distributed random variable can be transformed to a normal variable with a mean of $\mu_{\ln x}$ and a standard deviation of $\sigma_{\ln x}$. The advantage of such a transformation will become clear in the subsequent discussion. It should be noted that other probability distributions (such as the normal distribution) are possible choices for modeling soil properties.

In addition to the mean and the variance, a third parameter called correlation length θ is required to characterize the spatial variability of a random variable (Vanmarcke 1977). The correlation length is needed to define a correlation function, which describes how random variables are correlated at different separation distances. For example, the correlation function for Markov process is shown in Equation (2.11) and is adopted herein because of its widespread use.

6.4 Importance Sampling Method

6.4.1 Mathematical Formulation

Let us reconsider Equation (6.1), which presents a mathematical formulation for the failure probability. In the crude MCS solution (see Equation 6.4), samples of $\boldsymbol{x}$ are drawn directly from the PDF of interest (denoted as f in that equation). As alluded to earlier, the probability of failure is usually a very small number, which means that only a very small portion of samples from the region of interest can be drawn. Although the remaining samples do not contribute to the estimation of P_f, they are still used as inputs to evaluate the indicator function. As a result of the repetitive evaluation for those samples, the rate of convergence is slowed. To address this deficiency, one possible solution is to draw more samples from the region of interest (i.e., $G \leq 0$). This can be achieved through a carefully devised instrumental function in importance sampling.

If the instrumental function is denoted as h, the mathematical representation of importance sampling for Equation (6.1) can be expressed as:

$$\begin{aligned} P_{f,\mathrm{IS}} &= \int I\left[G \le 0\right] \frac{f\left(\boldsymbol{x}\right)}{h\left(\boldsymbol{x}\right)} h\left(\boldsymbol{x}\right) d\boldsymbol{x} \\ &\approx \frac{1}{n} \sum_{i=1}^{n} I_i\left[G \le 0\right] \frac{f\left(\boldsymbol{x}_i\right)}{h\left(\boldsymbol{x}_i\right)} \end{aligned} \tag{6.10}$$

where $f(\boldsymbol{x})/h(\boldsymbol{x})$ is the importance sampling quotient and the subscript "IS" indicates that the estimate is evaluated by importance sampling. Note that the random samples $\boldsymbol{x}$ in Equation (6.10) are drawn from $h(\boldsymbol{x})$ instead of $f(\boldsymbol{x})$. The importance sampling method has minimal constraints. It only requires that the support of f is contained in that of h such that the variance for the estimate is finite. Equation 6.10 is very useful, and it gives a different perspective on the estimation of P_f. By carefully selecting an instrumental function h, more samples are drawn from the region of interest, resulting in faster convergence. From a statistical point of view, the instrumental function is introduced to reduce the variance in the estimate in a MCS problem.

6.4.2 Important Considerations

The objective of applying importance sampling is to be able to conduct fast reliability evaluation without losing accuracy. When applying importance sampling to the reliability evaluation of axially loaded piles, there are a few fundamental considerations:

1. The number of dimensions in the reliability problem is high, and the IS estimator (i.e., Equation 6.10) should give the same unbiased estimate as does the crude MCS method;
2. The IS estimator should yield a fast rate of convergence; and
3. An efficient method for simulating the random samples from the instrumental function should be available.

The first consideration is related to the accuracy of the importance sampling technique, while the second and the third ones are related to the computational efficiency of the technique. In the analysis of axially loaded piles, the vertical movement under axial loading is evaluated by the load transfer method, in which the pile under consideration is discretized into a finite number of segments. The soil-pile interaction behavior for each segment is characterized by a *t-z* curve or a *q-w* curve. Thus, the number of dimensions is large in importance sampling. A common concern associated with the high-dimensional importance sampling problem is the question of whether the importance sampling estimator can converge or not. It is worthwhile to note that the convergence of the estimate comes with some conditions on *h* and cannot be taken for granted in high-dimensional importance sampling. Detailed discussions of those conditions can be found in Au and Beck (2003). Finally, it is important to note that the simulation of the random samples should be efficient, as the random samples are used as inputs to evaluate the indicator function and will directly affect the rate of convergence.

6.4.3 Implementation Scheme

The choice of the instrumental function *h* is a crucial step, because the instrumental function would not only directly affect how efficient it is to draw the random samples, but it would also affect the evaluation of the indicator function and the corresponding importance sampling quotient. The optimal choice for the instrumental function is determined by the following equation:

$$h_{opt}(\boldsymbol{x}) = \frac{I[G \le 0] f(\boldsymbol{x})}{\int I[G \le 0] f(\boldsymbol{x}) d\boldsymbol{x}} = \frac{I[G \le 0] f(\boldsymbol{x})}{P_f} \tag{6.11}$$

in which the variance of the estimate is equal to zero. Unfortunately, the optimal choice of the instrumental function is not feasible in practice, because it requires the knowledge of the integral

of interest (i.e., P_f), which is unknown! Though not practical, the optimal instrumental function gives important insights: it demonstrates that 1) h_{opt} covers the entire region of interest and has no support beyond that region; and 2) h_{opt} is proportional to the original joint PDF f by a factor of $1/P_f$ in the region of interest, regardless of $\boldsymbol{x}$. Taking advantage of these insights, the instrumental function is chosen so that significant probability content from the region of interest can be covered. It has been suggested that a design point $\boldsymbol{x}^*$ can be used to identify the region of interest (Melchers 1999). The design point $\boldsymbol{x}^*$, which is the point lying on the failure surface which has the maximum likelihood, is calculated as follows:

$$\boldsymbol{x}^* = \arg \max_{G=0} \left[f(\boldsymbol{x}) \right] \tag{6.12}$$

where "arg" is short for argument, and max[·] denotes the maximum value under the constraint $G = 0$. Once the design point is determined, a common strategy is to shift the original PDF f so that the mean is at the point $\boldsymbol{x}^*$ (e.g., Au and Beck 1999; Melchers 1999).

6.4.4 Locating Design Point

The objective of this section is to present the proposed approach for pinpointing the design point so that the region of interest can be characterized. Based on the well-accepted first order reliability method (FORM), Low and Tang (2007) have shown a geometric interpretation for the reliability index in that β is equal to the minimum distance from the failure surface to the origin in the **u**-space, where **u** is standard normal variable. In general, the design point is obtained by solving a constrained optimization problem. There are numerous algorithms for solving the optimization problem; among them is the gradient projection method, which has been proven to be an efficient algorithm to use in searching for the design point (e.g., Der Kiureghian and Stefano 1991; Der Kiureghian and Liu 1991). The method is summarized below:

1. Assume an initial point $\boldsymbol{x}_0$ for $\boldsymbol{x}$ in the $\boldsymbol{x}$-space and transform it to independent standard normal variable $\boldsymbol{u} = \boldsymbol{u}(\boldsymbol{x})$, choosing tolerances δ_1 and δ_2 for checking convergence.

2. Evaluate the gradient vector $\boldsymbol{\alpha}$:

$$\nabla G(\boldsymbol{u})^T = \left(\frac{\partial G}{\partial u_1}, \frac{\partial G}{\partial u_2}, \cdots, \frac{\partial G}{\partial u_k} \right) \tag{6.13}$$

$$\boldsymbol{\alpha} = \frac{\nabla G(\boldsymbol{u})}{\left\| \nabla G(\boldsymbol{u}) \right\|} \tag{6.14}$$

where $\|\cdot\|$ measures the Euclidean norm of a vector.

3. Determine search direction $\boldsymbol{v}$:

$$\boldsymbol{v} = \left[\frac{G(\boldsymbol{u})}{\left\| \nabla G(\boldsymbol{u}) \right\|} + \boldsymbol{\alpha}^T \boldsymbol{u} \right] \boldsymbol{\alpha} - \boldsymbol{u} \tag{6.15}$$

4. Assume a step size λ (e.g., $\lambda = 1$) and then find a new iteration point $\boldsymbol{u}_{\text{new}}$:

$$\boldsymbol{u}_{\text{new}} = \boldsymbol{u} + \lambda \boldsymbol{v} \tag{6.16}$$

5. Check whether convergence is achieved or not:

$$G(\boldsymbol{u}_{\text{new}}) \le \delta_1 \tag{6.17}$$

$$\left\| \boldsymbol{u}_{\text{new}} - \boldsymbol{\alpha}^T \boldsymbol{u} \boldsymbol{\alpha} \right\| \le \delta_2 \tag{6.18}$$

It is important to note that Equation (6.17) and Equation (6.18) must be satisfied simultaneously when convergence is obtained.

6. Repeat Steps 2 through 5 until convergence is achieved.

7. Evaluate the reliability index using the design point $\boldsymbol{u}^*$:

$$\boldsymbol{u}^* = \boldsymbol{u}_{\text{new}} \tag{6.19}$$

$$\beta = \boldsymbol{\alpha}^T \boldsymbol{u}^* \tag{6.20}$$

It should be noted that the design point $\boldsymbol{x}^*$ can be obtained by transforming $\boldsymbol{u}^*$ back to the original space.

6.4.5 Response Surface Method

The objective in using the response surface method is to construct a limit state function that can be used in the search of the design point. In the load transfer model, there is no explicit equation for calculating the vertical movement at the top of the pile. The vertical movement is solved iteratively through the use of numerical algorithms. Therefore, the limit state function should be established before applying FORM. An example of the limit state function by using the response surface method is given below:

$$G\left(\ln x_1, \ln x_2, \cdots, \ln x_k\right) = a + \sum_{i=1}^{k} b_i \ln x_i + \sum_{i=1}^{k} c_i \left(\ln x_i\right)^2 \tag{6.21}$$

where a, b and c are regression coefficients, (x_1, x_2, …, x_k) is a vector of random variables, and ln(·) denotes the natural logarithm. Note that the logarithms of soil properties are used as predictor variables in the response surface method. While using other forms of the limit state function would also be feasible, the use of a quadratic form makes it efficient to evaluate the gradient vector in the FORM.

6.4.6 Algorithm

Normal variables can be used as an example to illustrate the construction of an instrumental function. As mentioned earlier, it is assumed that soil properties are lognormally distributed. Normal variables can be obtained by taking logarithms of the soil properties. For example, suppose that $\boldsymbol{x}=(x_1,x_2,\ldots,x_k)^{\mathrm{T}}$ has a mean vector $\boldsymbol{\mu}$ and a covariance matrix $\boldsymbol{C}$. After the limit state function and the statistics of the random variables are defined, FORM analysis is conducted to pinpoint the design point $\boldsymbol{x}^*$ (where the center of the instrumental function is at $\boldsymbol{x}^*$).

There is little flexibility in choosing the covariance matrix in high-dimensional importance sampling problem. According to Au and Beck (2003), there are some restrictions on the covariance matrix. If the covariance matrix for *h* is not appropriate, the consequence is that the estimate of P_f will vanish or be biased, particularly in the case of a high-dimensional importance sampling problem. In order to have an unbiased estimate, the covariance matrix of the instrumental function *h* is taken as the same as in *f* in this study. Now it becomes clear that the random samples are drawn from $\phi(\boldsymbol{x}^*, \boldsymbol{C})$ instead of $\phi(\boldsymbol{\mu}, \boldsymbol{C})$, where $\phi(\cdot)$ denotes the joint PDF for normal variables. The advantage in using a normal distribution is that the joint PDF has an explicit form, so that it is efficient to use for evaluating the importance sampling quotient.

In summary, the instrumental function is shifted so that the mean is at the design point $\boldsymbol{x}^*$ while the covariance term remains unchanged. In this case, it is anticipated that approximately one half of the random samples will be drawn from the failure domain. Once the instrumental function is defined, the importance sampling quotient *R* is evaluated using the following equation:

$$R = \frac{f(\boldsymbol{x})}{h(\boldsymbol{x})} = \frac{\phi(\boldsymbol{x}|\boldsymbol{\mu},\boldsymbol{C})}{\phi(\boldsymbol{x}|\boldsymbol{x}^*,\boldsymbol{C})} = \frac{\exp\left[-\frac{1}{2}(\boldsymbol{x}-\boldsymbol{\mu})^T \boldsymbol{C}^{-1}(\boldsymbol{x}-\boldsymbol{\mu})\right]}{\exp\left[-\frac{1}{2}(\boldsymbol{x}-\boldsymbol{x}^*)^T \boldsymbol{C}^{-1}(\boldsymbol{x}-\boldsymbol{x}^*)\right]} \tag{6.22}$$

The variability of the estimator is measured by its COV, which is given by this equation:

$$\delta_p^{IS} = \frac{\sqrt{\mathrm{Var}(P_{f,\mathrm{IS}})}}{\mathrm{E}(P_{f,\mathrm{IS}})} \approx \sqrt{\frac{\sum_{i=1}^{n} I_i^2[G \le 0] R_i^2 - n P_{f,\mathrm{IS}}^2}{n(n-1)}} \Big/ P_{f,\mathrm{IS}} \tag{6.23}$$

where Var(·) denotes the variance for the estimate and E(·) denotes the expectation.

The algorithm for conducting fast reliability evaluation of axially loaded piles is summarized as follows:

1. Define the soil profile of interest and the associated statistics (mean $\boldsymbol{\mu}$ and covariance $\boldsymbol{C}$) for soil properties.
2. Determine the mechanical properties (EA) of the pile.
3. Define the allowable displacement as the failure criterion.
4. Obtain the design axial load.
5. Construct an approximated limit state function using the response surface method.
6. Search for the design point $\boldsymbol{x}^*$ using the described gradient projection method.
7. Construct the instrumental function $h(\boldsymbol{x}) = \phi(\boldsymbol{x} \mid \boldsymbol{x}^*, \boldsymbol{C})$.
8. Assume a sample size n (e.g., 300 to 1000) and draw random samples from $h(\boldsymbol{x})$.
9. Use the realizations of the random samples as inputs to compute the vertical movement of the pile.
10. Conduct statistical analysis using the realizations of the vertical movement and evaluate the failure probability using Equation (6.22) and Equation (6.23).

A computer program has been developed based on the above algorithm and has been tested. The following examples are presented to illustrate the proposed approach.

6.5 Examples

6.5.1 Example 1: Drilled shaft in a homogeneous soil deposit

The objective of Example 1 is to demonstrate the accuracy of the developed importance sampling algorithm. Consider a drilled shaft with a 1.10-m (3.61 ft) diameter and a 8.0-m (26.25 ft) length in a homogeneous clay soil deposit that is subjected to compression force Q of 1300 KN (292.24 kips). The adopted failure criterion is a vertical displacement y_a of 25 mm (1 in). Both y_a and Q are deemed deterministic in this example, although they can be treated as random

variables as well. The undrained shear strength S_u of the clay at that site has a mean of 100 KPa, a COV of 20%, and a correlation length of 1.0 m (3.28 ft). The correlation length is needed to evaluate the covariance matrix. Note that S_u is a lognormally distributed variable and that the correlation length of S_u is defined with respect to its logarithm. The statistics of S_u are needed to generate random fields in MCS. The reinforcement ratio is taken as 1%. The elastic modulus is taken as 200 GPa (29,000 ksi) for reinforcement and 26.6 GPa (3857 ksi) for concrete, which will be used to calculate the elastic modulus of the drilled shaft. The *t-z* curves and *q-w* curves for cohesive soils from AASHTO (2010) are used to represent the soil-structure interactions, which are considered to be deterministic. Finally, the unit weight of reinforced concrete is taken as 24 KN/m^3 (149.76 pcf), which is used to calculate the dead weight of the drilled shaft.

Figure 6.1 shows the convergence of the importance sampling estimate with a sample size of 1,000. As the number of samples increases, the estimate becomes stable. As an approximated measure of the computational efficiency, success rate η is defined as the ratio of the number of samples drawn from the region of interest n_1 to the sample size n; namely, $\eta = n_1 / n$. It should be noted that η is 44.7% (447/1000) in this run. The final estimate of P_f is 0.0012 with COV of 6.24%. The corresponding reliability index β is calculated as 3.035. For comparison, the reliability evaluation by FORM is also summarized in Figure 6.1, with a reliability index β = 2.939 and P_f = 0.0016. Although the reliability index by the importance sampling method is just 3.27% larger than that of FORM, the P_f by FORM is 33.33% larger than that of the importance sampling method as a result of the nonlinear relationship between P_f and β (see Equation 6.3).

To verify the results of the importance sampling method, a reliability analysis is conducted using the crude MCS method. Figure 6.2 shows the convergence of the estimate. It can be seen from this figure that the estimate converges with increasing sample size. The final estimate is a

P_f of 0.0013 with a COV of 5.24%. Note that the success rate is only 0.13% (i.e., 390/300,000 where n = 300,000) in this run for the crude MCS method, which is much lower than that for the importance sampling method (44.7%).

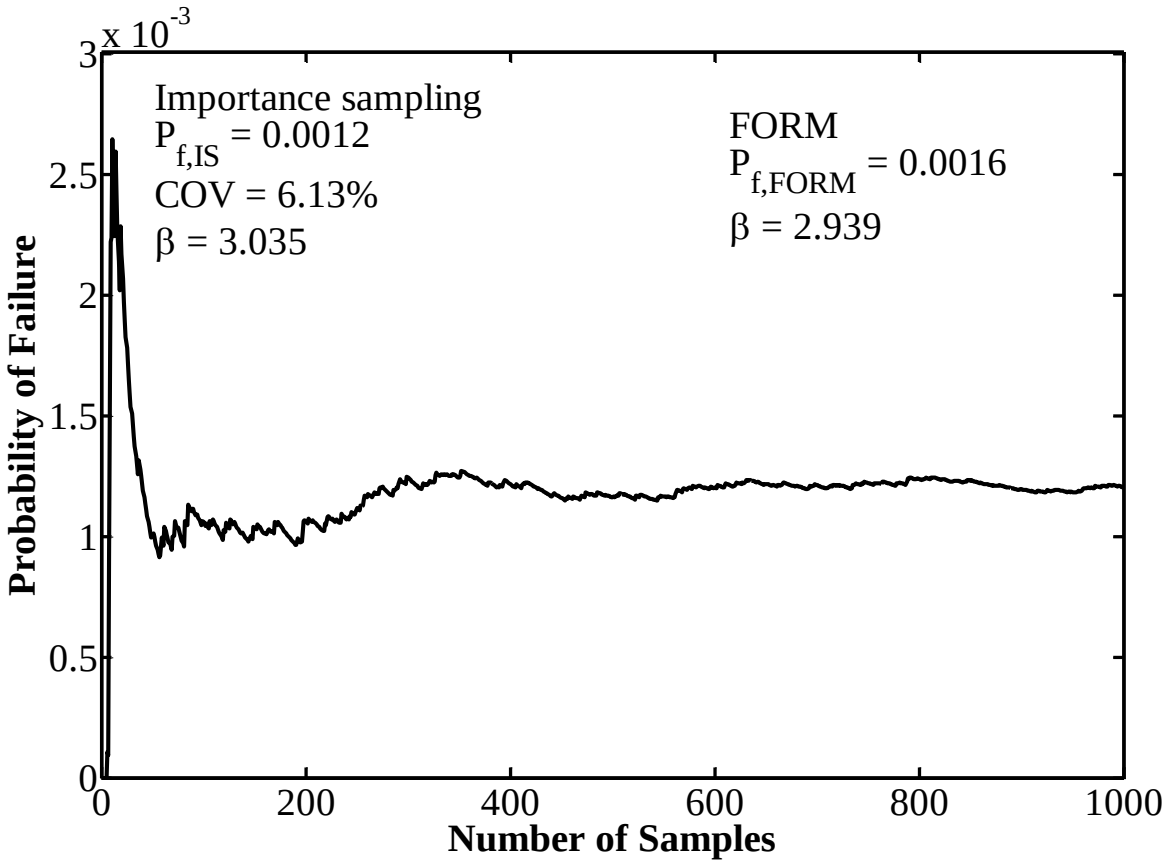

Figure 6.1 Reliability evaluations by IS method and FORM for Example 1

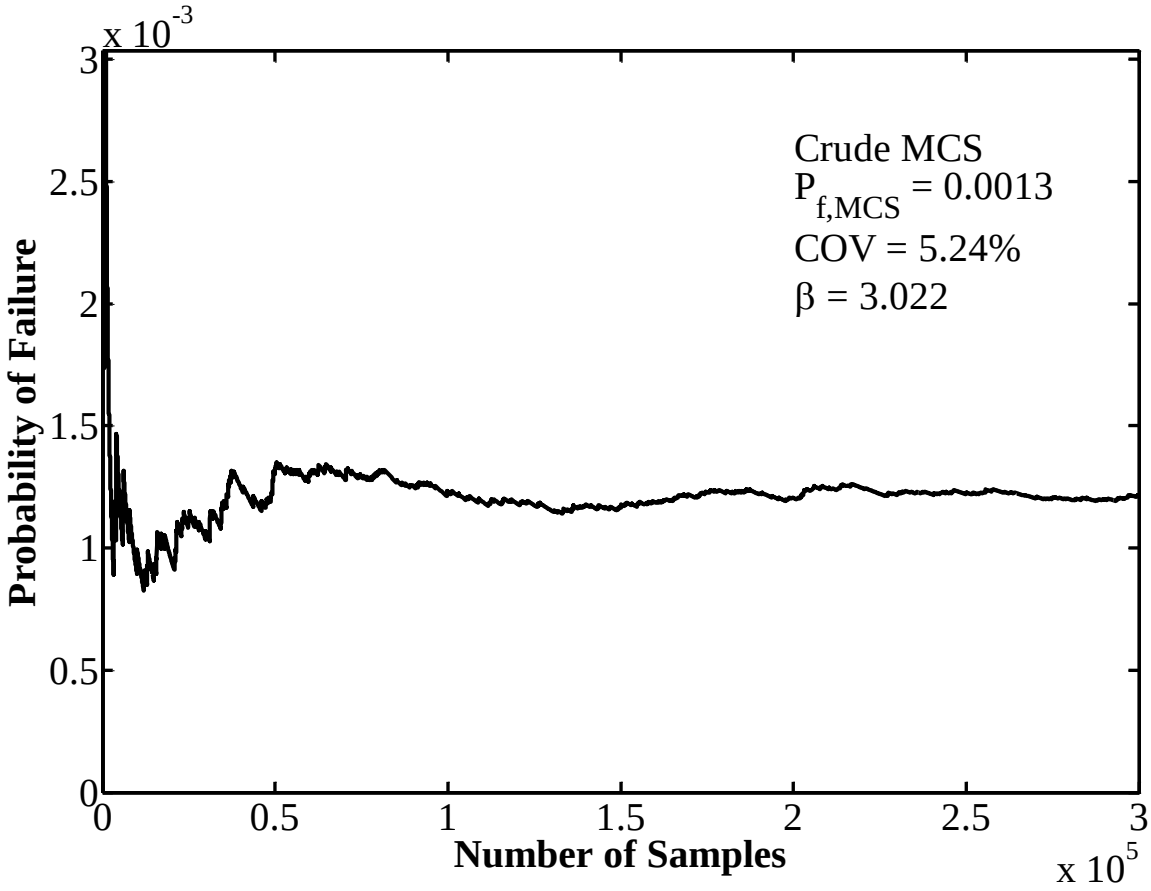

Figure 6.2 Convergence of crude MCS method for Example 1

Figures 6.1 and 6.2 indicate that the estimates of P_f by the importance sampling method and the crude MCS method are very close to each other. The difference between the results is minor and is expected to vanish as the sample sizes become larger. It can be concluded that the proposed importance sampling method can give unbiased estimates, as does the crude MCS method. However, the estimate of P_f by FORM significantly deviates from those of the sampling-based methods. This difference between the FORM estimate and the sampling-based estimates can be primarily attributed to two sources: 1) the limit state function is approximated by response surface method; and 2) the failure surface is replaced by a hyperplane FORM when the limit state function is nonlinear.

In order to investigate the influence of the correlation length θ (a measure of the correlation structure of soil properties) and the axial load Q; both θ and Q are varied while other parameters remain fixed. Figure 6.3 shows the relationships between P_f and the two parameters. It can be observed that P_f increases with increasing axial load. For a given Q, there is a significant variation in P_f if θ is different. It is worthwhile to note that the difference in P_f could be several orders of magnitude, particularly when P_f is a very small number (e.g., $P_f \leq 1/1000$). It can be concluded that considering θ would be critical in reliability analysis. Furthermore, if the correlation length is not properly accounted for, the estimate of P_f would probably become biased.

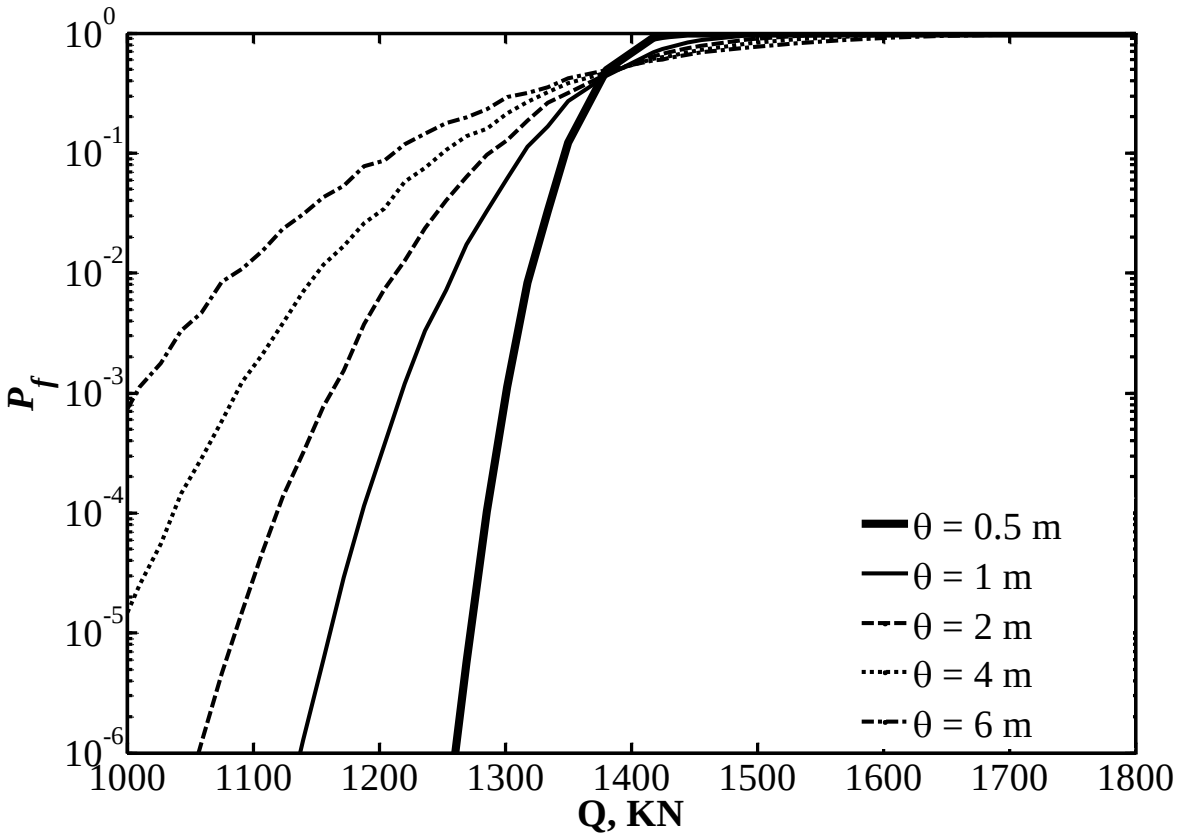

Figure 6.3 Influences of θ and Q

6.5.2 Example 2: Drilled shaft in heterogeneous soil deposit

The objective of Example 2 is to demonstrate the efficiency of the developed importance sampling method in a non-homogeneous clay deposit. Consider a drilled shaft that is 1.0 m (3.28 ft) in diameter and 10.0 m (32.81 ft) in length that is subjected to a compression force of 1400 KN. In contrast to the previous example, the mean of S_u (denoted as μ_{Su}) is varied over the depth z (in meter): the μ_{Su} is 90 KPa (13.05 psi) for the topmost 2.5 m (8.2 ft) of the shaft and then linearly increases at depths below 2.5 m (8.2 ft) as described in the equation μ_{Su} = 83.478+2.609z (KPa). The standard deviation of S_u is 18 KPa (2.61 psi) along the depth and the correlation length θ = 1.2 m (3.94 ft). The failure criterion in terms of vertical displacement is 25 mm (1 in). The reinforcement ratio is taken as 1%. The elastic modulus is taken as 200 GPa (29,000 ksi) for reinforcement and 26.6 GPa (3857 ksi) for concrete. The same *t*-*z* curves and *q*-*w* curves for cohesive soils from AASHTO (2010) are used to represent the soil-pile interactions.

Figure 6.4 shows the convergence of the estimate using the proposed IS based method. The final estimate is 0.00089 with COV of 6.11%, with a corresponding value for β of 3.122. The success rate is η = 45.7% (457/1000). For comparison, the reliability evaluation by FORM is also summarized in Figure 6.4, shows that β is equal to 2.984 (i.e., P_f = 0.0014). To validate the results of the importance sampling method, a reliability analysis using the crude MCS method is conducted, and the convergence of the MCS estimate with a sample size of 400,000 is presented in Figure 6.5. The estimate of P_f by the crude MCS method is 0.00086 with a COV of 5.37%, and the corresponding β of 3.133, which is very close to that of the importance sampling method. Although the reliability indices evaluated by different methods are close to each other, the P_f evaluated by FORM is approximately 60% larger than those of the sampling-based methods!

In order to demonstrate the improvement in computational efficiency of the importance sampling method, the sample sizes of the importance sampling method and the crude MCS method are compared when the estimates of P_f achieve the same COV by both methods. Taking the average of the results of 50 runs, the mean of $P_{f,\mathrm{IS}}$ is equal to 0.000891, while the average sample size needed to achieve a COV of 5% using the importance sampling method is 1570. Using $P_f = P_{f,\mathrm{IS}} = 0.000891$ and Equation (6.6), the sample size n of the crude MCS method is calculated as 448,533 – which is 286 times that of the importance sampling method! In this example, the difference in sample size is two orders of magnitude.

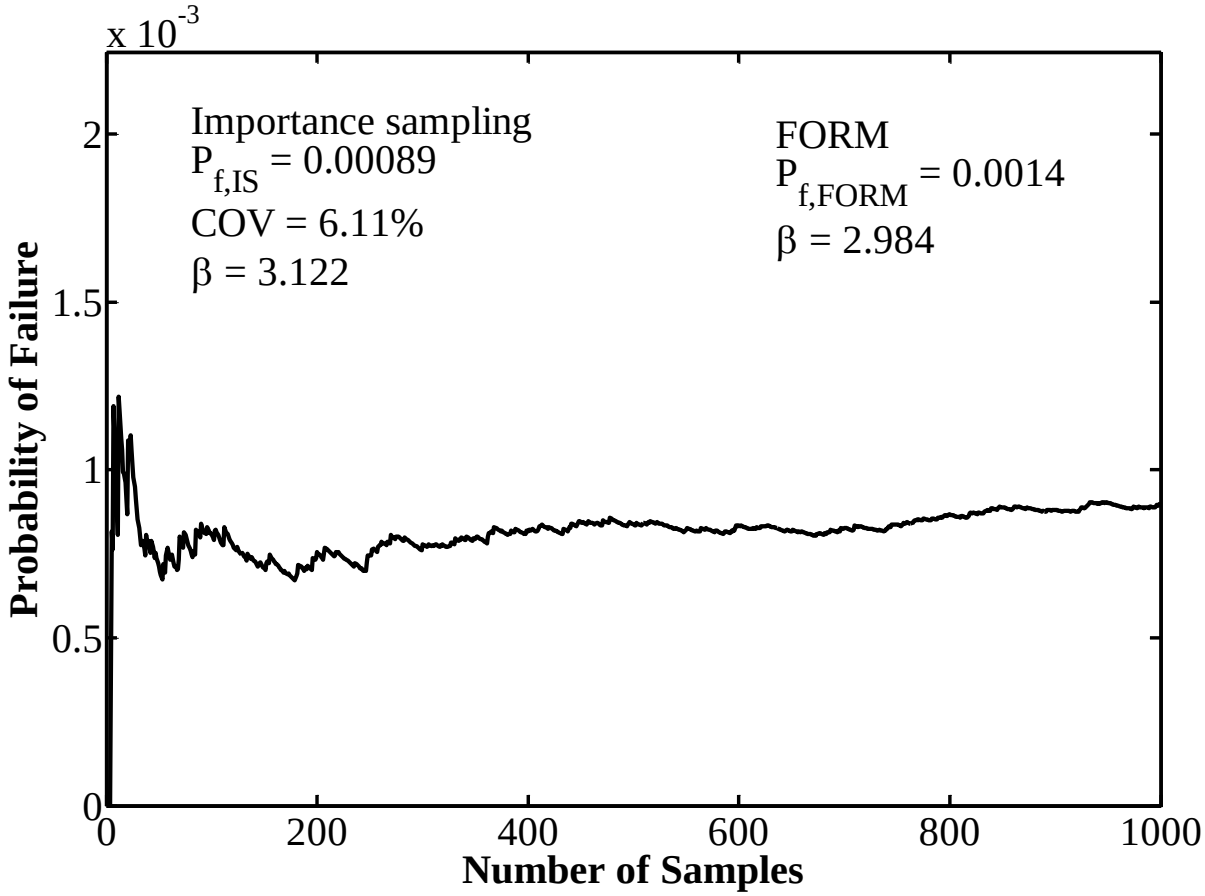

Figure 6.4 Reliability evaluations by IS method and FORM for Example 2

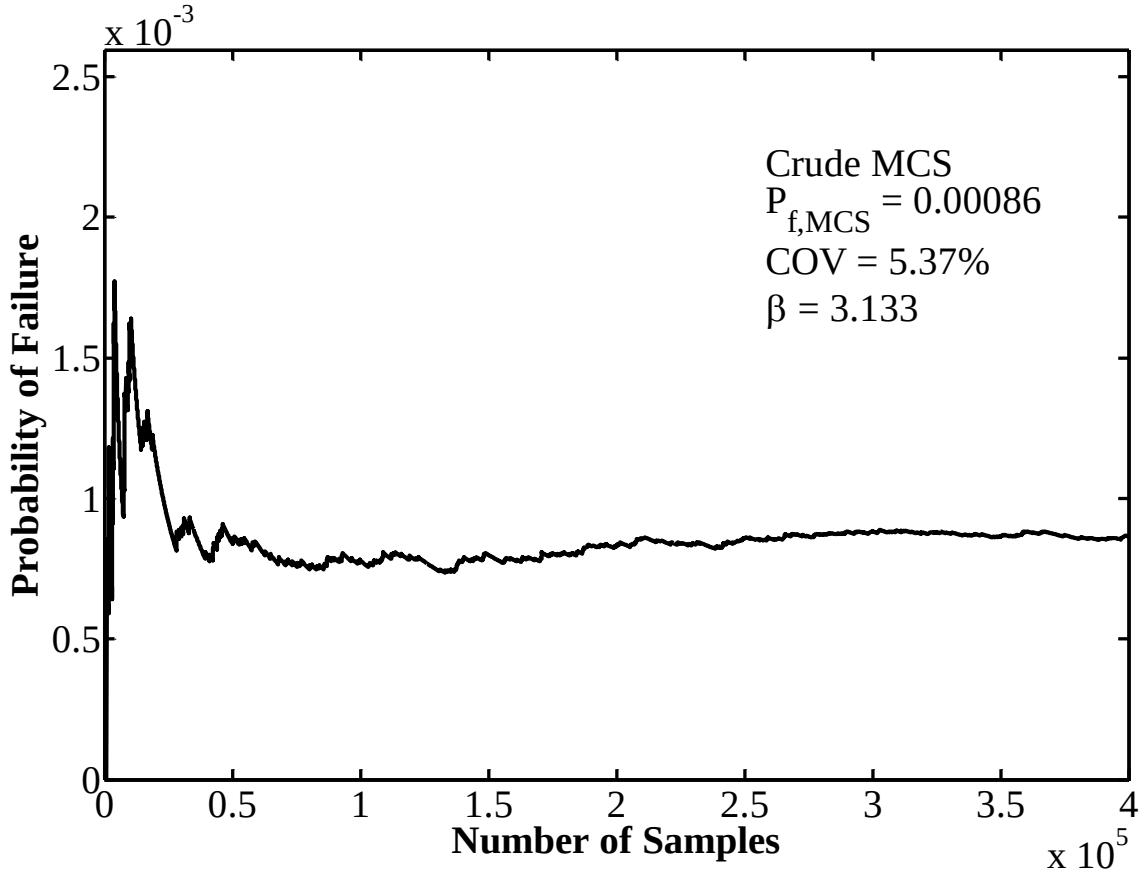

Figure 6.5 Probability of failure by crude MCS method for Example

In order to further investigate the performance of the proposed importance sampling method at different probability levels, the axial load Q is varied while other parameters in this example remain unchanged. Figure 6.6 shows the sample sizes that correspond to a COV of 5% for the estimates of P_f and the associated success rates when the results of 50 runs are averaged. As a result of the variation in the axial load, the probability of failure increases from 2.06×10^{-6} to 0.74. It can be seen that the average sample size of the importance sampling method slightly decreases from 2,555 to 518 until $P_f \geq 42.5\%$. Meanwhile, the average sample size of the crude MCS method decreases from 1.94×10^{8} to 140. In this example, the difference in sample size between the two methods is at least two orders of magnitude when $P_f \leq 1/1000$. Moreover, the difference becomes more noticeable when P_f becomes smaller.

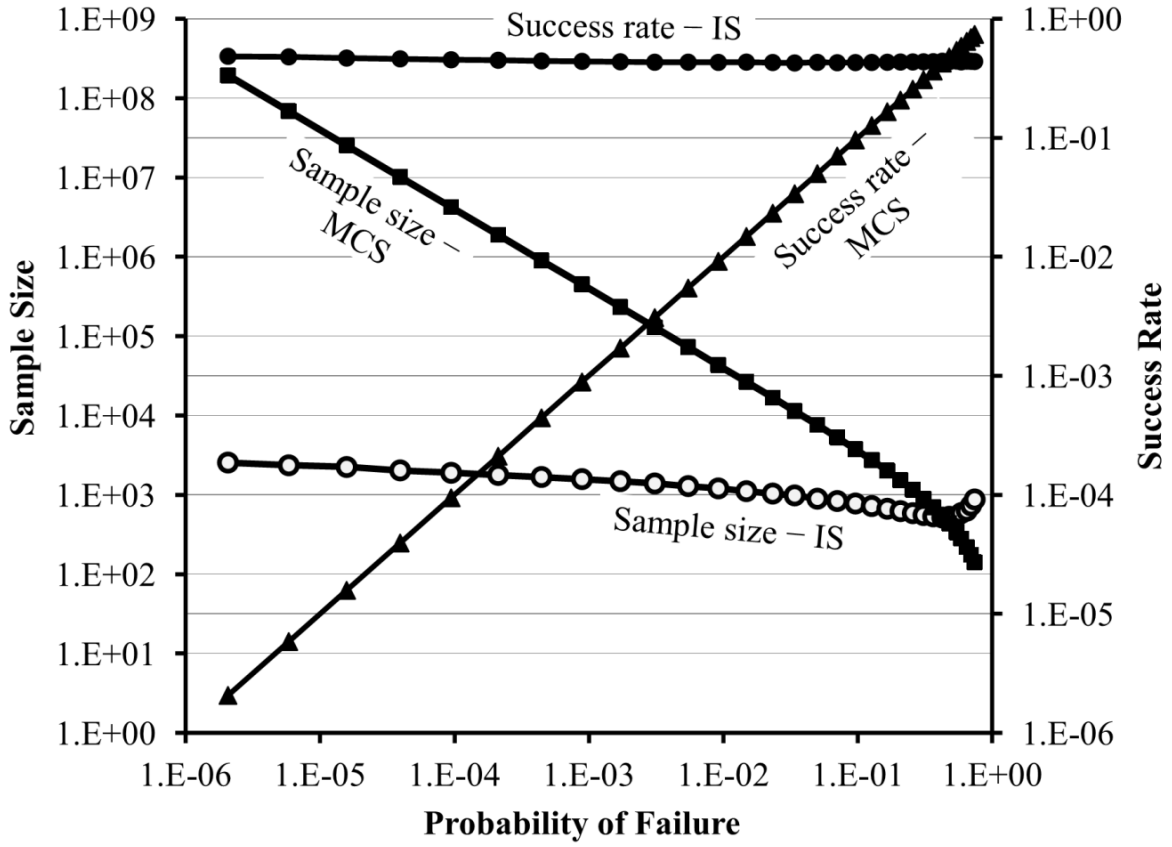

Figure 6.6 Computational efficiency of IS method

It can be noticed that the sample size in the crude MCS method is 75,900 times that of the importance sampling method when $P_f = 2.06 \times 10^{-6}$. However, the sample size of the crude MCS method is smaller than that of the importance sampling method when P_f is approximately equal to or larger than 50%, implying that the crude MCS method is more efficient than the importance sampling method when the failure probability is very large. This finding might be explained by the success rate. In this example, the average success rate of the importance sampling method decreases from 48.5% to 43.8%, while that of the crude MCS method increases from 2.06×10^{-6} to 0.74, which is equal to the corresponding P_f. When the failure probability is large, it is more efficient to draw samples from the failure region in the crude MCS method.

Based on the comparison in Example 2, it is clear that the importance sampling method brings considerable improvement in computational efficiency over the crude MCS method, particularly when P_f is a very small number. However, instead of the importance sampling method, the crude MCS method should be used if P_f is large (e.g., $P_f \geq 50\%$), from the standpoint of computational efficiency.

6.6 Summary and conclusions

The crude MCS method is known to be computationally demanding. In order to increase the computational efficiency, this research presents an importance sampling–based algorithm that can be applied to conduct fast reliability evaluation for axially loaded piles. The spatial variability of soil properties is considered by random field modeling, which characterizes the random field of a soil parameter by factoring the field mean, the field variance, the probability distribution, and the correlation structure into the model. In importance sampling, the instrumental function is constructed by shifting the original PDF such that the mean is at the point having the maximum probability density of the failure surface. A computer program has been developed in order to apply the proposed algorithm for conducting reliability analysis. Based on the two examples of drilled shaft design presented in this chapter, the following conclusions can be made:

1. The proposed importance sampling method gives the same unbiased estimate of the failure probability as the crude MCS method.
2. The proposed importance sampling method is much more efficient than the crude MCS method when evaluating a small probability of failure (e.g., $P_f \leq 1/1000$). By drawing more samples from the region of interest, the proposed method will achieve a faster rate

of convergence. With the same sample size, the estimate obtained by using the importance sampling method would have a much smaller coefficient of variation than the estimate obtained by the crude MCS method.

3. The importance sampling method is highly efficient in variance reduction for the estimate, and it is recommended to use the importance sampling method in the evaluation of small probabilities of failure.
4. It is demonstrated that the probability of failure is sensitive to the correlation length, θ. If θ is not considered in reliability assessment, the estimated probability of failure would probably be biased. Therefore, considering correlation length is warranted in the reliability analysis of deep foundations.

5. The probability of failure evaluated by the commonly used first order reliability method (FORM) significantly deviates from those of Monte Carlo statistical methods, although the reliability index by FORM is close to those of Monte Carlo statistical methods. The differences in the failure probabilities between FORM and Monte Carlo statistical methods are primarily attributed to the approximation of the limit state function in the response surface method and the linear truncation of the limit state function in the FORM.

CHAPTER 7. SPATIAL VARIABILITY OF SOIL PROPERTIES

7.1 Introduction

As a methodology of reliability based design (RBD), performance-based design approaches (Fan and Liang 2012, 2013a, 2013b) have been proposed in which the design criteria are defined in terms of allowable displacements. For drilled shaft under axial loading, the design criterion is defined with respect to the vertical movement (w) at the top of the shaft. For drilled shaft under lateral loading, the design criterion is defined with respect to the lateral deflection (δ) and the angular distortion (ψ) at the top. If any of the displacements (δ, ψ and w) is greater than the corresponding displacement, failure is to occur. That is

$$I\left(d, d_a\right) = \begin{cases} 1, & \text{for } d \geq d_a \\ 0, & \text{for } d < d_a \end{cases} \tag{7.1}$$

where $I(\cdot)$ is an indicator function, $d = \delta$, ψ or w, and d_a denotes the corresponding allowable displacement. In the proposed approaches, Monte Carlo simulation (MCS) is applied to estimate the probability of failure $P_{f,d}$

$$P_{f,d} = \frac{1}{K}\sum_{i=1}^{K} I_i \tag{7.2}$$

where K is the number of simulations. When the number of simulations is sufficiently large, the estimate in Equation (7.2) will approach its exact value. The advantage of using MCS method is that the estimate in Equation (7.2) is unbiased. Moreover, it is mathematically straightforward.

In order to calculate the probability of failure, the uncertainties associated with soil properties need to be accounted for. In the proposed performance based design approaches, the soil properties are modeled as random fields which are statistically characterized by a mean μ, a

standard deviation σ and a correlation length θ. The correlation length is needed to define a correlation function. For example, the one-dimensional Markovian correlation function is given below

$$\rho(\tau,\theta) = \exp\left(-\frac{2|\tau|}{\theta}\right) \tag{7.3}$$

where $\rho(\cdot)$ gives the correlation coefficient between two points and τ is the separation distance between the two points. The mean measures the center of a dataset, the variance measures the dispersion from the mean, and the correlation length measures how rapidly a random field varies in space. It has been demonstrated that the statistical descriptors (μ, σ and θ) have a significant impact on $P_{f,d}$ and the consideration of θ is important in reliability analysis (see Fan and Liang 2012, 2013a).

In RBD, the probabilistic model of soil profiles is as important as the computational methods of reliability analysis. The stochastic nature of the soils would directly influence the response of geotechnical structures to external loads, thus affecting the results of the reliability analysis. A realistic probabilistic model for soils is an essential part of the input to the computational methods for the reliability analysis of any geotechnical structure. As a part of the performance-based design methodology, it is necessary to develop statistical guidelines to characterize the uncertainties of soil profiles. The objectives of this study include:

1. To develop computational methods of determining the statistical descriptors (μ, σ and θ) of a random field for a soil property.
2. To identify the soil stratifications at a given location;

To make the computational methods usable to practicing engineers, data from standard penetration test (SPT) will be used as a means to estimate the statistical descriptors. SPT is

widely used in subsurface investigations, and soil samples can be retrieved during testing. The advantage of using SPT is that the retrieved soil samples allow for identification of soil stratification. The soil stratifications would dictate the use of the load transfer curves that may differ from one soil to another. It should be noted that the identification of soil stratification is as important as the determination of the statistical descriptors, because the knowledge of soil stratifications would directly affect the modeling of the soil-structure interaction. As a result, the displacements of drilled shafts under axial and lateral loads would be influenced, thus affecting the calculation of the failure probability. In this research, the identification of soil stratifications and the computational methods to determine the statistical descriptors will be introduced. Finally, real data from a site investigation will be used as an example to demonstrate the proposed approach.

7.2 Computational Methods

In the proposed performance-based design methodology, each soil property such as undrained shear strength (S_u) for clay and effective friction angle (ϕ') for granular soils is modeled as a random field which is statistically characterize by a mean μ, a standard deviation σ, and a correlation length θ. In order to accurately determine the statistical descriptors (μ, σ and θ) of a random field, a subsurface investigation should be performed on the construction site and a certain amount of soil data needs to be gathered to conduct a realistic statistical analysis. Note that in a subsurface investigation, the cone penetration test (CPT) and the standard penetration test are the most commonly used tests. In CPT, the cone tip resistance is recorded at every 2-cm or 5-cm interval and is measured continuously along the depth. Because of the nature of the data, CPT data may be more amenable to statistical analysis and probabilistic modeling. The random field based modeling for CPT data is available (see Fenton 1999). Unfortunately, SPT data is

quite different from CPT data. In SPT, the blow count is recorded for a 15-cm (6-in.) interval and may not be measured continuously. It is quite common that the blow counts may be missing for some intervals along the depth. Moreover, there are many factors that affect the SPT and its results (Sabatini et al. 2002), which make it difficult to repeat the SPT results. As a result, the analytical method in (Fenton 1999) for CPT data does not work for SPT data in most cases. However, in some construction projects, only the SPT data is available, and the CPT data is not available because of the cost of conducting the test. In order to make the developed performance-based design approach usable to those projects, the statistical guidelines and the computational methods designated to SPT data should be developed.

The objective of this section is to develop a probabilistic model for SPT data and determine the statistical descriptors of soil properties using SPT data. The following steps are taken:

1. Two commonly-used empirical correlations with SPT data are employed to obtain an estimate of the soil strength parameter (S_u and ϕ') that will be viewed as observations in Bayesian approach.
2. The statistical descriptors (μ, σ and θ) are parameterized and a probabilistic model is established to evaluate the probability of observing the SPT data.
3. Given the SPT data, Bayesian approach is applied in which the statistical descriptors (μ, σ and θ) are the parameters of the probabilistic model.
4. Markov chain Monte Carlo is applied to draw samples of μ, σ and θ, according to the established probabilistic model in Step 3.
5. Statistical analysis is conducted using the samples of μ, σ and θ, and the estimates of μ, σ and θ can be obtained accordingly.

7.2.1 Correlations with SPT Data

In SPT, only the second and third blow counts (denoted as N_1 and N_2) are summed to obtain the N value, where $N = N_1 + N_2$. Note that the N value can be converted to undrained shear strength for cohesive soils or effective friction angle for granular soils, employing commonly used empirical correlations (see Das 2011):

$$S_u = 0.29 N_{60}^{0.72} \cdot p_a \tag{7.4}$$

$$\phi' = \tan^{-1}\left[\frac{N_{60}}{12.2 + 20.3\left(\frac{\sigma'_0}{p_a}\right)}\right] \tag{7.5}$$

where N_{60} ($N_{60} = N \cdot ER/60$ where ER is the energy efficiency) is the N value corrected to 60% energy efficiency, p_a is the atmospheric pressure (p_a = 101.325 KPa), $\tan^{-1}(\cdot)$ denotes the inverse tangent, and σ'_0 is the effective vertical stress. Note that other correlation equations may be used to obtain S_u or ϕ'. It is recognized that the correlation equations have model error. However, the calibration of the model error is beyond the scope of the study.

7.2.2 Bayesian Approach

Because of the nature of the data, the method of moments in which the samples are averaged to determine the mean and variance may not work well on SPT data. In SPT, the blow counts are recorded along the depth, which gives a rough indication of the soil strength. It is well understood that soil properties along the depth may change for a variety of reasons. For example, the undrained shear strength of normally consolidated clay may increase with depth, as a result of the increasing confining stress. In this case, if the samples of undrained shear strength obtained at different elevations are used to conduct a pooled statistical analysis directly, the

estimate of the mean will be probably erroneous and the associated standard deviation would be overestimated! Furthermore, the sample size of the blow counts for a particular geological stratum may be limited, depending on the thickness of the soil stratum. There is one blow count for every 0.152-m (6 in.) interval. Although there may be multiple soil borings at the construction site, the *N* values collected at different locations should not be pooled to form a larger sample size. This is because the samples from different locations may not come from the same population, from the standpoint of statistics. Hence, it may be problematic to directly evaluate the statistical averages using the method of moment.

As an alternative to the method of moments, Bayesian approach can be applied to model the uncertainties of SPT data. The objective of applying Bayesian approach is to estimate the statistical descriptors (μ, σ and θ) using SPT data. In this study, the parameters of interest are $\boldsymbol{\lambda} = (\mu, \sigma, \theta)$ and will be treated as random variables in the Bayesian approach. Given any observational data $\boldsymbol{X}$, the posterior probability density distribution (PDF) of $\boldsymbol{\lambda}$ can be expressed as

$$f''(\boldsymbol{\lambda}) = c \cdot L(\boldsymbol{\lambda} \mid \boldsymbol{X}) \cdot f'(\boldsymbol{\lambda}) \tag{7.6}$$

where $f'(\boldsymbol{\lambda})$ and $f''(\boldsymbol{\lambda})$ are the prior PDF and posterior PDF, respectively; c is a normalizing constant such that the integration of $f''(\boldsymbol{\lambda})$ over the entire space would be unity; and $L(\boldsymbol{\lambda}|\boldsymbol{X})$ is the likelihood function that gives the probability of observing $\boldsymbol{X}$ given that the parameters of the underlying probabilistic model is $\boldsymbol{\lambda}$.

To implement the Bayesian approach, observational data and a probabilistic model of the data are needed. In this study, the observational data is the estimated soil properties (S_u and ϕ') that are converted using the empirical correlations. In order to establish a probabilistic model for the SPT data, three assumptions are introduced:

A1. Each N value (450-mm interval) is considered as a unit, and the corresponding second and the third blow counts (N_1 and N_2) of the unit are used as two observations of the soil properties in the Bayesian approach;

A2. The soil properties are second-order stationary in the unit, that is, the mean and the standard deviation are constant over the interval; and

A3. The soil properties are lognormally distributed.

As indicated in Assumption A1, there are two blow counts (N_1 and N_2) in a unit. Since each blow count just corresponds to a 15-cm interval while the SPT N value corresponds to a 30-cm interval, an "equivalent" N_{60} is defined as

$$N'_{60} = 2N_i \frac{ER}{60}, \quad i = 1, 2 \tag{7.7}$$

where N'_{60} is the equivalent N_{60}, and ER is the energy efficiency same as in $N_{60} = N \cdot ER/60$. With the equivalent N_{60}, the soil properties (S_u and ϕ') can be obtained according to the empirical correlations.

With Assumption A2 and A3, the probability of observing the SPT data (N_1 and N_2) can be expressed as

$$L(\lambda \mid \boldsymbol{X}) = \frac{1}{2\pi\sigma\sqrt{1-\rho^2}} \exp\left[-\frac{1}{2\sigma^2\left(1-\rho^2\right)} \left(\boldsymbol{X}-\mu\right)^T \boldsymbol{R} \left(\boldsymbol{X}-\mu\right) \right] \tag{7.8a}$$

$$\boldsymbol{R} = \begin{pmatrix} 1 & -\rho \\ -\rho & 1 \end{pmatrix} \tag{7.8b}$$

where $L(\cdot)$ denotes the likelihood function, $\boldsymbol{X} = [\ln(x_1), \ln(x_2)]^T$ where $x = S_u$ or ϕ', the subscripts "1" and "2" of x corresponds to N_1 and N_2, respectively; $\ln(\cdot)$ denotes the natural logarithm and $\exp(\cdot)$ denotes the exponential function; μ and σ are the mean and the standard deviation of the random variable $\ln(x)$, respectively; the superscript "T" denotes transpose; and ρ is the

correlation coefficient between $\ln(x_1)$ and $\ln(x_2)$. Indeed, ρ is a function of the parameter θ, that is, $\rho = \rho(\theta)$. Note that the exact form of $\rho(\theta)$ is dependent upon what kind of correlation function is in use. An example of the correlation function is given in Equation (7.3), where τ is equal to 0.152 m (6 in.). As a result of the functional relationship between the correlation coefficient ρ and θ, the parameter vector $\boldsymbol{\lambda}$ is re-written as (μ, σ, ρ) for notational simplicity. Since the soil properties are lognormally distributed according to Assumption A3, the logarithms of S_u or ϕ' will be normally distributed. It is preferable to have normally distributed variables, because an analytical form of the joint probability density function is available. Now the advantage of invoking Assumption A2 and A3 become clear.

In addition to the likelihood function, the prior PDF of the parameters $\boldsymbol{\lambda} = (\mu, \sigma, \rho)$ should be determined. Prior to the statistical analysis, the knowledge of the parameters is limited. In Bayesian statistics, it is common to assume that the parameters of interest (μ, σ and ρ) follow uniform distributions or normal distributions. In most cases, there are no general guidelines to determine the corresponding distribution parameters. Rough estimates of the parameters based on the observational data should be adequate. In the context of SPT, the soil properties ($x = S_u$ or ϕ') can be estimated according to the empirical correlations with the N value. With the estimated soil properties, the mean μ_x and the standard deviation σ_x of the soil properties may be assumed according to those used in the study by Phoon and Kulhawy (1999). Since the soil properties are lognormally distributed, the distribution parameters ($\mu_{\ln x}$ and $\sigma_{\ln x}$) of $\ln(x)$ can be calculated as

$$\mu_{\ln x} = \ln\left(\frac{\mu_x^2}{\sqrt{\mu_x^2 + \sigma_x^2}}\right) \tag{7.9}$$

$$\sigma_{\ln x} = \sqrt{\ln\left(\sigma_x^2 / \mu_x^2 + 1\right)} \tag{7.10}$$

Once the distribution parameters are determined, the range of $\mu_{\ln x}$ and $\sigma_{\ln x}$ can be roughly estimated. Physically, the correlation coefficient between adjacent soil properties should be positive. Thus, the prior PDF of the parameters $\boldsymbol{\lambda}$ can be expressed as follows:

$$f'(\boldsymbol{\lambda}) = f'(\mu,\sigma,\rho) = f_{\mu}(\mu)\cdot f_{\sigma}(\sigma)\cdot f_{\rho}(\rho) \tag{7.11}$$

where $f_{\mu}(\cdot)$, $f_{\sigma}(\cdot)$, and $f_{\rho}(\cdot)$ denote the PDF of μ, σ, and ρ, respectively. Note that other probability distributions may be assumed as the prior PDF for μ, σ and ρ, depending on the setting of the problem.

7.2.3 Implementation Using Markov Chain Monte Carlo

The objective of applying Markov chain Monte Carlo (MCMC) is to draw the samples of μ, σ, and ρ according to the formulation of the Bayesian approach presented previously. The advantage of using MCMC is that the normalizing constant c in Equation (7.8) can be avoided. In MCMC, the samples can be drawn directly without knowing c. More importantly, it is more straightforward to conduct statistical analysis using the resulting samples generated through MCMC, instead of using numerical integration with respect to the posterior probability density function. The advantages of using MCMC will be clear in the following paragraphs. The details of MCMC can be found in Robert and Casella (2004). Figure 7.1 shows the flow chart of the computational method. The following steps are taken to implement the computational method:

1. Establish the likelihood function (see Equation 7.8a).
2. Assume a prior PDF of the parameters (see Equation 7.11).
3. Assume an initial point of the parameters to start the simulation of the parameter using MCMC.
4. Conduct statistical analysis of the resulting samples.
5. Obtain the estimates of μ, σ and ρ.

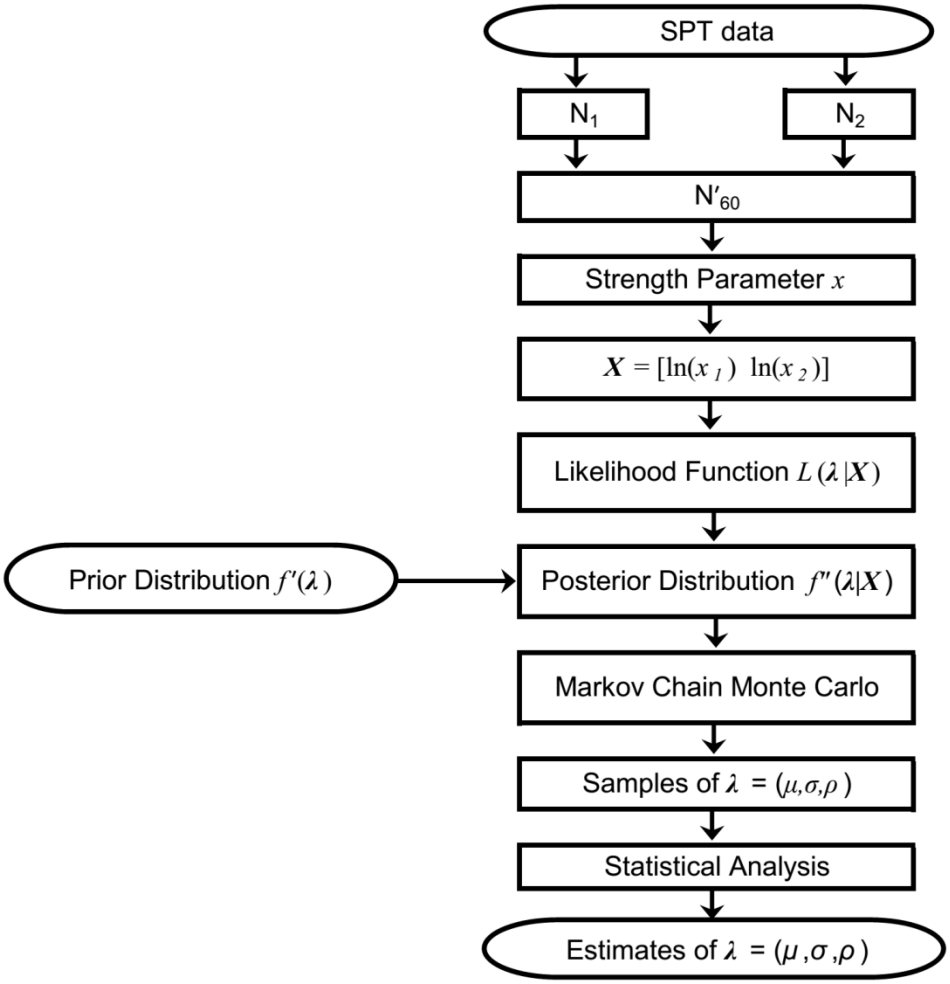

Figure 7.1 Flow Chart of the computational method

In this study, the computer program MATLAB© is used to implement MCMC. Through MCMC, a sequence of random samples can be obtained and is denoted as $\boldsymbol{U} = (u_1, u_2, \ldots, u_n)$ where $u = \mu$, σ or ρ, and n is the length of the sequence. The estimates of the mean for the parameter u can be expressed as follows:

$$\mu_u = \frac{1}{n}\sum_{i=1}^{n} u_i \tag{7.12}$$

where μ_u denotes the mean of u. The mean of the samples may be used as an estimate of the parameter. Note that the estimate of θ can be obtained by plugging the mean of ρ into Equation (7.3).

7.3 Geostatistical Analysis

The methods of estimating statistical parameters (μ, σ and θ) are discussed previously. Once the three statistical parameters are available, and the soil variability model is defined. However, in practice, drilled shafts may not be installed at exactly the same location where soils are sampled for analysis. The objective of this section is to present the geostatistical principles that can be applied to interpret the soil profile.

A number of geostatistical techniques called kriging are available for estimating unknown values based on available observations. Kriging is a collection of generalized linear regression methods which includes ordinary kriging, polygon, triangulation, local sample mean, and inverse distance method. Basically, a kriging estimator is a linear combination of known or observed data. The accuracies and comments about these methods can be referred to in the literature (Isaaks and Srivastava 1989). For illustration purposes, the inverse distance method is presented as follows:

$$T_0 = \sum_{j=1}^{m} w_j T_j \tag{7.13a}$$

$$w_j = l_j^{-v} \Big/ \sum_{i=1}^{m} l_i^{-v}, j = 1, 2, \cdots, m \tag{7.13b}$$

where T_0 is an estimate of the unknown value, T_j is the j-th observation with a distance of l_j to the desired location, w_j is the relative weight for the j-th observation, m is the number of observations, and v is a power term that can be adjusted. A different u would usually result in a

different estimate. If v is taken as 1.0, the weights are inversely proportional to the distance. In the inverse distance method, the estimator is a weighted mean of nearby samples. The advantage of using inverse distance method is that more weight is given to the closest samples and only the distances are needed to determine the weights. It should be noted that kriging techniques other than the inverse distance method may be possible alternatives, depending on the data at hand and the specific settings of the problem.

Note that in Equation (7.13a), the term "T" is a quantity of interest. For example, it can be the thickness of a soil layer, a strength parameter, or a statistic of soil properties. In application, the distances between the desired location and the locations that have observations need to be determined first. Once that information is obtained, the relative weight of each observation is evaluated by assuming a power term v.

7.4 Example

The example is taken from a project that is intended to create a grade-separation between State Route 58 and the existing CSXT Railroad tracks in Wellington, Ohio. To carry the railroad tracks, a bridge was constructed and the bridge is supported by two abutments, each of which consists of 17 drilled shafts. One of the drilled shafts is shown in Figure 7.2. In this figure, the locations where SPT was conducted are denoted as BR1 and BR2 The dead axial load applied to the drilled shaft is Q_D = 351.39 KN (79 kips), while the live axial load is Q_L = 631.62 KN (142 kips). The lateral load of V_D = 162.72 KN (36.58 kips) applied at the top of the drilled shaft results from the lateral earth pressure and should be considered as dead load. All the given loads are unfactored. The load eccentricity of the lateral load is 1.69 m (5.54 ft) and will be used to calculate the bending moment at the top of the drilled shaft. The elevations at the top at the three locations are 258.3 m (847.44 ft) and 258.0 m (846.46 ft), respectively. The maximum allowable

displacements are specified as 0.0254 m (1 in) for both vertical movement and lateral deflection. The angular distortion at the top is not considered in this example. Using load and resistance factor design approach, the final design is a drilled shaft that is 25.30 m (83 ft) in length and 1.07 m (42 in) in diameter. The cross section is reinforced by a total of 20 No. 11 rebars, and the cover thickness is 7.6 cm (3 in.). Note that the elevation of the top of the drilled shaft is 253.0 m. Hence, the drilled shaft does not penetrate through the topmost three soil layers.

7.4.1 Subsurface Investigation

It is known that the site lies within the glaciated portion of Ohio where the topmost soils consist of moraine materials. From the site investigation, the general subsurface conditions can be described in the descending order as follows:

1. 0.05 m (2 in) to 0.30 m (0.99 ft)of topsoil;
2. 0.91 m (2.99 ft) to 5.18 m (17 ft) of stiff to very hard dark brown mottled with gray silt and clay;
3. 2.60 m (8.53 ft) to 8.08 m (26.51 ft) of hard gray silt, and soft to medium stiff brownish gray clay;
4. 1.98 m (6.5 ft) to 4.72 m (15.49 ft) of very stiff to hard brown and gray clay;
5. 5.50 m (18 ft) to 9.14 m (30 ft) of stiff to hard gray and brown clay, silty clay and some silt;
6. SPT was terminated at the depth of 30.39 m (99.7 ft) at BR1 and 28.99 m (95.1 ft) at BR2 after very dense sand and silt.

The SPT data are shown in Figure 7.3. The ground water is found at the depth of 13.10 m (43 ft) at BR1 and 20.7 m (67.91 ft) at BR2.

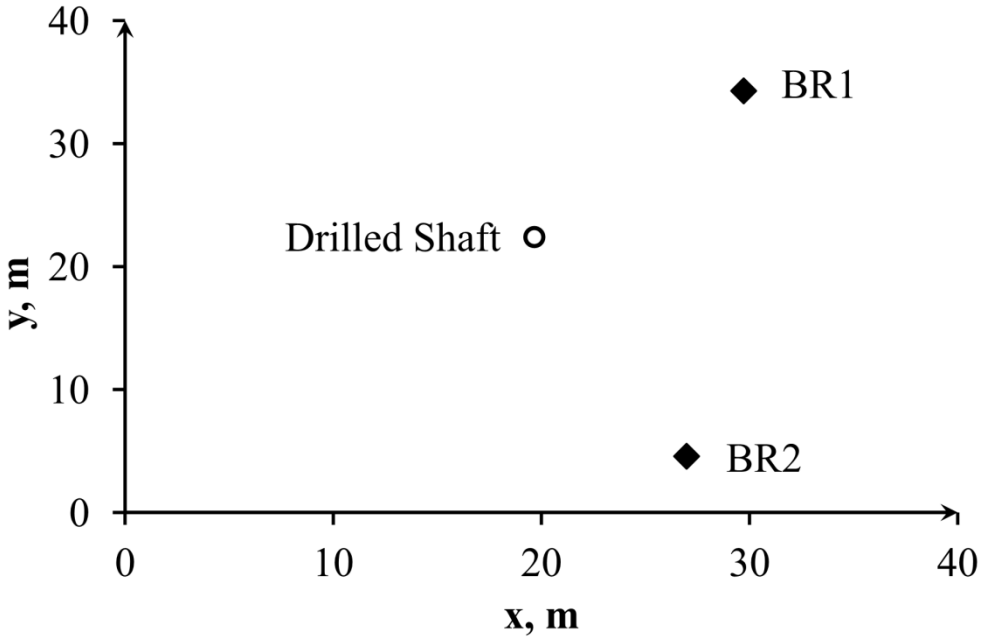

Figure 7.2 Layout of borings and drilled shaft

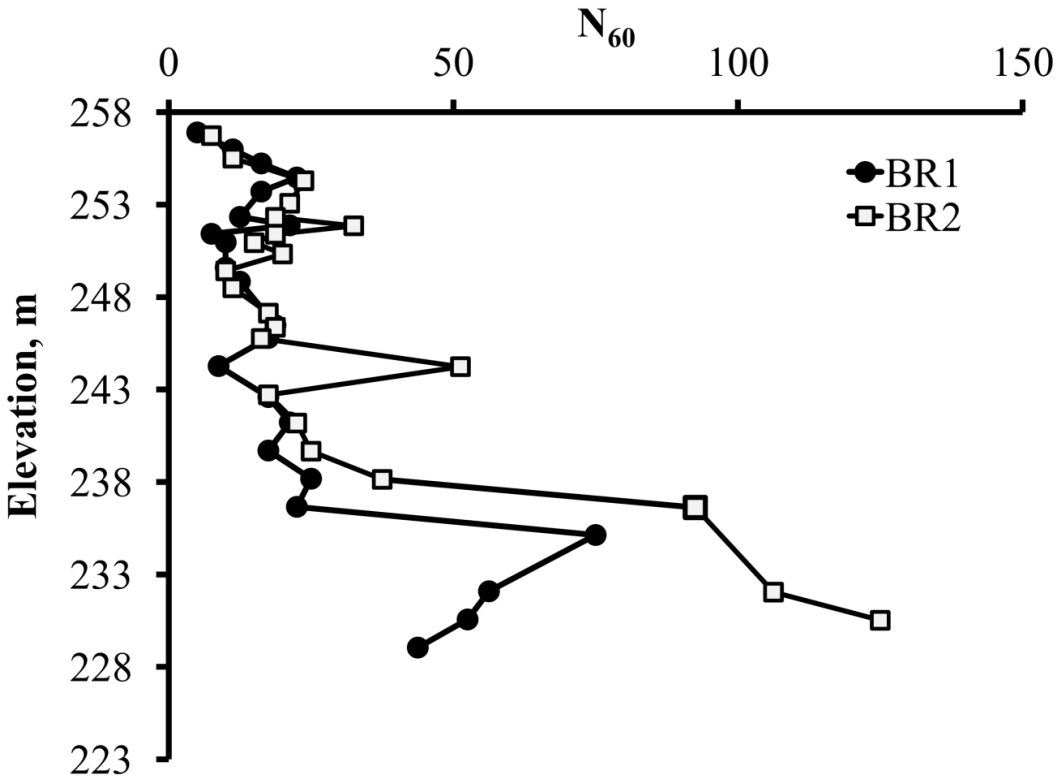

Figure 7.3 SPT data of the project

7.4.2 Random Field Modeling Using SPT Data

The proposed method is applied to establish the probabilistic model for soil parameters. For demonstration purposes, the N value from a silt and clay layer at BR1 is used as input where N_1 = 2, N_2 = 2, and ER = 75%. Hence, the corresponding N'_{60} = 5 for both N_1 and N_2. The resulting undrained shear strength of x = 93.62 KPa (13.57 psi) is obtained using Equation (7.4). Next, the observational vector $\boldsymbol{X}$ = [ln(93.62), ln(93.62)] = [4.54, 4.54]. Plugging $\boldsymbol{X}$ into Equation (7.8a), the likelihood function $L(\boldsymbol{\lambda}|\boldsymbol{X})$ can be obtained. According to Phoon and Kulhawy (1999), the COV of undrained shear strength can be assumed as 25%. Taking advantage of the lognormality assumption for soil properties and applying Equation (7.9) and Equation (7.10), the distribution parameters of undrained shear strength can be calculated as $\mu_{\ln x}$ = 4.414 and $\sigma_{\ln x}$ = 0.500 given μ_x = 93.62 KPa (13.57 psi) and σ_x = 50.00 KPa (7.25 psi). Following the steps shown in the flow chart, it is assumed that μ follows a normal distribution with mean of 4.414 and COV of 40%, σ follows truncated normal distribution ($\sigma > 0$) with mean of 0.500 and COV of 40%, and ρ follows the standard uniform distribution. With all these inputs, the built-in function "slicesample" of *MATLAB*© is run to implement MCMC. Accordingly, the random samples of μ, σ, and ρ can be drawn and shown in Figure 7.4. In order to reduce the effect of the initial value that is needed to start the Markov chain, the first 200 samples are discarded. It can be seen from Figure 7.4 that the samples generated by MCMC converge to the posterior distribution. Figure 7.5 show the posterior marginal cumulative distribution functions (CDF) of μ, σ and ρ. It can be seen that the CDFs of μ and ρ become steeper with the incorporation of the observational data. However, the posterior CDF of σ is almost the same as the prior CDF. These observations indicate that the incorporation of the observational data is effective in reducing the variability of μ and ρ but is ineffective for σ. The mean values of μ, σ,

and ρ are 4.549, 0.502 and 0.663, respectively. The resulting correlation length θ can be calculated as 0.742 m (2.43 ft) by plugging a ρ value of 0.666 into Equation (7.3). By employing Equation (7.9) and Equation (7.10), the mean and the standard deviation of the undrained shear strength are determined to be 107.204 KPa (15.54 psi) and 57.353 KPa (8.31 psi), respectively.

The same computational procedures can be repeated for the remaining SPT data. The computational results for the boring are presented in Table 7.1 for BR1 and in Table 7.2 for BR2; in these tables, the "Soil Strength" column gives the values for the undrained shear strength or the effective friction angle that are calculated according to the empirical correlations. Moreover, the "μ_x" column gives the local average of soil properties for the interval in SPT, while the "σ_x" column gives the corresponding standard deviation of the soil properties. It can be noticed from these tables that each of the values for the soil strength x is close to the corresponding μ_x, indicating that the proposed computational method can preserve the local average of the soil properties and the spatial trend of soil properties. This is an advantage of the proposed method. Additionally, the correlation length θ also has some variations, and these are related to the variation of the correlation coefficient ρ. The larger ρ is, the longer θ will be.

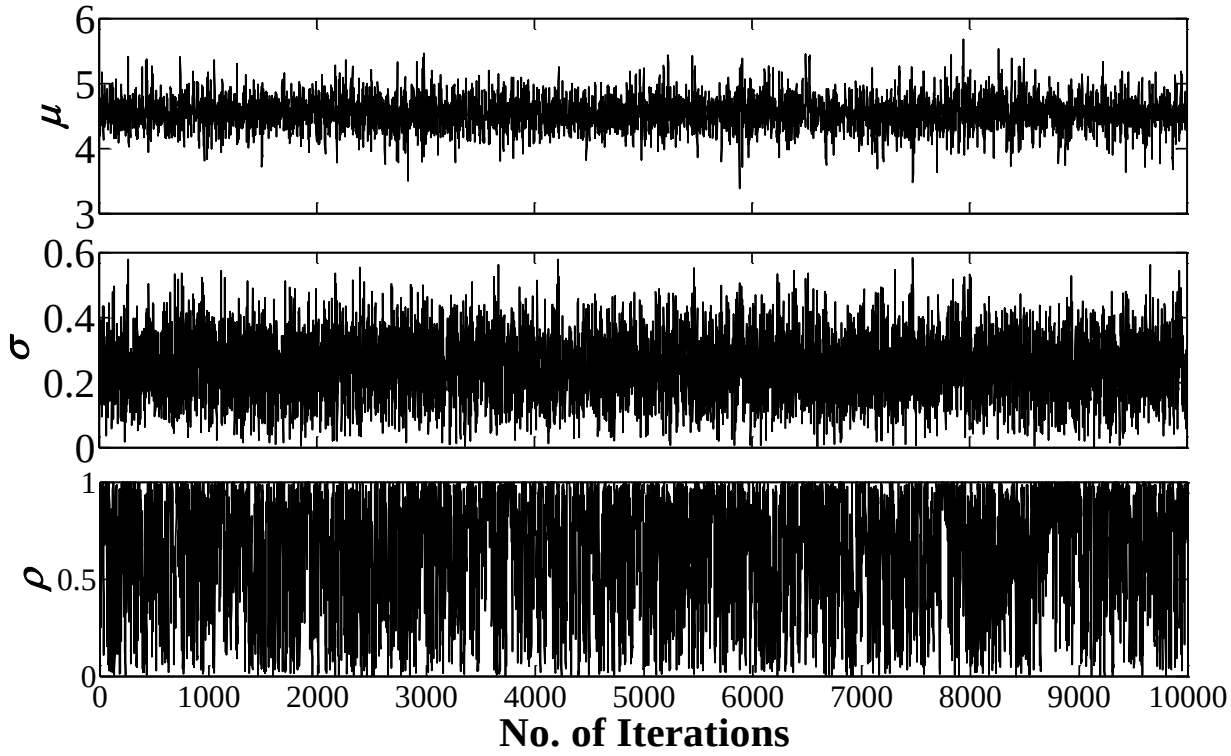

Figure 7.4 Random samples generated by MCMC

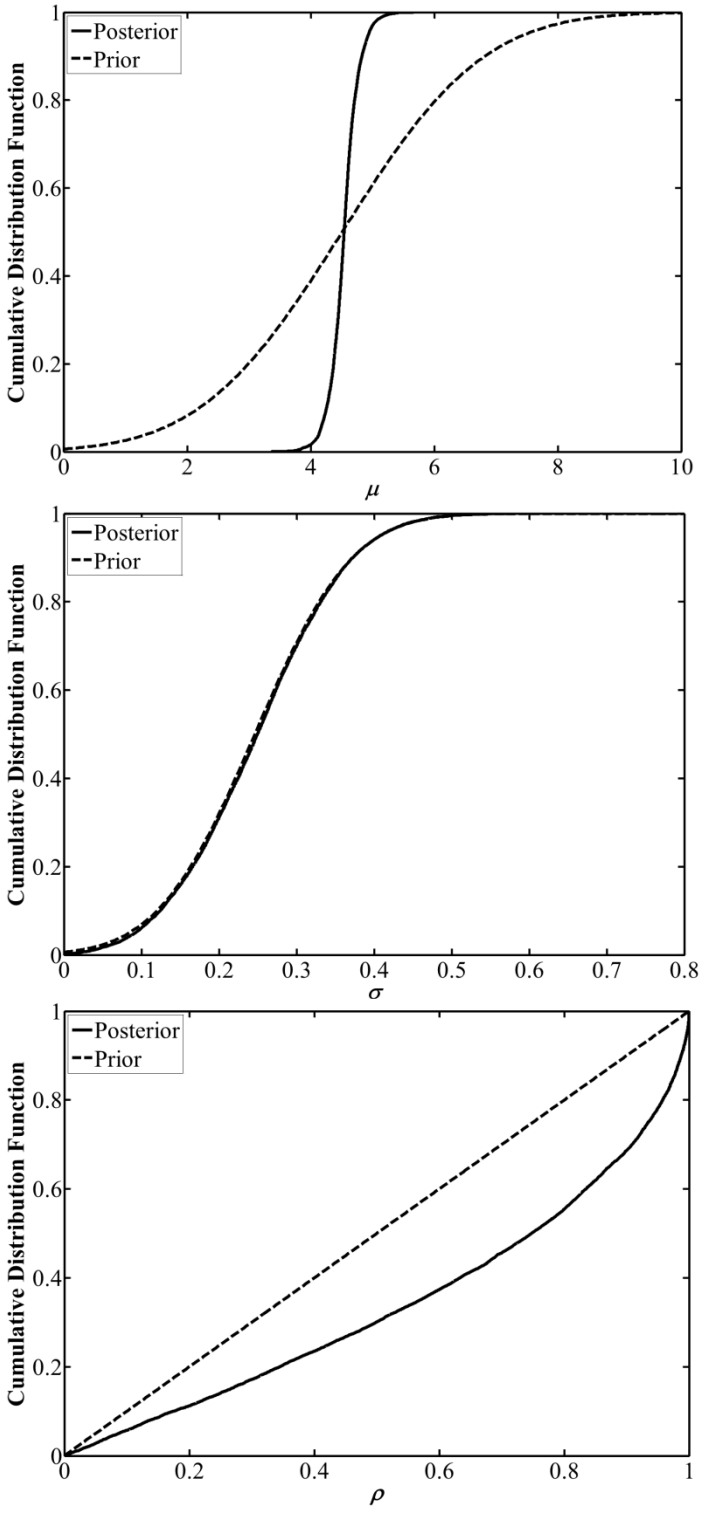

Figure 7.5 Posterior marginal CDFs of μ, σ and ρ

Table 7.1 Statistics of Soil Properties at BR1

Elevation (m)	x	Soil Strength	μ	σ	ρ	θ (m)	μ_x	σ_x
257.4	S_u	93.621	4.549	0.502	0.663	0.742	107.204	57.353
256.5	ϕ'	39.987	3.688	0.111	0.536	0.489	40.222	4.473
255.8	S_u	218.740	5.360	0.285	0.392	0.326	221.553	64.375
255.0	S_u	276.494	5.605	0.233	0.359	0.298	279.323	65.931
254.2	ϕ'	39.877	3.681	0.108	0.557	0.521	39.932	4.330
252.9	ϕ'	35.769	3.570	0.131	0.460	0.392	35.821	4.726
252.4	ϕ'	40.291	3.698	0.106	0.579	0.559	40.575	4.317
252.0	ϕ'	30.333	3.410	0.131	0.666	0.750	30.523	4.026
251.5	ϕ'	32.418	3.480	0.124	0.668	0.756	32.710	4.057
250.1	ϕ'	31.294	3.432	0.154	0.436	0.367	31.315	4.852
249.4	ϕ'	32.679	3.480	0.143	0.467	0.400	32.780	4.705
247.8	ϕ'	35.269	3.563	0.121	0.568	0.539	35.536	4.307
247.1	ϕ'	34.144	3.532	0.118	0.674	0.771	34.443	4.078
246.3	S_u	140.075	4.927	0.386	0.517	0.462	148.642	59.627
244.8	ϕ'	32.931	3.491	0.138	0.513	0.457	33.122	4.583
243.1	S_u	265.346	5.573	0.231	0.406	0.338	270.271	63.153
241.8	S_u	230.729	5.436	0.252	0.456	0.388	236.820	60.584
240.2	S_u	298.285	5.695	0.168	0.651	0.711	301.595	50.941
238.7	S_u	276.494	5.602	0.234	0.361	0.299	278.403	66.092
237.2	ϕ'	44.805	3.790	0.115	0.376	0.312	44.551	5.152
232.6	ϕ'	41.019	3.713	0.108	0.531	0.481	41.209	4.480
231.1	ϕ'	40.048	3.692	0.105	0.603	0.603	40.340	4.238
229.6	ϕ'	38.017	3.630	0.124	0.465	0.398	38.001	4.744

Note: $x = S_u$ or ϕ'. If $x = S_u$, the units of "Soil Strength", "μ_x" and "σ_x" are KPa. Otherwise, the corresponding units are in degrees.

Table 7.2 Statistics of Soil Properties at BR2

Elevation (m)	x	Soil Strength	μ	σ	ρ	θ (m)	μ_x	σ_x
257.0	S_u	125.360	4.819	0.388	0.666	0.751	133.458	53.730
255.8	ϕ'	39.144	3.666	0.114	0.550	0.510	39.359	4.486
254.6	S_u	287.470	5.663	0.190	0.557	0.520	293.332	56.351
253.4	ϕ'	41.683	3.728	0.102	0.581	0.561	41.820	4.278
252.6	ϕ'	39.587	3.679	0.108	0.565	0.533	39.819	4.310
252.1	ϕ'	44.409	3.792	0.098	0.563	0.530	44.578	4.360
251.7	ϕ'	38.625	3.653	0.111	0.568	0.538	38.840	4.339
251.2	ϕ'	36.089	3.586	0.111	0.665	0.746	36.325	4.046
250.6	S_u	254.013	5.533	0.229	0.459	0.392	259.741	60.367
249.7	S_u	154.211	5.015	0.382	0.429	0.360	162.105	64.184
248.8	S_u	167.859	5.115	0.326	0.537	0.490	175.558	58.740
247.4	S_u	230.729	5.428	0.255	0.465	0.398	235.233	60.997
246.7	S_u	242.480	5.482	0.225	0.545	0.502	246.510	56.143
246.0	ϕ'	33.016	3.496	0.130	0.573	0.547	33.273	4.331
244.5	ϕ'	42.908	3.753	0.111	0.434	0.365	42.925	4.779
243.0	S_u	230.729	5.437	0.253	0.461	0.393	237.289	60.912
241.5	S_u	276.494	5.604	0.233	0.347	0.288	279.005	65.844
240.0	S_u	298.285	5.696	0.195	0.471	0.405	303.210	59.553
238.4	ϕ'	36.940	3.602	0.128	0.460	0.393	36.958	4.763
236.9	ϕ'	45.076	3.802	0.101	0.502	0.443	45.040	4.576
232.3	ϕ'	45.588	3.808	0.107	0.417	0.348	45.327	4.869
230.8	ϕ'	46.905	3.846	0.089	0.608	0.613	47.009	4.187

Figure 7.6 and Figure 7.7 show the CDFs of θ for cohesive soils and granular soils, respectively. It can be observed that θ is distributed over the range of 0.2 m (0.66 ft) to 0.8 m (2.62 ft) in this example, regardless of whether the soils are cohesive or not. This finding is consistent with Phoon and Kulhawy (1999). The mean value of θ for both cohesive soils and

granular soils are approximately 0.45 m (1.48 ft), while the standard deviation is roughly 0.14 m (0.46 ft).

Since the computational method is applied per N value and there may be multiple N values in a single soil layer, there are multiple μ_x, σ_x and θ for the soil layer. Note that μ_x can preserve the local average of the soil strength. As a result, the values of μ_x along the depth give a spatial trend of soil strength. The mean values of σ_x and θ should be taken as the corresponding representative values for the soil layers, which will be used in random field generation. The representative values of σ_x and θ are summarized in Table 7.3.

Table 7.3 Representative Values of σ_x and θ

Soil Layer	BR1		BR2		Interpreted	
	σ_x	θ (m)	σ_x	θ (m)	σ_x	θ (m)
#1	57.35	0.74	53.73	0.75	56.01	0.75
#2	4.47	0.49	4.49	0.51	4.48	0.50
#3	65.15	0.31	56.35	0.52	61.90	0.39
#4	4.38	0.56	4.27	0.58	4.34	0.57
#5	59.63	0.46	60.09	0.43	59.80	0.45
#6	4.58	0.46	4.55	0.46	4.57	0.46
#7	60.19	0.43	62.10	0.36	60.90	0.41
#8	4.65	0.45	4.60	0.45	4.63	0.45

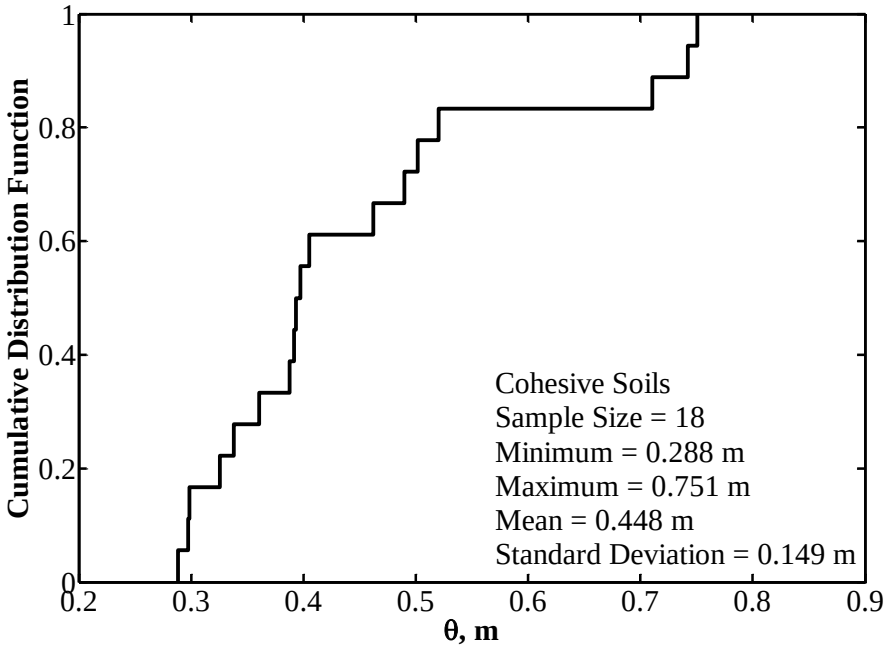

Figure 7.6 CDF of correlation length for cohesive soils

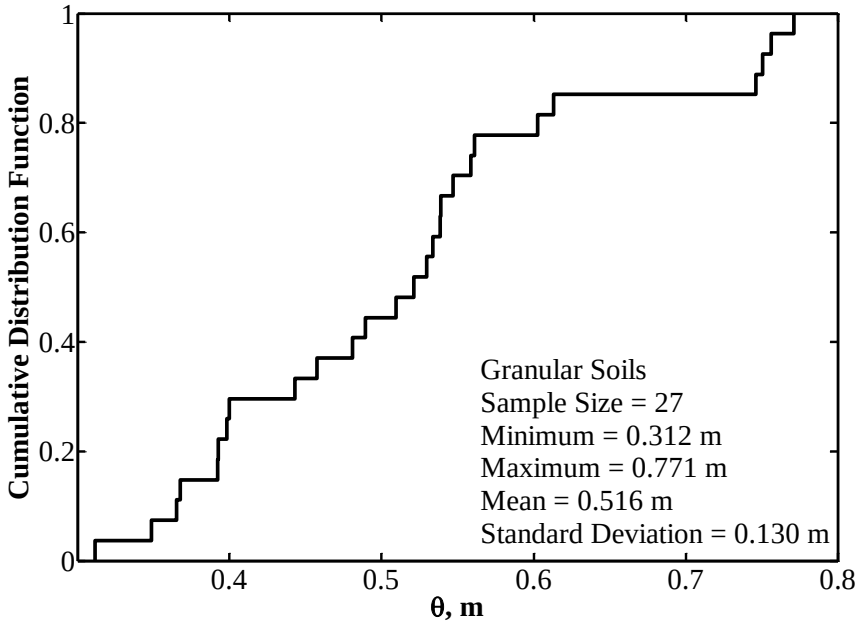

Figure 7.7 CDF of correlation length for granular soils

(Note: 0.3 m = 0.98 ft; 0.4 m = 1.31 ft; 0.5 m = 1.64 ft; 0.6 m = 1.97 ft; 0.7 m = 2.3 ft; 0.8 m = 2.62 ft.)

7.4.3 Determination of Soil Profile for Reliability Analysis

It has been shown in Figure 7.2 that the drilled shaft is not constructed at the locations where SPT was conducted. As a result, the soil profile at the location where the drilled shaft is constructed should be determined based on the findings of the subsurface investigation. The objective of this section is to demonstrate the use of inverse distance method in interpreting the soil profile given the adjacent boring logs.

In subsurface investigation, the soil samples are retrieved. Hence, the soil stratifications at the boring locations can be established and the thickness of each soil layer is known. In order to identify the soil stratifications at the desired location, it is assumed that the same soil stratifications are still present at that location. However, the thickness of each soil layer may be different. With this assumption, the thicknesses of the soil layers at the desired location need to be determined using the inverse distance method, and the distance between two points can be calculated based on their coordinates. In this example, the distances from the location where the drilled shaft is constructed to the locations of BR1 and BR2 are 15.6 m (51.18 ft) and 19.3 m (63.32 ft), respectively. The relative weight for BR1 and BR2 would be 0.63 and 0.37, assuming a v equal to 2.5 in Equation (7.13b). Figure 7.8 shows the interpreted soil stratifications for the drilled shaft based on the adjacent borings. It can be seen that the interpreted soil stratifications are close to those at BR1 and BR2, because the inverse distance method gives a weighted average based on the adjacent observations. Likewise, the inverse distance method can be applied to estimate other parameters based on the boring logs of BR1 and BR2. The "Interpreted" column in Table 7.3 summarizes the representative values of σ_x and θ at the location where the drilled shaft is constructed, while Table 7.4 summarizes the spatial trend of the strength parameter x.

Table 7.4 Spatial Trend of Strength Parameter along the Depth

Elevation(m)	x	μ_x
253.0	ϕ'	36.2
251.0	ϕ'	36.2
251.0	S_u	199.5
250.5	S_u	199.4
250.0	S_u	199.2
248.9	S_u	199.0
248.9	ϕ'	35.8
243.7	ϕ'	35.8
243.7	S_u	271.8
242.9	S_u	271.9
242.4	S_u	272.0
240.4	S_u	272.3
237.8	S_u	272.7
237.8	ϕ'	42.1
235.3	ϕ'	42.1
234.8	ϕ'	42.0
230.7	ϕ'	41.9
227.7	ϕ'	41.9

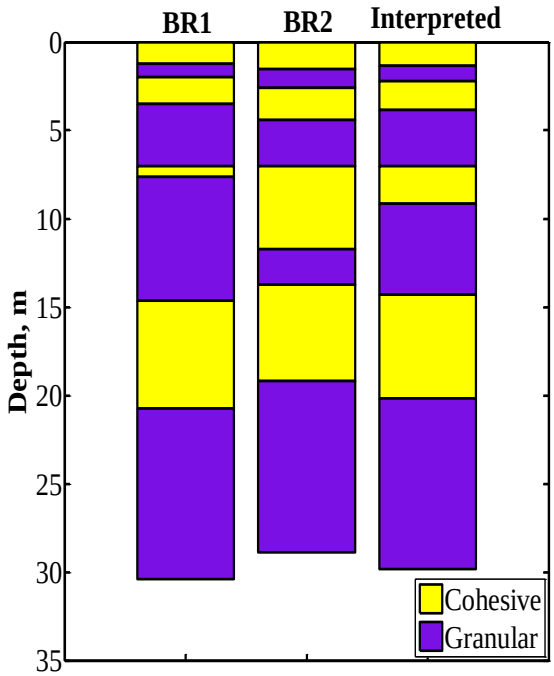

Figure 7.8 The interpreted soil stratifications based on adjacent borings

7.4.4 Reliability Analysis and Design

The objective of this section is to perform reliability analysis for the drilled shaft and determine a feasible design that achieves the target reliability. The statistics of the soil profiles have been determined and summarized in Table 7.3 and Table 7.4 in the previous section according to the inverse distance method. In addition to the soil profiles, the statistics of the concrete strength, the yield strength of steel, the model errors of *p*-*y* curves, *t*-*z* curves and *q*-*w* curves, and the allowable displacements are needed and summarized in Table 7.5, which will be used as inputs to the computer codes developed in Fan and Liang (2012, 2013a, 2013b).

Note that in Table 7.5 f'_c = compressive strength of concrete; f_y = yield strength of steel; E_s = elastic modulus of steel; e = model error with subscripts "py", "tz" and "qw" corresponding to *p*-*y* curves, *t*-*z* curves and *q*-*w* curves (see Fan and Liang 2012, 2013a, 2013b); and $d_{a,d}$ = allowable displacement where $d = \delta$, ψ or w, V_L = the live lateral load. The means of f'_c, f_y and E_s are specified as 31 MPa, 415 MPa and 200 GPa, respectively. The corresponding COVs for these parameters are taken as 7%, 5% and 5%, respectively. These values are typical and can be found in literature (ACI 2002; Mirza and MacGregor 1979). Note that the statistics of model errors are assumed in Table 7.5, because they are unavailable. To the best knowledge of the authors, there have been no statistics of the model errors reported in literatures. The means of e_{py}, e_{tz} and e_{qw} are all assumed as 1.0, implying that the load transfer curves do not underestimate or overestimate the soil reactions. Their COVs are just taken as 10% for demonstration purposes. According to Zhang and Ng (2005), the tolerable displacement in foundation design is indeed uncertain to some degree. To account for the uncertainty of the tolerable displacements, both the COVs of the tolerable vertical movement and the tolerable lateral deflection are specified as 10% for demonstration purposes. The lateral load that primarily results from the lateral earth pressure

and the surcharge on the ground surface is deemed a dead load. Because of the uncertainties in the unit weight of soils and the empirical model that is used to calculate the distribution of the lateral earth pressure along the elevation, the COV of the lateral load is taken as 25%. The provided unfactored axial loads are used as the means of the corresponding component. For demonstration purposes, the COVs of the live component and the dead component of the axial load are taken as 10% and 50%, respectively. Both of these COVs are typical, according to Nowak and Collins (2000). Moreover, the probability distributions of all the aforementioned random variables are assumed to be lognormal for the sake of simplicity, although other probability distributions such as the gamma distribution may be applicable.

Table 7.5 Statistics of Random Variables

Variable	Distribution	Mean	COV	Remarks
f'_c	Lognormal	31 MPa	7%	ACI (2002)
f_y	Lognormal	415 MPa	5%	Mirza and MacGregor (1979)
E_s	Lognormal	200 GPa	5%	Mirza and MacGregor (1979)
e_{py}	Lognormal	1	10%	(Assumed)
e_{tz}	Lognormal	1	10%	(Assumed)
e_{qw}	Lognormal	1	10%	(Assumed)
$d_{a,\delta}$	Lognormal	2.54 cm	10%	Zhang and Ng (2005)
$d_{a,w}$	Lognormal	2.54 cm	10%	Zhang and Ng (2005)
$d_{a,\psi}$	—	—	—	—
V_D	Lognormal	162.72 KN	25%	Nowak and Collins (2000)
V_L	—	—	—	—
Q_D	Lognormal	351.39 KN	10%	Nowak and Collins (2000)
Q_L	Lognormal	631.62 KN	50%	Nowak and Collins (2000)

With all the inputs defined previously, reliability analysis can be conducted using the computer codes. The target failure probability P_T is specified as 0.001 (reliability index β = 3.09). The failure probabilities of the original design are shown in Figure 7.9. It is found that the

original design (diameter = 1.07 m (42 in) and length = 25.30 m (83 ft)) has a $P_{f,w}$ of zero for the vertical movement limit state. However, the failure probability for the lateral deflection limit state is equal to 0.0028, which is greater than the target failure probability, indicating that the diameter and/or length should be adjusted to optimize the design. By trial and error, a different design is selected with diameter of 1.07 m (42 in) and a length of 16.76 m (55 ft), and the cross-section is reinforced by a total of 22 No. 11 bars with a cover thickness of 7.62 cm (3 in). Figure 7.10 shows the convergence of the failure probabilities for the new design. Although in the reliability analysis, the COV of the live axial load is as much as 50% and the COV of the dead axial load is 10%, the failure probability of the vertical movement limit state is just 4.4E-4, which is still much lower than the target probability of failure. It can be seen that the failure probability of the system (P_f = 5.1E-4) is smaller than the target failure probability (P_T = 0.001). Hence, it is considered a feasible design.

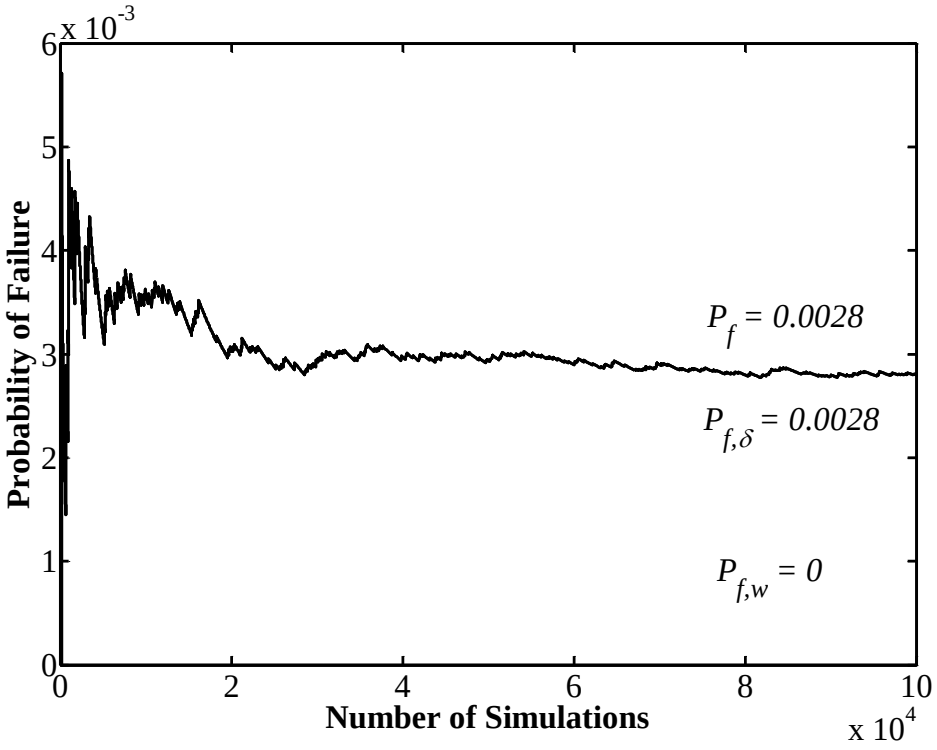

Figure 7.9 Failure probabilities of the original design

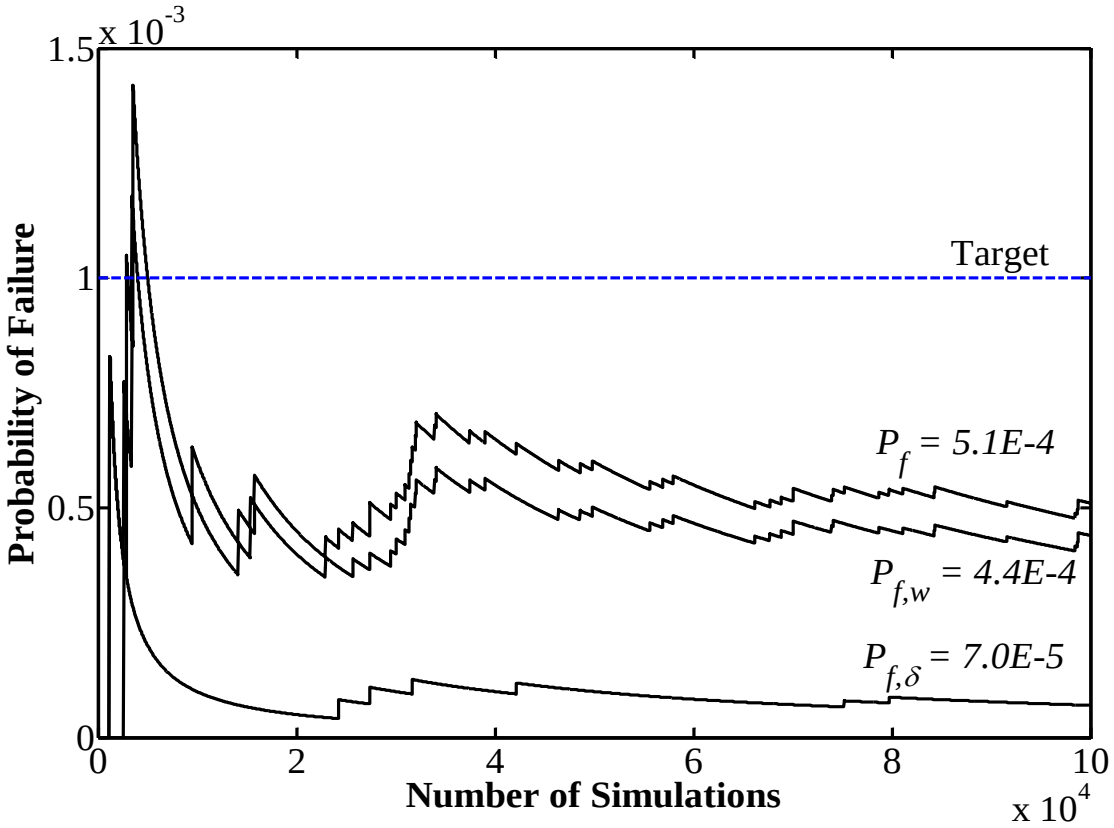

Figure 7.10 Failure probabilities by MCS

The new design by the proposed performance based design approach is compared with the original design (diameter = 1.07 m (42 in) and length = 25.30 m (83 ft)). First, the diameter of the new design is the same as that of the original design, and the new design has two more longitudinal bars than the original design as reinforcements. On the other hand, it is noticeable that the new design has a much shorter length than the original design: the new design is just 66% as long as the original design. While the difference in reinforcing rebars between the two designs is minimal, the difference in the length between the two designs is significant. This finding can be attributed to the design for the axial loads. Note that the average axial capacity of the original design in Monte Carlo simulation is 5125.9 KN (1152.30 kips), which is obtained according to the performance criterion (allowable displacement of 2.54 cm (1 in)). Likewise, the average axial capacity of the new design is just 3254.6 KN (731.63 kips) using the same performance criterion.

Notice that the summation of the unfactored dead load and the unfactored live load is 351.39 + 631.62 = 983.01 KN (220.98 kips). Accordingly, the factor of safety would be 5.215 for the original design and 3.311 for the new design. There is a significant difference between the factors of safety.

As indicated by the factors of safety, the original design may be too conservative for the axial loads. This same conclusion can be reached from the viewpoint of the failure probability. Notice that failure probability of the vertical movement limit state is zero for the sample size of 100,000, much lower than the target failure probability. In spite of the length of 25.30 m (83 ft), the system failure probability of the original design is just 0.0028 in relation to the failure probability of the lateral deflection limit state, indicating that the design is unable to achieve the target reliability. This is because the transfer of lateral loads occurs primarily in the upper zone of the drilled shaft and additional length is no longer ineffective in reducing the lateral deflection at the top of the drilled shaft.

Furthermore, it should be pointed out that the system reliability has been considered in the new design. As concluded in the Fan and Liang (2013a), the failure probability of the system is greater than those of the individual failure modes in reliability analysis. In the consideration of the system reliability, although the new design has slightly bigger diameter and slightly higher reinforcement ratio, the system failure probability for the new design is just 9.9E-4. From the viewpoint of the system failure probability, the new design is more reliable than the original design.

7.5 Summary and Conclusions

The stochastic nature of soil properties plays an important role in reliability-based design and risk management. This research presents a Bayesian approach that can be applied to

characterize the spatial variability of soil properties using SPT data. In order to establish a probabilistic model for SPT data in the Bayesian approach, it is assumed that the mean, the standard deviation and the correlation structure in the interval of each *N* value remain unchanged. Moreover, it is assumed that the strength parameter such undrained shear strength for cohesive soils and effective friction angle for granular soil follows lognormal distribution. With the establishment of the probabilistic model, Markov chain Monte Carlo is implemented to draw samples of the parameters (μ, σ, ρ). The resulting samples can be used to estimate (μ, σ, ρ). The mean μ measures the center of a dataset, the standard deviation measures the variability of a random variable while the correlation length measure how rapidly a random field varies in space. Furthermore, a kriging technique called inverse distance method is presented to interpret the soil profiles based on adjacent borings. Finally, an example is given and the following conclusions are made:

1. The computational method can be applied to characterize the spatial variability of soil properties using SPT data. It is applied per *N* value. If there are multiple *N* values in a single soil layer, then σ_x and θ should be averaged, and the average values should be taken as the representative values for the soil layer.
2. The resulting correlation length in this study is distributed over the range from 0.2 m (0.66 ft) to 0.8 m (2.62 ft). The corresponding mean is approximately 0.45 m (1.48 ft), while the standard deviation is about 0.15 m (0.49 ft).
3. The computational method can preserve the local average of the soil properties. The values of μ_x along the depth give a spatial trend of the soil strength.

4. The inverse distance method provides a simple means to interpret the soil profiles according to the adjacent borings. In the inverse distance method, more weight is given to the observations that are close to the desired location.
5. In the example, the feasible design by the performance based design approach is significantly different from the original design that was obtained using load and resistance factor design. The factor of safety of the new design is just 3.311. However, the factor of safety of the original design is as much as 5.215, indicating that the original design might be too conservative.

CHAPTER 8. SUMMARY AND CONCLUSIONS

8.1 Summary of the Research

Reliability-based design of deep foundations, such as drilled shafts and driven piles, has become increasingly important due to the heightened awareness of the shortcomings of the conventional allowable stress design approach. For example, the load and resistance factor design has been implemented by American Association of State Highway Transportation Officials (AASHTO) since 2007. Nevertheless, there are still many unsolved issues regarding the implementation of load and resistance factor design. For example, there is no generally accepted guidance on the statistical characterization of soil properties. Moreover, the serviceability limit check in LRFD is still deterministic. No uncertainties arising in soil properties, loads and design criteria are taken into account in the current version of LRFD for the serviceability limit check. In current practice, the load factors and resistances are taken as unity and deterministic models are applied to evaluate the displacements of geotechnical structures.

In order to address the aforementioned issues of LRFD, the computational method for conducting reliability analysis and the computational tools for statistically characterizing the variability of soil properties are needed. The main objectives of the research are:

1. To develop mathematically sound computational tools for conducting reliability analysis for deep foundations; and
2. To develop the associated computational method that can be used to determine the variability model of soil properties.

In this research, to achieve a consistency between the strength limit check and the serviceability limit check of the LRFD framework, performance-based design methodology was developed for deep foundation design. In the proposed methodology, the design criteria are defined in terms of the displacements of the structure that are induced by external loads. If the displacements are within the specified design criteria (i.e., the allowable displacement of the foundation system), the design is considered satisfactory. Otherwise, failure is said to occur. To calculate the probability of failure, Monte Carlo simulation is employed. In Monte Carlo simulation, the variability of the random variables that are involved in the reliability analysis is captured by simulating a large number of the samples according to their respective probability distributions. Then the simulations of the random variables are used as the input to the commonly-used deterministic numerical algorithms including the *p-y* method for lateral load and the *t-z* model for axial load to evaluate the load-displacement behavior. With the calculated displacements, it can be determined whether or not failure occurs. Accordingly, the failure probability is calculated as the number of failure events to the total number of simulations.

8.1.1 Computational Tools for Reliability Analysis

A series of computer codes have been developed to facilitate the computation of reliability analysis. Specifically, *P-LPILE* has been developed for laterally loaded drilled shafts, *P-TZPILE* has been developed for axially loaded piles, and *XPILE* has been developed for piles under combined axial and lateral loads. Furthermore, a computer code based on importance sampling has been developed for axially loaded piles in order to have a faster rate of convergence in estimating the failure probability.

Various sources of uncertainties are accounted for in the proposed reliability methodology. In all the aforementioned computer codes, the soil properties are modeled as random fields that

are statistically characterized by the mean, the standard deviation and the correlation length. The mean measures the center of a dataset, the standard deviation measures the variability of a random variable, and the correlation length measures how rapidly a random field varies in space. The probability distribution of the soil properties is assumed to be lognormal, just for mathematical simplicity and the ease of simulation. In addition to the variability of soil properties, the variability of the external loads, concrete properties, steel properties, the design criteria and the model uncertainty of the load transfer curves can be systematically taken into account.

Extensive validations were carried out to ensure accuracy and robustness of the developed computer codes. Furthermore, these computer codes were used for conducting a series of parametric studies as well as performing several illustrative design examples.

8.1.2 Computational Method for Determining Soil Variability

The method of determining the relevant variability model for soil properties based on the standard penetration test (SPT) data was developed. The computational method is based on Bayesian approach. To make the computational method usable to practicing engineers, data from the SPT is used in the computational method. The objective of developing the method is to determine the required input including the mean μ, standard deviation σ, and correlation length θ of soil properties in reliability analysis and foundation analysis. Several assumptions are invoked in formulating the approach: 1) each N value in SPT is considered as a unit in the computation; 2) the mean, standard deviation and the correlation structure of soil properties remain unchanged in the interval of each N value; and 3) soil properties follow lognormal distributions. In Bayesian approach, the parameters of interest are $\boldsymbol{\lambda} = (\mu, \sigma, \theta)$. With these assumptions, the probabilistic model of the blow counts in SPT can be established as multivariate normal distribution.

Accordingly, the posterior distribution of $\boldsymbol{\lambda}$ can be formulated. Markov chain Monte Carlo is implemented to draw the samples of (μ, σ, θ). The advantages of implementing Markov chain Monte Carlo are that: 1) the normalizing constant in the posterior distribution of the parameters can be avoided; and 2) it is straightforward to use the resulting samples of the parameters (μ, σ, θ) to conduct statistical analysis. An example was given to demonstrate the application of the proposed site variability characterization method. In addition, the design based on the proposed reliability method is compared with that based on the current LRFD approach. The comparison indicates that the current LRFD method yields a very conservative design.

8.2 Conclusions

Using the developed computer codes and the computational method, a series of parametric studies are conducted. Furthermore, to demonstrate the application of the proposed methodology, real data from a construction project is used, and the proposed computational method is employed to determine the variability of the soil properties. Next, the determined variability model of soil properties is used as input to the developed computer codes in the reliability analysis. Based on the results of parametric studies and the reliability analysis, the following conclusions are made:

- Reliability Analysis Of Piles Under Axial And Lateral Loads

    1. The spatial variability of soil properties, particularly the COV and correlation length of undrained shear strength for cohesive soils, could exert significant influences on the computed probability of failure for the specified performance criteria. The difference in the computed probability of failure caused by different correlation length of S_u could be several orders of magnitude.

2. Apart from soil spatial variability, the proposed performance based design approach provides a systematic procedure to consider uncertainties of the computational model and the applied loads. A random bias factor is introduced to account for the uncertainty of p-y curves. The estimated probability of failure increases if the uncertainty of the adopted p-y curves is considered. The uncertainty of loads is considered by sampling from their probability distributions and using the samples as input. The calculated probability of failure increases when the uncertainty of loads is considered.

3. The proposed approach is useful to conduct reliability analysis for serviceability limit check in the current LRFD framework. Based on the conducted parametric studies, the reliability for the serviceability limit design of a laterally loaded pile is sensitive to the spatial correlation of soil properties, soil variability, uncertainty of p-y curves and loads.

4. The proposed approach is very versatile, as it allows practicing engineers to input the means, variances and probability distributions of the load model, soil properties and the bias factor of p-y curves. Furthermore, they can specify the target reliability index according to the intended functions of the structures under consideration.

5. Probabilistic approaches that do not take into consideration of spatial variance of soil properties may potentially result in a foundation design that would not meet the performance criteria with the target reliability. It is demonstrated that the probability of failure is sensitive to correlation length, θ. If θ is not considered in reliability assessment, the estimated probability of failure would probably be biased. Therefore, considering correlation length is warranted in the reliability analysis of deep

foundations. There is a strong incentive to use a reliability method that considers the correlation structure of soil properties for deep foundations.

❖ The Importance Sampling Technique

6. The proposed importance sampling method gives the same unbiased estimate of the failure probability as the crude MCS method. Nevertheless, the proposed importance sampling method is much more efficient than the crude MCS method when evaluating a small P_f (e.g., $P_f \leq 1/1000$). By drawing more samples from the region of interest, the proposed method will achieve a faster rate of convergence. With the same sample size, the estimate obtained by using the importance sampling method would have a much smaller coefficient of variation than the estimate obtained by the crude MCS method. It is recommended to use the importance sampling method in the evaluation of small P_f.

7. The probability of failure evaluated by the commonly used FORM may significantly deviate from those of Monte Carlo statistical methods, although the reliability index by FORM is close to those of Monte Carlo statistical methods. The differences in the failure probabilities between FORM and Monte Carlo statistical methods are primarily attributed to the approximation of the limit state function in the response surface method and the linear truncation of the limit state function in the FORM.

❖ The Analysis Of The System Reliability

8. The failure probability of the system, P_f, is greater than any of the three component failure modes. In addition, P_f is less than the summation of the failure probabilities of

the three component failure modes. The failure probability of the system may be underestimated if multiple failure modes are not considered simultaneously.

9. It is recommended to use the system reliability if multiple failure modes exist. In the current LRFD approach, different limit states are considered separately, which leads to overestimation in the reliability.

❖ The Importance Analysis Of Random Variables

10. The importance analysis of the random variables indicate that the major sources of uncertainties affecting the reliability of a designed drilled shaft come from external loads, the allowable displacement, soil property S_u, and the model factors of the load transfer curves. The variability in concrete and reinforcement is relatively less important.

❖ Site Variability Characterization

11. A computational method has been developed that can be applied to characterize the spatial variability of soil properties using SPT data. It is applied per N value. If there are multiple N values in a single soil layer, then σ_x and θ should be averaged and the average values should be taken as the representative values for the soil layer.
12. The resulting correlation length in this study is distributed over the range from 0.2 m to 0.8 m. The corresponding mean is approximately 0.45 m while the standard deviation is about 0.15 m.

13. The computational method can preserve the local average of the soil properties. The values of μ_x along the depth give a spatial trend of soil strength.
14. The inverse distance method provides a simple means to interpret the soil profiles according to the adjacent borings. In the inverse distance method, more weights are given to the observations that are close to the desired location.
15. In the example given in Chapter 7, the feasible design by the performance based design approach is significantly different from the original design that was obtained using load and resistance factor design. The factor of safety of the new design is just 3.513. However, the factor of safety of the original design is as much as 5.215, indicating that the original design might be too conservative.

8.3 Recommendations for Future Research

Although the computer codes have been developed for conducting reliability analysis and the computational method has been proposed to determine the variability model for soil properties, there is a need to continue the current research on the following aspects:

1. To provide statistical guidance to determine the variability of external loads. In the importance analysis, although the COV of external loads is small, it is noticeable that the reliability of a design is very sensitive to the external loads. The failure probability can vary significantly when the COVs of the external loads changes.
2. To calibrate the model uncertainty of the load transfer curves (*p*-*y* curves, *t*-*z* curves and *q*-*w* curves). Even though the COVs of the load transfer curves are small in the importance analysis, it can have a big impact on the reliability of a design.
3. To compile a database of the tolerable displacements of deep foundations. The displacements of interest include lateral deflection, angular distortion and vertical

movement. This is because the design criteria are defined by the displacements and it directly influences the final design. If specified tolerable displacements are too small, it may lead to conservative designs. Otherwise, unconservative designs will be obtained.

4. To develop a computer code that can be used to conduct reliability analysis on a group of piles. The computer codes developed in the research only apply to a single drilled shaft. However, drilled shafts are often constructed as a group. Therefore, it is highly desirable to develop a computer program for a group of drilled shafts such that the group effect can be considered in reliability analysis.
5. To continue the research on the effects of the spatial variability on the reliability of the designed structures and the use of kriging techniques to estimate unknown parameters.

REFERENCES

Allen, T. M., Nowak, A. S. and Bathurst, R. (2005) *Calibration to Determine Load and Resistance factors for Geotechnical and Structural Design*. No. E-C079, Transportation Research Board, Washington, D.C.

American Association of State Highway and Transportation Officials (AASHTO). (2010). *AASHTO LRFD Bridge Design Specifications*, 5th Edition. American Association of State Highway and Transportation OfficialsWashington, DC.

American Concrete Institute. (2002). *Evaluation of Strength Test Results of Concrete*. ACI 214-R2. American Concrete Institute , Farmington Hills, Michigan.

Ang, A. H-S., and Tang, W. H. (1984). *Probability Concepts in Engineering Planning and Design*, Vol. II.. Hoboken, New Jersey: John Wiley and Sons.

Ang, A. H-S., and Tang, W. H. (2007). *Probability Concepts in Engineering: Emphasis on Applications in Civil and Environmental Engineering*. Hoboken, New Jersey: John Wiley and Sons.

Au, S. K., and Beck, J. L. (2003). "Importance sampling in high dimensions." *Structural Safety*, No. 25, 139-163.

Au, S.K, and Beck, J.L. (1999). "A new adaptive importance sampling scheme for reliability calculations." *Struct. Safety* 21: 135-158.

Brown, D. A., Turner, J. P., and Casetelli, R. J. (2010). "Drilled shaft: construction procedures and LRFD design methods." *No. FHWA-NHI-10-016*, Federal Highway Administration, Washington, D.C.

Ching, J. Y., and Phoon, K. K. (2011). "A quantile-based approach for calibrating reliability-based partial factors." *Structural Safety*, 33(2011): 275-285.

Ching, J.Y., Phoon, K.K., Chen, J.R., and Park, J.H. (2013). "Robustness of constant load and resistance factors for drilled shafts in multiple strata." *J. Geotech. Geoenviron. Engr.*, ASCE, Vol.139(7):1104-1114.

Coyle, H. M., and Reese, L. C. (1966). "Load transfer for axially loaded piles in clay." *Journal of Soil Mechanics and Foundation Division*, 92(2): 1-26.

D'Andrea, A., and Tsai, C. N. (2009). "Louisiana Department of Transportation's experience with LRFD." *Implementation status of geotechnical load and resistance factor design in state department of transportation*, No. E-C136, pp. 1-10.

Das, B. (2011). *Principles of Foundation Engineering*. Stamford, Connecticut: Cengage Learning. pp. 84-88.

Der Kiureghian, A., and Ke, J.-B. (1995). "Finite-element based reliability analysis of frame structures." *Proc., ICOSSAR '85, 4th Int. Conf. on Structural Safety and Reliability*, IASSAR, New York, 1, 395–404.)

Der Kiureghian, A., and Liu, P. L. (1991). "Optimization algorithms for structural safety." *Struct. Safety*, 9:161-177.

Der Kiureghian, A., and Stefano, M. D. (1991). "Efficient algorithm for second-order reliability analysis." *J. Engr. Mech.*, 117(12): 2904-2922.

Ditlevsen, O., and Madsen, H.O. (1996). *Structural reliability methods.* Chichester, UK: Wiley..

Ellingwood, B., and Tekie, P. B. (1999). "Wind load statistics for probability-based structural design." *J. Struct. Eng*., 125 (4), 453-463.

Ellingwood, B., Galambos, T. V., MacGregor, J. G., and Cornell, C. A. (1980). *Development of a Probability Based Load Criterion for American National Standard A58*. NBS Special Publication 577. Washington, D.C.: National Bureau of Standards.

Fan, H. J., and Liang, R. (2012). "Reliability-Based Design of Axially Loaded Drilled Shafts using Monte Carlo Method." *Int. J. of Num. and Analyt. Methods in Geomech.* (In Press).

Fan, H. J., and Liang, R. (2013a). "Probabilistic framework of drilled shaft design considering soil spatial variability." *Journal of the Transportation Research Board*. (In Press)

Fan, H. J., and Liang, R. (2013b). "Performance-Based Reliability Analysis of Laterally Loaded Drilled Shafts." *Journal of Geotechnical and Geoenvironmental Engineering*, ASCE. http://dx.doi.org/10.1061/(ASCE)GT.1943-5606.0000954 (In Press)

Fenton, G. (1999). "Random field modeling of CPT data." *Journal of Geotechnical and Geoenvironmental Engineering*, ASCE, 125 (6), 486-498.

Fenton, G. A., and Griffiths, D. V. (2008). *Risk Assessment in Geotechnical Engineering*, Hoboken, New Jersey: Wiley and Sons.

Fishman, G. S. (1996). *Monte Carlo: Concepts, Algorithms and Applications*. New York: Springer

Griffiths, D. V., Huang, J., and Fenton, G. (2009). "Influence of spatially variability on slope reliability using 2-D random fields." *J. Geotech. Geoenviron. Eng*., ASCE, 135 (10), 1367-1378.

Isaaks, E. H., and Srivastava, R. M. (1989) *Introduction to Applied Geostatistics*. Oxford University Press, Inc., New York, pp. 249-277.

Klammler, H., McVay, M., Horhota, D., and Lai, P. (2010). "Influence of spatially variable side friction on single drilled shaft resistance and LRFD resistance factors." *J. Geotech. Geoenviron. Eng*., ASCE, 136 (8), 1114-1122.

Kung, G. T. C., Juang, C., Hsein, H., Evan, C. L., and Hashash, Y. M. A. (2007). "Simplified model for wall deflection and ground-surface settlement caused by braced excavation in clays." *Journal of Geotechnical and Geoenvironmental Engineering*, 133(6): 731-747.

Lai, P. W. (2009). "Florida Department of Transportation's experience with LRFD." In: *Implementation Status of Geotechnical Load and Resistance Factor Design in State Departments of Transportation*, Transportation Research Circular No. E-C136, 11-20. Transportation Research Board, Washington, D.C.

Lee, I. K., White, W., and Ingles, O. G. (1983). *Geotechnical Engineering*. Melbourne, Australia: Sir Isaac Pitman and Sons. p. 62

Low, B.K., and Tang, W.H. (2007). "Efficient spreadsheet algorithm for first order reliability method." *J. Engr. Mech.* 133(12): 1378-1387.

Luo, Z., Atamturktur, S., Cai, Y. and Juang, C. H. (2012). "Simplified approach for reliability-based design against basal heave failure in braced excavations considering spatial effect." *J. Geotech. Geoenviron. Eng*., 128(4), 441-450.

Melchers, R. (1999). *Structural Reliability Analysis and Prediction*. London: John Wiley and Sons, Ltd.

Mirza, S.A., and MacGregor, J.G., "Variability of Mechanical Properties of Reinforcing Bars." *Journal of the Structural Division*, ASCE. Vol. 105, No. ST5, 1979, pp. 921-937.

Nowak, A. S., and Collins, K. R. (2000). *Reliability of structures*. New York: McGraw-Hill.

Paice, G. M., Griffiths, D. V., and Fenton, G. A. (1996). "Finite element modeling of settlements on spatially random soil." *J. Geotech. Eng.*, ASCE, 122(9), 777-779.

Phoon, K. K, Kulhawy, F. H., and Grigoriu, M. D. (1995). "Reliability-based design of foundations for transmission line structures." Rep. TR-105000, Electric Power Research Institute, Palo Alto, California.

Phoon, K. K, Kulhawy, F. H., and Grigoriu, M. D. (2003a). "Development of a reliability-based design framework for transmission line structure foundations." *J. Geotech. Geoenviron. Eng*., ASCE, 129 (9), 798-806.

Phoon, K. K, Kulhawy, F. H., and Grigoriu, M. D. (2003b). "Multiple resistance factor design for shallow transmission line structure foundations." *J. Geotech. Geoenviron. Eng*., ASCE, 129 (9), 807-818.

Phoon, K. K., and Kulhawy, F. H. (1999). "Characterization of geotechnical variability." *Can. Geotech. J.*, Vol. 36, 612-624.

Phoon, K. K., and Kulhawy, F. H. (2005). "Characterization of model uncertainties for laterally loaded rigid drilled shafts." *Geotechnique*, Vol. 55(1), 45-54.

Reese, L. C. (1977). "Laterally loaded piles: program documentation." *J. Geotech. Eng. Division*., Vol. 103 (GT4), ASCE, 287-305.

Reese, L. C., Wang, S. T, and Isenhower, W. M., and Arrellaga, J. A. (2004). *Computer program LPILE Plus version 5.0 technical manual*. Austin, Texas: Ensoft. Inc.

Robert, C. P., and Casella, G. (2004). *Monte Carlo Statistical Methods*, Springer, New York.

Roberts, L. A., and Misra, A. (2010). "Performance-based design of deep foundation systems in load and resistance factor design framework." *Journal of the Transportation Research Board*, No. 2186, 29-37.

Sabatini, P. J., Bachus, R. C, Mayne, P. W., Schneider, J. A., and Zettler, T. E. (2002). Evaluation of Soil and Rock Properties. *Report No. FHWA-IF-02-034*. Federal Highway Administration, Washington, D.C..

Vanmarcke, E. H. (1977). "Probabilistic modeling of soil profiles." *Journal of the Geotechnical Engineering Division*, 103(11), 1227-1246.

Wang, Y., Au, S. K., and Kulhawy, F. H. (2011). "Expanded reliability-based design approach for drilled shafts." *J. Geotech. Geoenviron. Eng*., 137(2), 140-149.

Zhang, L. M., and Ng, Agnes, M. Y. (2005). "Probabilistic limiting tolerable displacements for serviceability limit state design of foundations." *Geotechnique*, 55(2), 151-161.

Zhu, H., and Chang, M. F. (2002). "Load transfer curves along bored piles considering modulus degradation." *Journal of Geotechnical and Geoenvironmental Engineering* 2002, ASCE, 128 (9): 764-773.